NACA

RESEARCH MEMORANDUM

A WIND-TUNNEL INVESTIGATION OF THE AERODYNAMIC CHARACTERISTICS OF A FULL-SCALE SWEPTBACK PROPELLER AND TWO RELATED STRAIGHT PROPELLERS

By Albert J. Evans and George Liner

Langley Aeronautical Laboratory
Langley Field, Va.

NATIONAL ADVISORY COMMITTEE
FOR AERONAUTICS

WASHINGTON

January 4, 1951
Declassified August 23, 1954

NATIONAL ADVISORY COMMITTEE FOR AERONAUTICS

RESEARCH MEMORANDUM

A WIND-TUNNEL INVESTIGATION OF THE AERODYNAMIC CHARACTERISTICS OF A FULL-SCALE SWEPTBACK PROPELLER AND TWO RELATED STRAIGHT PROPELLERS

By Albert J. Evans and George Liner

SUMMARY

An investigation of an NACA 10-(1.7)(062)-057-27 two-blade swept propeller has been conducted in the Langley 16-foot high-speed tunnel over a range of blade-angle setting from 20° to 60°. The maximum value of helical tip Mach number was about 1.15.

Two related straight propellers were also tested over the same operating range as the swept propeller. The straight propellers were tested for comparison purposes to evaluate the merits of the sweptback-blade design. At the design blade-angle setting the swept propeller maintained its low-speed level of maximum efficiency to a value of helical tip Mach number that was about 6 percent higher than that for the straight propellers. Results of the tests indicated, however, that the range of operation where the sweepback may be desirable for a propeller design is very narrow. When the propeller was operating at the design condition, the power absorbed by the swept propeller was only 50 percent of the design power coefficient, whereas the straight-blade propellers absorbed close to 100 percent of the power for which they were designed.

INTRODUCTION

Numerous investigations of the effects of sweep on the aerodynamic characteristics of wings have shown that the onset of the adverse effects of compressibility can be delayed by sweep to appreciably higher free-stream Mach numbers. Since a propeller blade is essentially a rotating wing, the incorporation of sweep in a propeller would therefore be expected to delay the onset of compressibility losses of the propeller to higher tip speeds. Investigation of the effect of sweeping the tips of a propeller (reference 1) indicated that the use of sweep in the design of a

propeller blade should give improved performance at high propeller tip speeds. Results of flight tests (reference 2) and other wind-tunnel tests (reference 3) of a sweptback propeller did not show any significant delay in the adverse effects of compressibility on propeller efficiency through the use of sweep. The fact that these tests did not show any significant gains for the swept propeller may have been due to insufficient amounts of sweep incorporated in the propeller design. In addition, in the case of the wind-tunnel tests, the propeller-section speeds were not high enough to show the beneficial effects of sweep.

As a result of these preliminary tests a sweptback-propeller program was inaugurated by the National Advisory Committee for Aeronautics. One phase of the program included tests of two swept-propeller models and a comparable straight propeller in the Langley 8-foot high-speed tunnel. These two swept propellers differed only in pitch distribution and were designed to yield the highest possible efficiency at the highest possible speed, as described in reference 4. The sweep of these propellers was 45° at the design radius station. The results of these tests are reported in references 5 and 6. The other phase of the NACA program was tests of a full-scale swept propeller and two related straight propellers in the Langley 16-foot high-speed tunnel. The full-scale propeller differed from those tested in the Langley 8-foot high-speed tunnel in that it was designed to operate at moderate power and speeds. This paper presents the results of the tests in the 16-foot high-speed tunnel and a brief description of the design of the propeller blades.

SYMBOLS

b	blade width parallel to resultant air stream at the design condition (chord), feet
C_P	power coefficient $\left(P/\rho n^3 D^5\right)$
C_T	thrust coefficient $\left(T/\rho n^2 D^4\right)$
C_T'	elemental thrust coefficient
c_{l_d}	design section lift coefficient
D	propeller diameter, feet
h	blade-section maximum thickness, feet
J	advance ratio (V/nD)

J_o advance ratio for $C_T = 0$

M air-stream Mach number

M_t helical tip Mach number $\left(M\sqrt{1 + \left(\frac{\pi}{J}\right)^2}\right)$

n propeller rotation speed, revolutions per second

P power, foot-pounds per second

R propeller-tip radius, feet

r radius to a blade element, feet

T thrust, pounds

V velocity of advance, feet per second

x fraction of propeller-tip radius (r/R)

β blade angle, degrees

$\beta_{0.70R}$ blade angle at 0.7 tip radius, degrees

γ angle whose tangent is the ratio of drag to lift

η efficiency $\left(\frac{C_T}{C_P} J\right)$

Λ sweep angle for design condition (see reference 4), degrees

ρ air density, slugs per cubic foot

$\phi_{0.70R}$ aerodynamic helix angle at 0.7 tip radius, degrees

APPARATUS

Propeller Dynamometer and Survey Rake

The tests were made with a 2000-horsepower propeller dynamometer in the Langley 16-foot high-speed tunnel. A complete description of the dynamometer is contained in reference 7. A photograph of the dynamometer in the tunnel test section with the sweptback propeller installed is shown as figure 1. A total-pressure survey rake was installed behind

the propeller, as shown in figure 1, to measure the radial thrust load distribution on the propeller blades.

Propeller Blades

General description.- Three two-blade propellers were designed and tested at the Langley 16-foot high-speed tunnel. One of the propellers incorporated sweepback. The other two propellers had straight blades whose design parameters were related to those of the sweptback blades for comparison of the aerodynamic characteristics. The design condition for all the propellers, chosen to obtain supercritical section speeds and to obtain the theoretically optimum value of blade-angle setting at the design radius for maximum efficiency, that is, $\beta_{0.70R} = \phi_{0.70R} = 45^{\circ} - \frac{\gamma}{2}$, was an advance ratio of 2.0 at a helical tip Mach number of 1.1. The values of section speeds and the extent of the blade radius operating at supercritical speeds were limited by the maximum tunnel speed and rotational speed obtainable.

The blades were made up of NACA 16-series airfoil sections and the radial thickness-ratio distribution was the same for the three propellers, being 6.2 percent at the design radius. The sections of the swept blades were positioned in the blades such that they lay in a plane which was perpendicular to a radial line drawn from the axis of rotation to the centroid of the section.

The pitch distribution was the same for the three propellers and was such that the chord line of each section lay in a plane parallel to the resultant section velocity corrected for the induced flow for the design advance ratio, $J = 2.0$. The induced flow was calculated according to Goldstein's theory for straight propellers. The three propellers had a distribution of width and lift coefficient so that they would have the Betz loading for minimum induced energy loss when operating at the design condition. The three propellers were 10 feet in diameter at the design blade-angle setting, and were of solid-aluminum-alloy construction (76S-T-61). Blade-form characteristic curves for the three propellers are presented in figure 2 and a photograph of the blades is presented as figure 3.

Sweptback blades.- The sweptback propeller is designated as the NACA 10-(1.7)(062)-057-27 design and in the figures of the present paper is noted as propeller I. The digits in the designation indicate a 10-foot-diameter propeller with the following design parameters at the 0.70-radius station: section design lift coefficient of 0.17, thickness ratio of 0.062, solidity of 0.057 per blade, and sweepback of 27°.

The blades of the sweptback propeller were swept in accordance with simple infinite-span-wing sweep theory, so that theoretically all the

swept sections reached the critical speed simultaneously at the design condition. The equation of the curve of sweepback was derived by using the following design parameters: Critical Mach number of the blade sections ($M_{cr} = 0.80$), propeller rotational speed (2,000 rpm), and design advance ratio ($J = 2.0$). Sweepback was provided outboard of the radial station $\left(\frac{r}{R} = 0.56\right)$ where the unswept section critical Mach number was reached at the design condition. The locus of the points of minimum pressure for the sections was originally chosen to define the sweepback angle. The stress computations were simplified, however, by actually applying the sweep curve to the locus of the section centroids which is practically the locus of points of minimum pressure for the sections. The radial distribution of the sweepback is shown in figure 2.

An arbitrary curve of sweepforward was applied to the locus of the centroids of the inboard sections to offset completely, for the design condition, the large bending moment at the blade shanks caused by the centrifugal forces acting on the sweptback sections. Although the sweepforward alleviated the high bending stresses due to the sweepback for the shanks and the inboard sections, high bending stresses still existed on the outboard or sweptback sections and were highest at the trailing edge of the section at the knee of the blade. In order to relieve the stresses at the knee, the chords of the sections were arbitrarily increased so that the value of the maximum stress on the blade finally achieved was 25,000 pounds per square inch. The large chords necessitated by structural considerations required the use of relatively low values of design lift coefficient for the blade sections because of the limited power available in the dynamometer. For the values of lift coefficient used, the lift-drag ratios for the sections were relatively low and were far from the optimum values that could have been used had the power available been sufficient.

The stresses in the upper and lower surfaces of the swept blade sections were eliminated by the method described in reference 8. This method resulted in the blades having a small amount of dihedral. The introduction of dihedral into the structure tended to change the sweep angles slightly, but by adjusting the initial values of sweep angle it was possible to maintain the design values of sweep after the correct amount of dihedral was applied.

Straight blades.- The straight blades were designated NACA 10-(1.7)(062)-051 design and NACA 10-(1.5)(062)-057 design and in the figures of the present paper are noted as propellers II and III, respectively. From elementary sweepback theory for wings it was determined that the lift coefficients of the sections on the swept blades would be directly proportional to the cosine of the sweep angle. It was necessary therefore, in order to maintain the same loading on the swept blades and the straight blades, to adjust the values of the section lift coefficients

or the section chord lengths of the sections on the straight blades. In the case of the NACA 10-(1.7)(062)-051 blades the section design lift coefficients were the same as those for the swept blade but the chords were reduced from the values for the swept blades by the cosine law, while in the case of the NACA 10-(1.5)(062)-057 blades the section chords were the same as for the sweptback blades and the section design lift coefficients were reduced by the cosine law. In this way the design loading for the three propellers was the same.

TESTS AND REDUCTION OF DATA

Scope of tests.- Thrust, torque, rotational speed, and wake pressure measurements were made for each of the three propellers at blade angles of 20°, 25°, 30°, 35°, 40°, 45°, 50°, 55°, and 60° at the 0.70R (42-inch) station. A constant rotational speed was used for each test and a range of advance ratio was covered by changing the tunnel airspeed, which was varied from about 60 miles per hour to 460 miles per hour.

In order to cover a range of tip Mach number, the tests were run at rotational speeds of 1,140, 1,350, 1,600, 1,680, 1,800, 1,900, 2,000, and 2,100 revolutions per minute. Because of the limited torque available, however, high rotational speeds were not run at high blade angles and for this reason high tip speeds were obtained by operating the tunnel at constant high values of airspeed and variable dynamometer rotational speeds.

The values of tip Mach number obtained in the tests covered a range from 0.55 to 1.15. Table I shows the propeller operational range covered together with the numbers of the figures in which the test data are presented.

Tares and aerodynamic data.- The spinner tare forces and the propeller aerodynamic forces were determined as described in reference 7. The shape of the sweptback blades caused the diameter of the sweptback propeller to change when the blades were turned in the propeller hub. The propeller diameter was 10 feet at the design blade angle of 45° and increased as the blade angle was reduced, or decreased as the blade angle was increased, from the design angle. The diameter of the sweptback propeller is recorded in table I for each blade angle tested and is the diameter used in the computation of the propeller aerodynamic coefficients for the sweptback propeller.

Wake pressure measurements were made during the tests to determine the thrust loading on the blades. The survey rake was placed 16.5 inches behind the center line of the propeller hub at an angle of 105° from a vertical center line measured in a counterclockwise direction when looking downstream in the tunnel, as shown in figure 1. The relatively large

distance of the rake downstream from the propeller-hub center line was necessary in order for the sweptback-propeller tip to clear the rake tubes at the higher blade angles. The rake consisted of 19 total-pressure tubes located inside the slipstream. No attempt was made to obtain torque data by slipstream measurements.

Wind-tunnel interference.- All data presented have been corrected to equivalent free-air conditions by the application of the Glauert tunnel-wall correction (reference 9). The correction amounted to a change in the tunnel indicated velocity of 2 percent at low tunnel speeds and was negligible at high speeds.

RESULTS AND DISCUSSION

The aerodynamic data obtained during the tests are presented in figures 4 to 36 as faired curves of thrust coefficient, power coefficient, propeller efficiency, air-stream Mach number, and helical tip Mach number plotted against propeller advance ratio. Discontinuities in the Mach number curves are caused by changes in the tunnel temperature which occurred from day to day.

Envelope efficiency.- A comparison of the envelope efficiency for the three propellers is presented in figure 37 for each test rotational speed. In general, the three propeller curves have a high level of efficiency and show a difference between the three propellers of less than about $2\frac{1}{2}$ percent over most of the range. The swept propeller has a lower level of efficiency at the lower values of rotational speed than the straight blades and a higher level of efficiency at the higher rotational speeds. Of the two straight propellers, the wider blade propeller with the lower values of section design lift coefficient was generally less efficient at all rotational speeds than the narrower straight propeller.

As structural considerations required a large blade width for the swept propeller, relatively low values of section design lift coefficient were required because of the limited power and rotational speed of the dynamometer. As a result of this consideration, the section lift-drag ratios and consequently the efficiencies were lower than the maximum attainable. The efficiency of the straight propellers was also lowered by this consideration as these propellers were closely related to the swept propeller for the purpose of comparison of performance.

Effect of compressibility on maximum efficiency.- By plotting the envelope curves of figure 37 against the propeller helical tip Mach number another envelope can be drawn over the original envelope curves as shown

in figure 38 for the three subject propellers. Plots of this kind afford a comparison of the maximum efficiency obtainable with the respective propellers over a speed range. A comparison of the envelope is made in figure 39.

Figure 39 shows that at subcritical values of Mach number the swept propeller is slightly less efficient than either of the straight propellers. The higher-cambered, narrow, straight propeller is the most efficient in the low speed range with the swept propeller about 1 percent less efficient and the lower-camber, straight propeller about 1/2 percent less efficient at a helical tip Mach number of about 0.75. At a helical tip Mach number of 0.95 the three propellers attained the same values of efficiency.

At helical tip Mach numbers just above 0.95 the swept propeller sustained a gradual loss in its subcritical level of efficiency while the straight propellers suffered appreciably greater losses. At a helical tip Mach number of 1.10, however, the slopes of the three efficiency curves are about the same, the swept propeller being about $2\frac{1}{2}$ percent more efficient than the straight propellers. The two straight propellers have about the same value of efficiency at helical tip Mach numbers above 0.95. It thus appears that sweepback offers some delay in the adverse effects of compressibility.

Results of tests of an NACA 10-(3)(062)-045A propeller (reference 10) are also shown in figure 39. The NACA 10-(3)(062)-045A propeller had the same thickness-chord ratio as the three propellers of the present program at the design radius but was narrower, which allowed the use of a design lift coefficient of 0.30. As a design lift coefficient of 0.30 is closer to the optimum for maximum lift-drag ratio for 16-series sections, higher efficiencies than that of the three related propellers were obtained at low tip speeds as shown by figure 39. This propeller is just as efficient as the swept propeller in the range of tip Mach number beyond 0.95.

It seems clear, however, that a swept propeller could be made to have greater efficiency than the NACA 10-(3)(062)-045A propeller at tip Mach numbers above 0.95 at about equal power if the diameter were reduced to permit use of more nearly ideal blade-section cambers. Such a procedure could not be used for these tests, however, because of the limitation in rotational speed of the dynamometer. It thus appears that careful attention should be given to the specified design operating conditions if any advantage is to be gained by using a swept propeller in lieu of a straight propeller.

A clear indication of the delay in compressibility loss due to sweepback is given by plots of maximum efficiency against tip Mach number for given values of blade-angle setting as shown in figure 40. It is evident that the largest delay was obtained when the blades were set at the design value of 45°, the amount of delay in the onset of compressibility losses

diminishing as the blade angle was increased or decreased from the design value.

For the design blade angle (45°) the tip Mach number for the efficiency break for the swept propeller was about 6 percent higher than the value for the straight propeller. This increase is only about 30 percent of that predicted by the simple sweep theory and is of the order of magnitude of results of propeller tests reported in reference 5. Discrepancies between the simple theory and experimental results have also been observed in the case of wings, although not of such large magnitude. Some of the lack of agreement between the theory and experiment in the propeller tests is probably due to the radial flow of the boundary layer, a radial Mach number gradient, and the effects of the propeller-tip relief. All these factors affect the blade section aerodynamic characteristics and are not accounted for in the simple theory.

Effect of sweep on power coefficient.- The curves of figures 39 and 40 illustrate the effects of sweep on maximum efficiency only and do not meet the design conditions of equal power absorption of the three propellers. The differences in power of the three propellers are shown in figures 41 and 42. Figure 41 shows the variation of power coefficient with helical tip Mach number for the three propellers when operating at the design values of blade-angle setting and advance ratio. It is shown in figure 41 that the swept propeller absorbs considerably less power than do the straight propellers. Part of this occurrence is probably caused by the tendency of the swept blades to turn into the plane of rotation due to centrifugal forces acting on the swept sections and thus causing the swept blades to operate at lower blade angles. Though most of the moments occurring in the swept blades have been eliminated for the design condition of operation in the design of the blades, the moment about the pitch-change axis cannot be reduced below a minimum value which is fairly great in comparison with the moment about the pitch-change axis of an unswept propeller (reference 8). Evidence of the large magnitude of this torsional moment was observed during the testing of the blades when special precautions[1] were required to keep the swept blades from turning in the propeller hub to a lower value of blade angle than that set for the test.

The data of figures 4 to 36 indicate that a shift in the value of advance ratio for zero thrust occurs due to sweep. Figure 43 shows that, as the blade angle is increased, that is, as the swept portions of the propeller blades are turned farther from the plane of rotation, the differences in the value of advance ratio for zero thrust between the swept blade and the straight blade become greater. Also, at any given

[1]The special precautions consisted of sprinkling carborundum dust between the propeller shanks and the hub barrels before clamping the blades in the hub.

blade angle, the difference becomes greater with increasing rotational speed. These facts indicate that appreciable torsional deflection of the swept blades occurs in a direction so as to reduce the aerodynamic load (power coefficient) of the swept propeller relative to the straight propellers.

All of the differences in power absorption shown in figure 41 may not be due to deflection of the swept blades as indicated in figure 42 where power coefficient at maximum efficiency for the three propellers is plotted against helical tip Mach number for the design blade-angle setting ($\beta_{0.70R} = 45^{\circ}$). Figure 42 shows that when operating at maximum efficiency the swept propeller absorbs less power than the straight propellers.

When operating at the design condition (fig. 41) the swept propeller attained only 50 percent of the design power coefficient due to aerodynamic losses and blade deflections, while the straight blades absorbed close to 100 percent of the design power. Both the small delay in the adverse effects of compressibility and the failure to attain the design value of power coefficient indicate that the simple cosine relation used for predicting the effect of sweep is not completely adequate.

To obtain comparable power-absorption properties with the straight blades, the section design lift coefficients or the diameter of the swept propeller should be increased. An increase of the section design lift coefficient would be the advisable alternative since a higher design lift coefficient would result in better values of section lift-drag ratio.

Constant-power propeller operation.- Because the swept and straight propellers absorbed different amounts of power when operating at the same conditions of advance ratio, blade-angle setting, and rotational speed, the efficiencies of the three propellers are compared for given values of power coefficient in figure 44. From figure 44 it is readily seen that the use of sweep in the present design did not improve the efficiency in the high speed range by any significant amount except at a power coefficient of 0.05 at the highest tip speeds. In most cases the swept propeller is inferior to one of the straight propellers.

Of the two straight propellers, the lower-cambered propeller is the least efficient in the higher range of propeller rotational speeds. In the lower range of rotational speeds the efficiencies of the straight propellers are within 1 percent to 2 percent of one another.

Effect of sweep on propeller-blade loading.- Wake pressure measurements were made simultaneously with the force measurements during the present tests to obtain information on the effect of sweep on the propeller-blade loading. The position of the survey rake during the tests was such that accurate values of absolute thrust were not obtained, but any comparison of loadings along the blades will give accurate differences in the values of elemental thrust.

Comparison of the thrust loadings are presented in figure 45 for several values of propeller-tip Mach number for a given value of propeller power coefficient at the design blade angle. The loading on the inboard sections of the swept propeller is higher than that of the straight propellers through the entire speed range tested. Since the swept propeller absorbs less power at a given value of advance ratio, it is necessary to operate the swept propeller at a lower value of advance ratio to attain a given value of power coefficient at a given blade-angle setting. The lower values of advance ratio and consequently the higher values of section geometric angles of attack on the unswept inboard sections (any sweep of less than 10° can be considered insignificant) cause the inboard sections to produce higher loadings. The higher thrust loadings for the swept propeller in figure 45 are due to the differences in the value of advance ratio for the straight and swept propellers.

At values of tip Mach number above 0.95 the swept propeller maintains its low-speed loading on the outboard sections while the straight propellers suffer compressibility losses on the outboard sections. A glance back at figure 44 shows that at values of rotational speed close to those of figure 45 the efficiency of the swept propeller is very little if any higher than that of the straight propeller when the propellers are compared at equal values of advance ratio and power coefficient. It is therefore evident that sweepback can be utilized to delay the onset of adverse compressibility effects of propeller sections but that careful analysis and design procedure are essential if the over-all propeller performance is not to be impaired.

General remarks.- The results of the present investigation show that the swept propeller offers little aerodynamic advantage over a straight propeller. Furthermore when the design and fabrication complications involved with a swept propeller are considered, any advantage for the swept propeller appears even smaller. Some of the factors to be considered in determining the relative merits of swept propellers and straight propellers include the possibility of increased weight of the swept blades, larger pitch-change mechanism to counteract the larger twisting moments of the blades, the presence of unavoidable high stresses which require high-strength alloys, and the difficulty of manufacture. In addition, for a given propeller installation, the higher stresses encountered in a swept propeller blade will require thicker sections than would be required by an unswept blade design with the result that any advantage achieved by the use of sweep is partly nullified by the requirement of relatively thick blade sections.

In general the results of the present investigation show that a straight-blade propeller with its relative ease of design and manufacture should be carefully considered before being discarded in favor of a swept propeller.

CONCLUSIONS

Tests in the Langley 16-foot high-speed tunnel at forward Mach numbers up to 0.65 of the NACA 10-(1.7)(062)-057-27 swept propeller and two related straight propellers lead to the following conclusions:

1. The value of helical tip Mach number at which the adverse effects of compressibility on propeller efficiency become appreciable for the swept propeller was 6 percent higher than for a related straight propeller; this 6-percent delay was only 30 percent of that predicted by simple sweep theory.

2. When operating at the design condition, the power absorbed by the swept propeller was only 50 percent of the design power coefficient while the straight-blade propeller absorbed close to 100 percent of the power coefficient for which the propeller was designed.

3. At equal values of power coefficient the swept propeller was no more efficient than the straight propellers except at a low value of power coefficient at values of helical tip Mach number above 1.0.

4. Total-pressure surveys in the propeller slipstream indicate that at supercritical section speeds which result in total-pressure losses for the sections of conventional straight-blade propellers, the outboard sections of the swept propeller operate with subcritical effectiveness.

Langley Aeronautical Laboratory
National Advisory Committee for Aeronautics
Langley Field, Va.

REFERENCES

1. Evans, Albert J., and Klunker, E. Bernard: Preliminary Investigation of Two Full-Scale Propellers to Determine the Effect of Swept-Back Blade Tips on Propeller Aerodynamic Characteristics. NACA RM L6J21, 1947.

2. Holford, Fred R., and Kasley, J. H.: Flight Test Comparisons of Propeller with 836-14C2-18R1, 109390, 109494, and 109498 Blades in Level Flight Conditions. Rep. No. C-1795, Curtiss Propeller Div., Curtiss-Wright Corp., March 6, 1947.

3. Gray, W. H.: Wind-Tunnel Tests of a Swept-Blade Propeller and Related Straight Blades Having Thickness Ratios of 5 and 6 Percent. NACA RM L8H19, 1948.

4. Whitcomb, Richard T.: A Discussion of the Design of Highly Swept Propeller Blades. NACA RM L50A23, 1950.

5. Delano, James B., and Harrison, Daniel E.: Investigation of the NACA 4-(4)(06)-057-45A and NACA 4-(4)(06)-057-45B Two-Blade Swept Propellers at Forward Mach Numbers to 0.925. NACA RM L9L05, 1950.

6. Delano, James B., and Harrison, Daniel E.: Investigation of the NACA 4-(4)(06)-04 Two-Blade Propeller at Forward Mach Numbers to 0.925. NACA RM L9I07, 1949.

7. Corson, Blake W., Jr., and Maynard, Julian D.: The NACA 2000-Horsepowe Dynamometer and Tests at High Speed of an NACA 10-(3)(08)-03 Two-Blade Propeller. NACA RM L7L29, 1948.

8. Whitcomb, Richard T.: Method for Stress Analysis of a Swept Propeller. NACA RM L8F11, 1948.

9. Glauert H.: The Elements of Aerofoil and Airscrew Theory. American ed., The Macmillan Co., 1943, pp. 222-226.

10. Maynard, Julian D., and Steinberg, Seymour: The Effect of Blade-Section Thickness Ratios on the Aerodynamic Characteristics of Related Full-Scale Propellers at Mach Numbers up to 0.65. NACA RM L9D29, 1949.

TABLE I

SUMMARY OF TESTS

Figure	Rotational speed (rpm)	Tunnel speed, M	Blade angle at 0.70 radius, $\beta_{0.70R}$ (deg)								
NACA 10-(1.7)(062)-057-27, propeller I											
4	1140	Varied	20	25	30	35	40	45	50	55	60
5	1350	Varied	20	25	30	35	40	45	50	55	
6	1600	Varied	20	25	30	35	40	45			
7	1680	Varied						45			
8	1800	Varied				35	40	45			
9	1900	Varied					40				
10	2000	Varied	20	25	30	35	40				
11	2100	Varied	20		30	35	40				
12	Varied	0.56						45	50		
13	Varied	0.60						45	50		
14	Varied	0.65							50	55	60
Propeller diameter, ft			10.10	10.09	10.07	10.05	10.03	10.00	9.97	9.94	9.91
NACA 10-(1.7)(062)-051, propeller II											
15	1140	Varied	20	25	30	35	40	45	50	55	
16	1350	Varied	20	25	30	35	40	45	50	55	
17	1600	Varied	20	25	30	35	40	45			
18	1680	Varied						45			
19	1800	Varied				35	40	45			
20	1900	Varied					40				
21	2000	Varied	20	25	30	35	40				
22	2100	Varied	20	25	30	35	40				
23	Varied	0.56						45	50		
24	Varied	0.60						45	50		
25	Varied	0.65							50	55	60
Propeller diameter, ft			10.00	10.00	10.00	10.00	10.00	10.00	10.00	10.00	10.00
NACA 10-(1.5)(062)-057, propeller III											
26	1140	Varied	20		30	35	40	45	50	55	60
27	1350	Varied	20	25	30	35	40	45	50	55	
28	1600	Varied	20	25	30	35	40	45			
29	1680	Varied						45			
30	1800	Varied				35	40	45			
31	1900	Varied					40				
32	2000	Varied	20	25	30	35	40				
33	2100	Varied	20	25	30	35	40				
34	Varied	0.56						45	50		
35	Varied	0.60						45	50		
36	Varied	0.65							50	55	60
Propeller diameter, ft			10.00	10.00	10.00	10.00	10.00	10.00	10.00	10.00	10.00

NACA

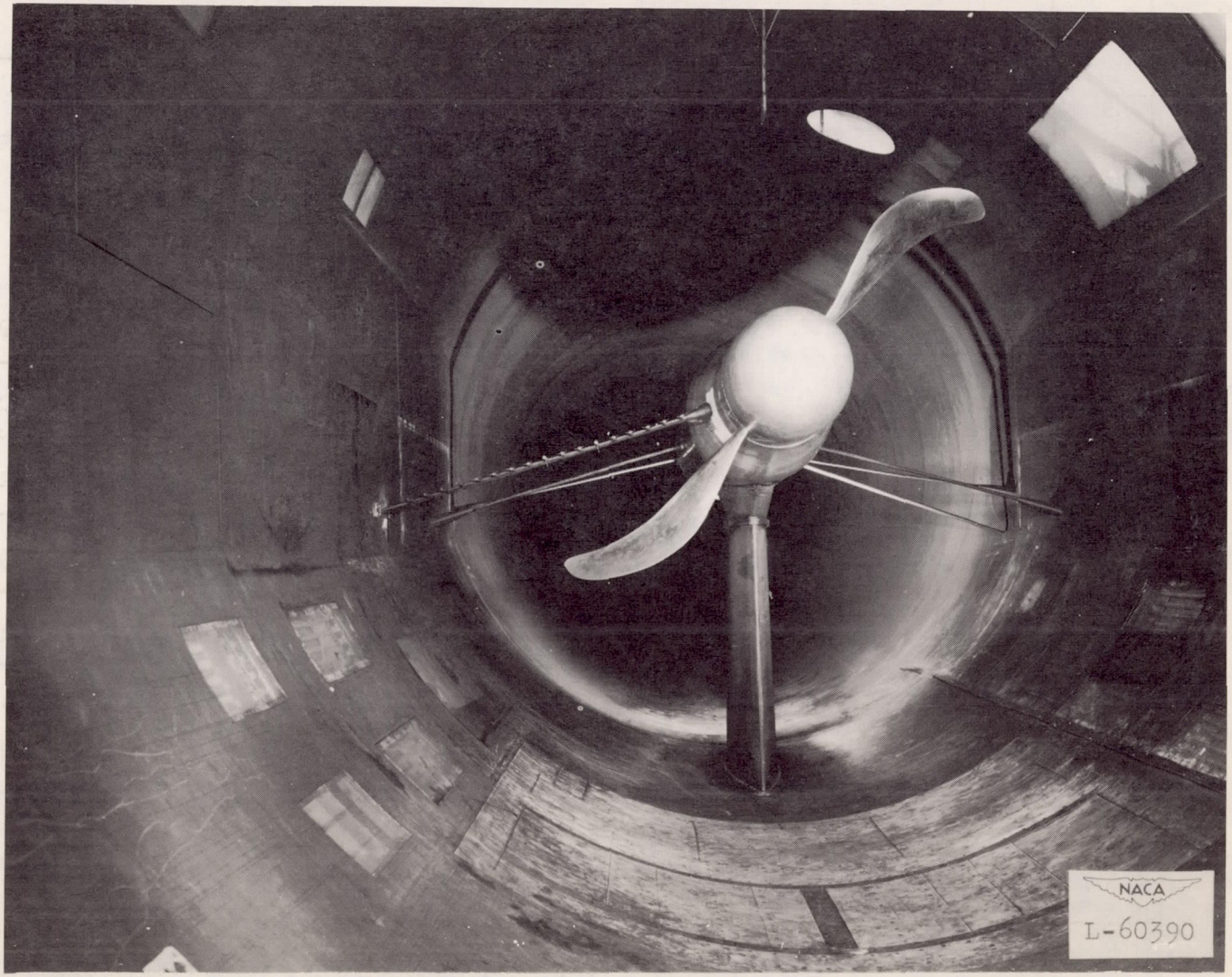

Figure 1.- Swept propeller in Langley 16-foot high-speed tunnel.

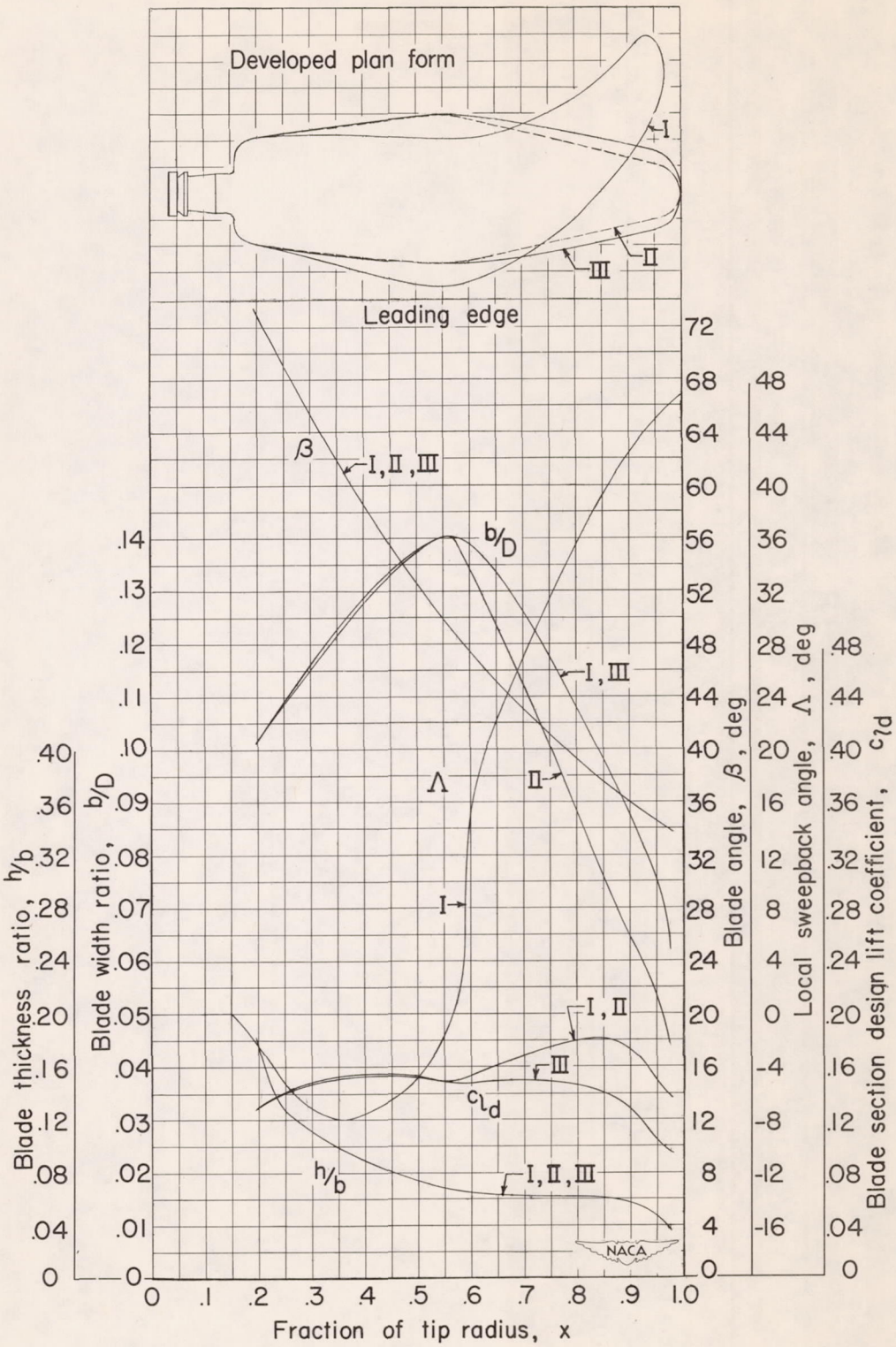

Figure 2.- Blade-form characteristic curves for swept and unswept propeller blades.

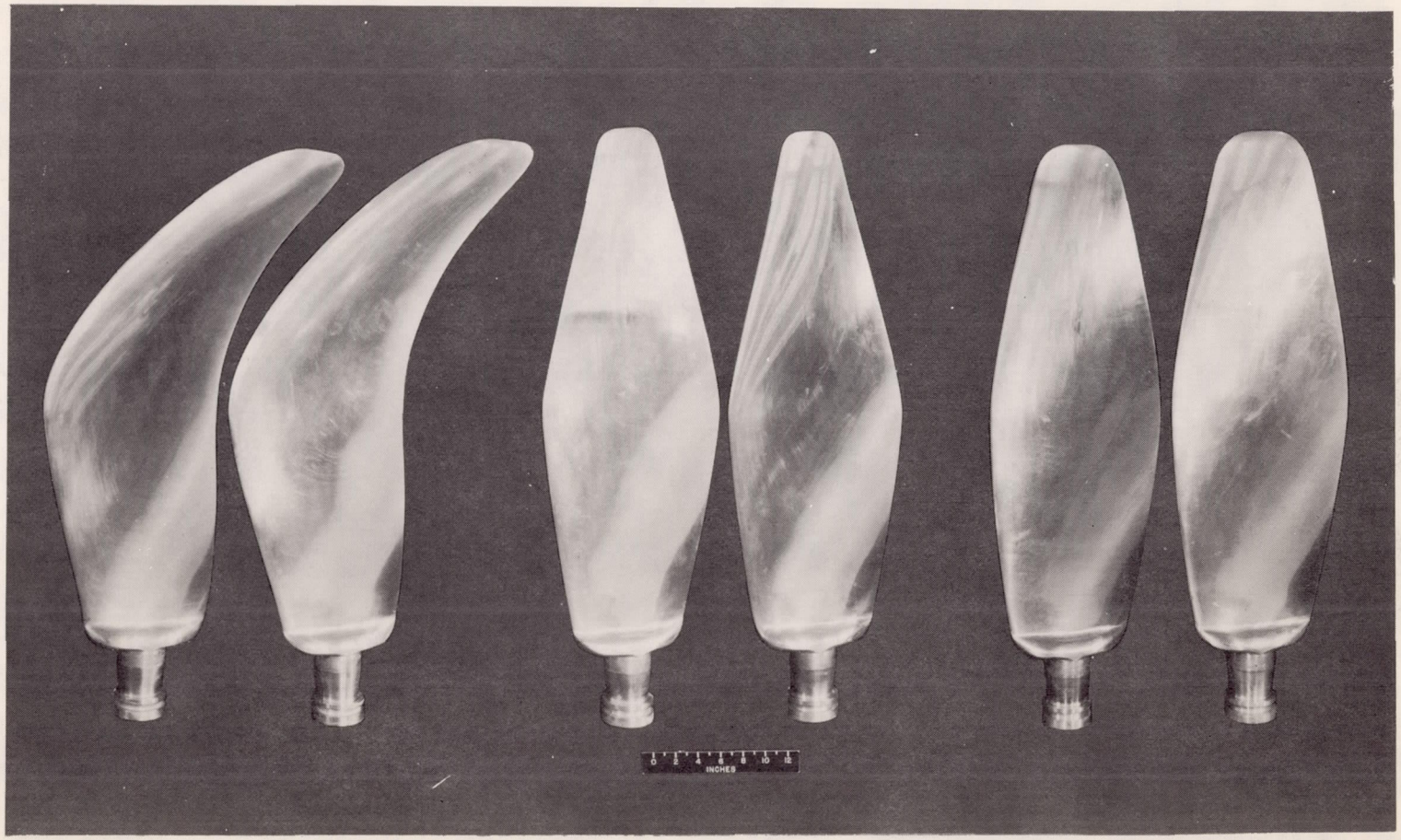

NACA
L-64935

Figure 3.- Propeller blades used in sweep investigation.

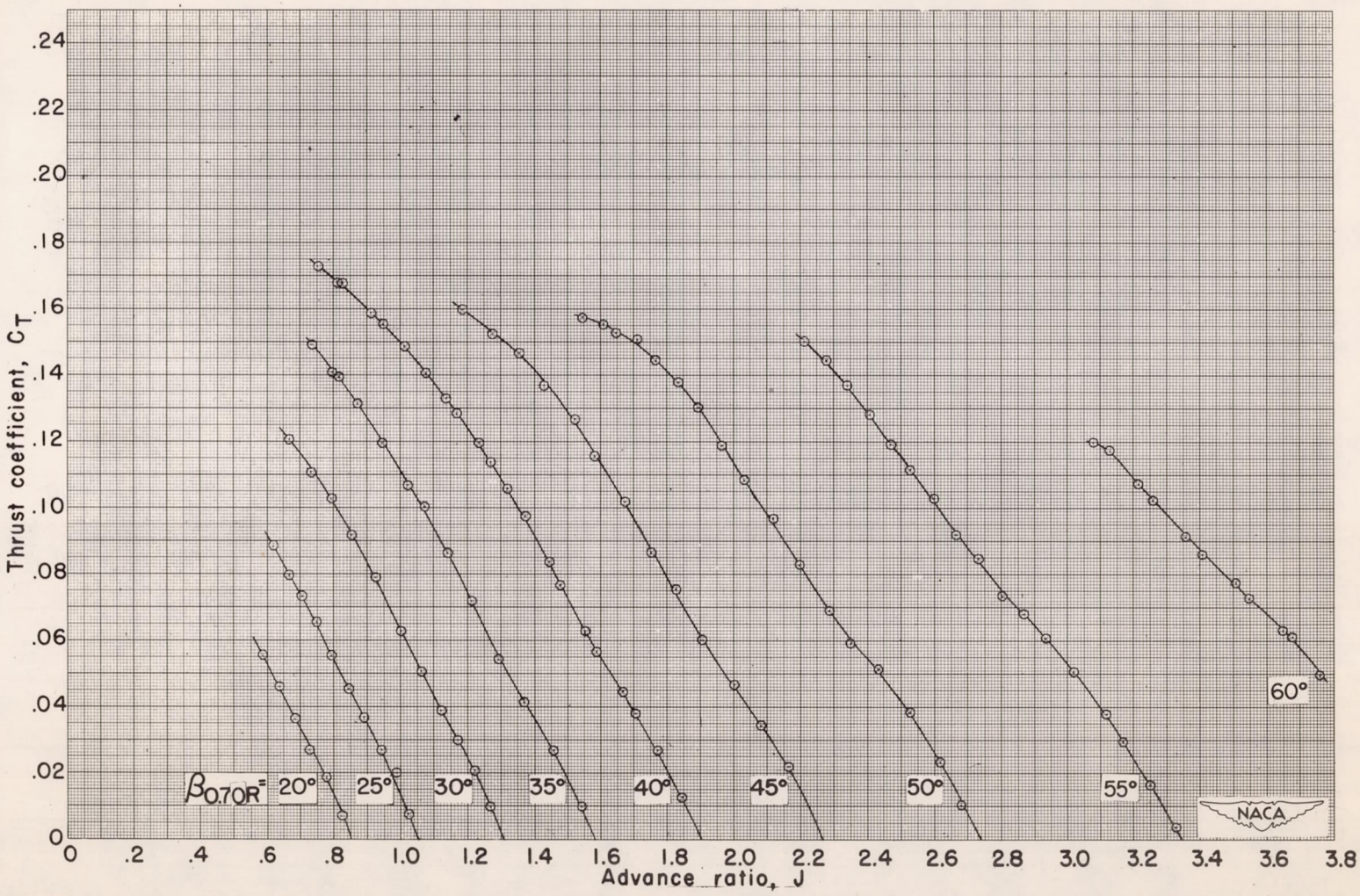

(a) Thrust coefficient.

Figure 4.- Characteristics of NACA 10-(1.7)(062)-057-27 propeller; 1140 rpm.

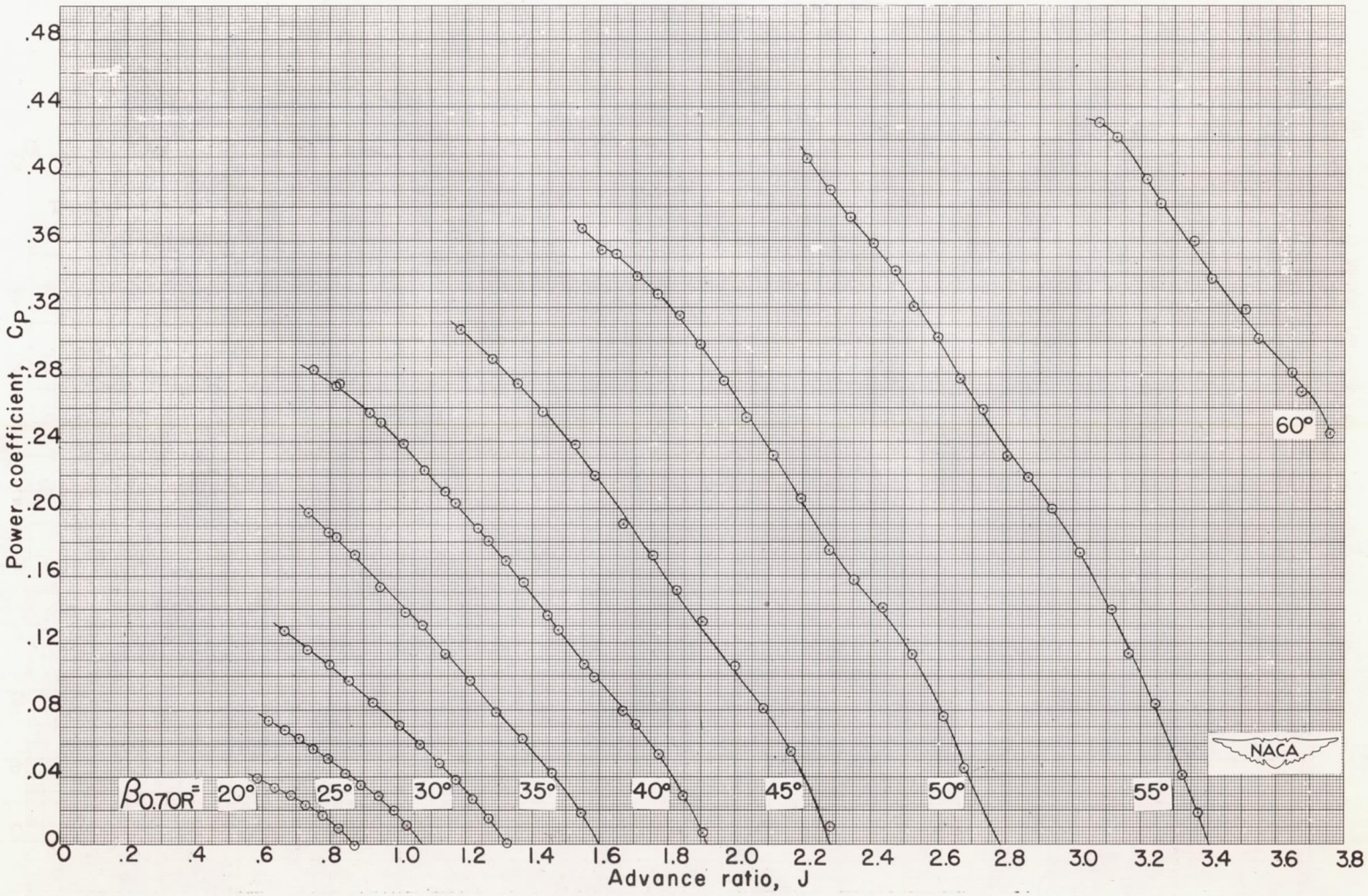

(b) Power coefficient.

Figure 4.- Continued. 1140 rpm.

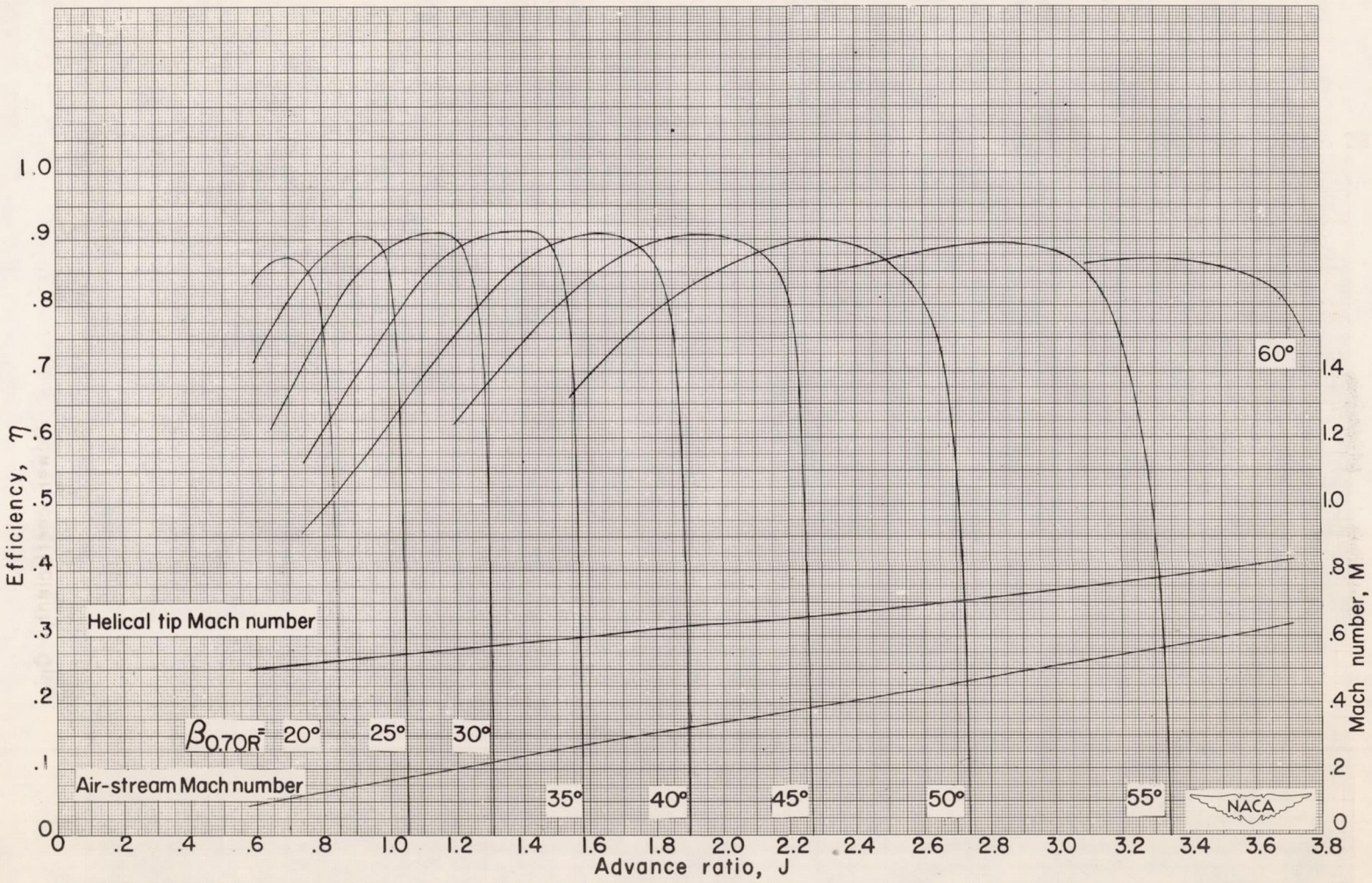

(c) Efficiency.

Figure 4.- Concluded. 1140 rpm.

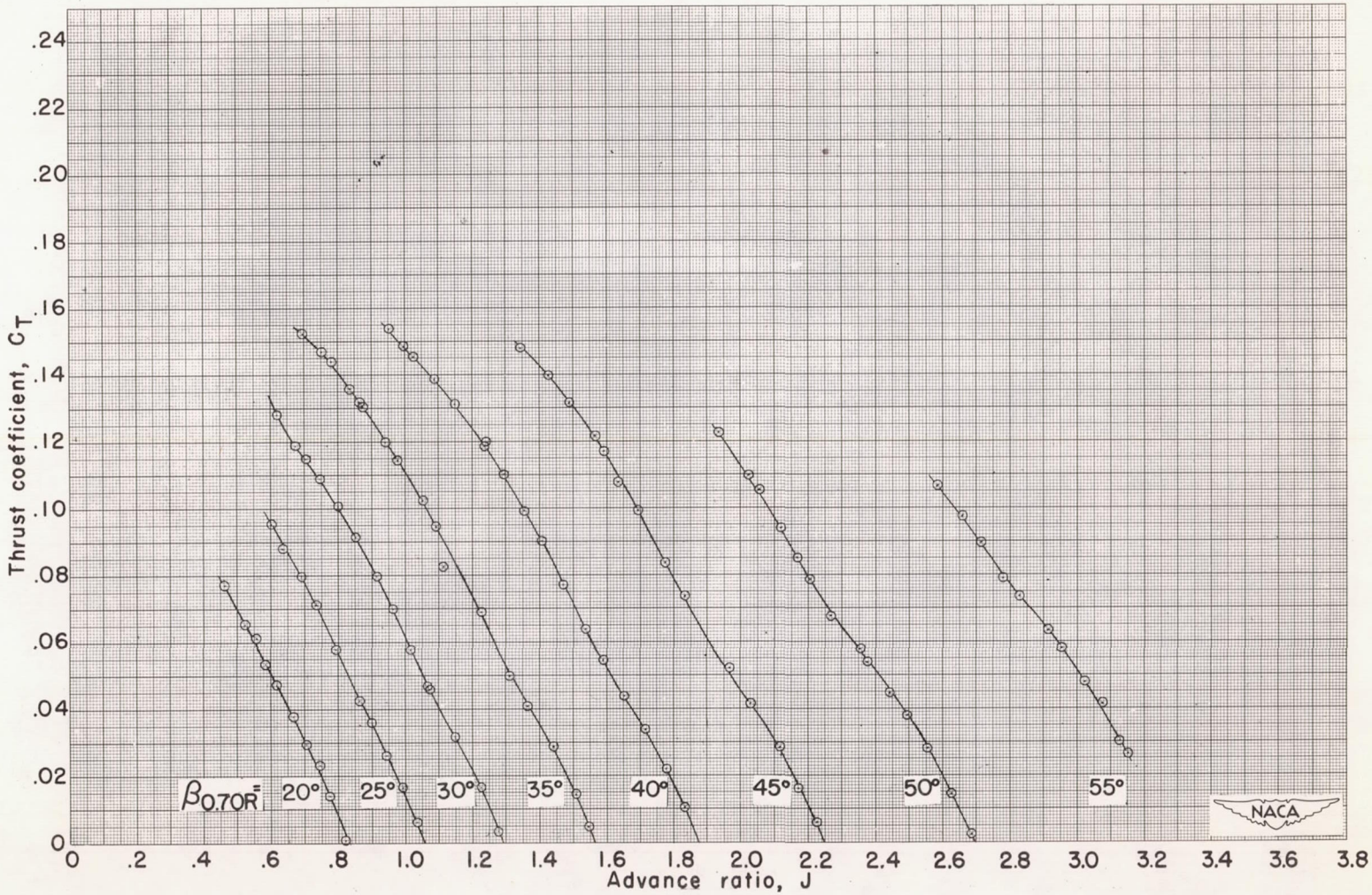

(a) Thrust coefficient.

Figure 5.- Characteristics of NACA 10-(1.7)(062)-057-27 propeller; 1350 rpm.

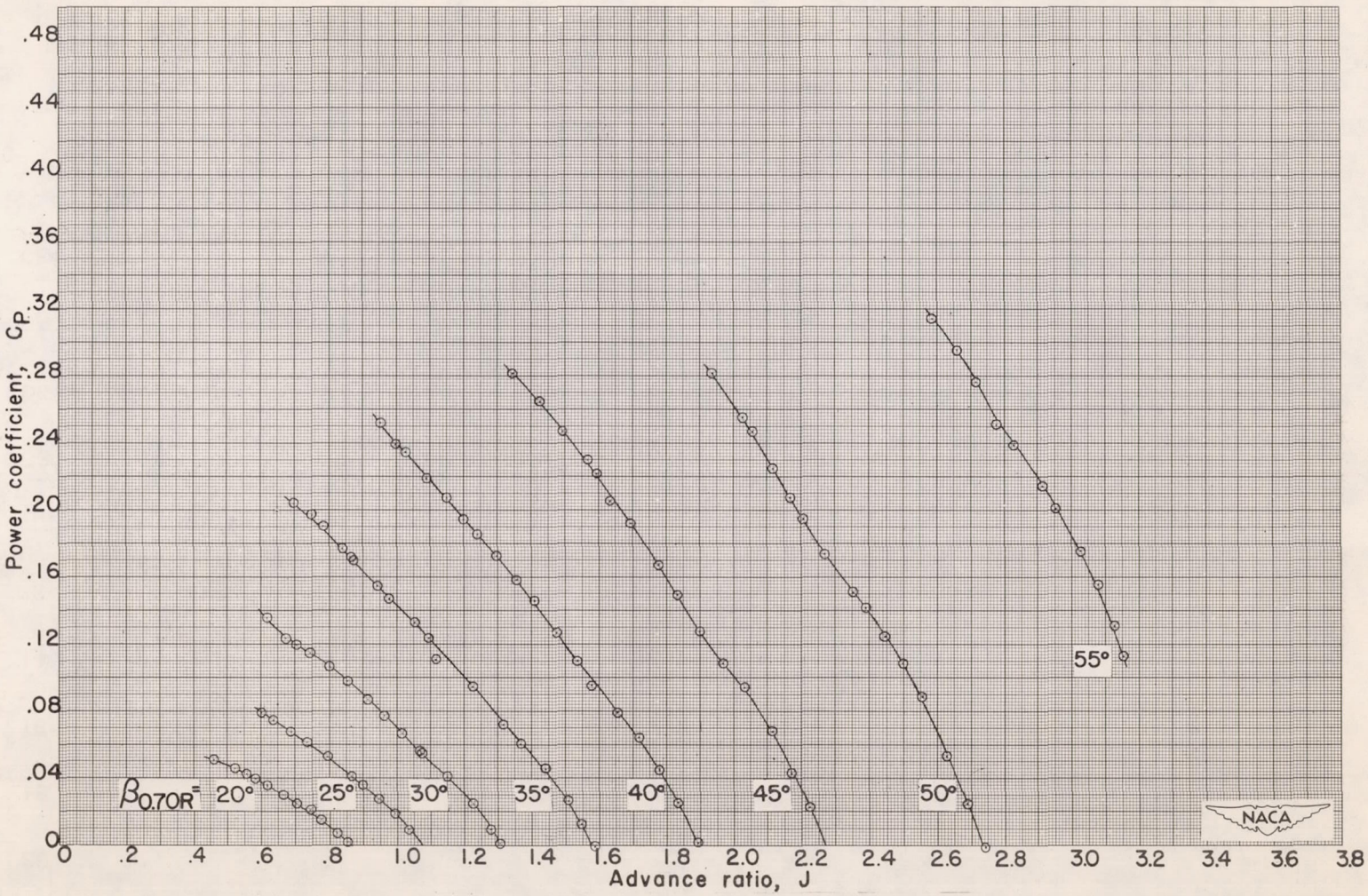

(b) Power coefficient.

Figure 5.- Continued. 1350 rpm.

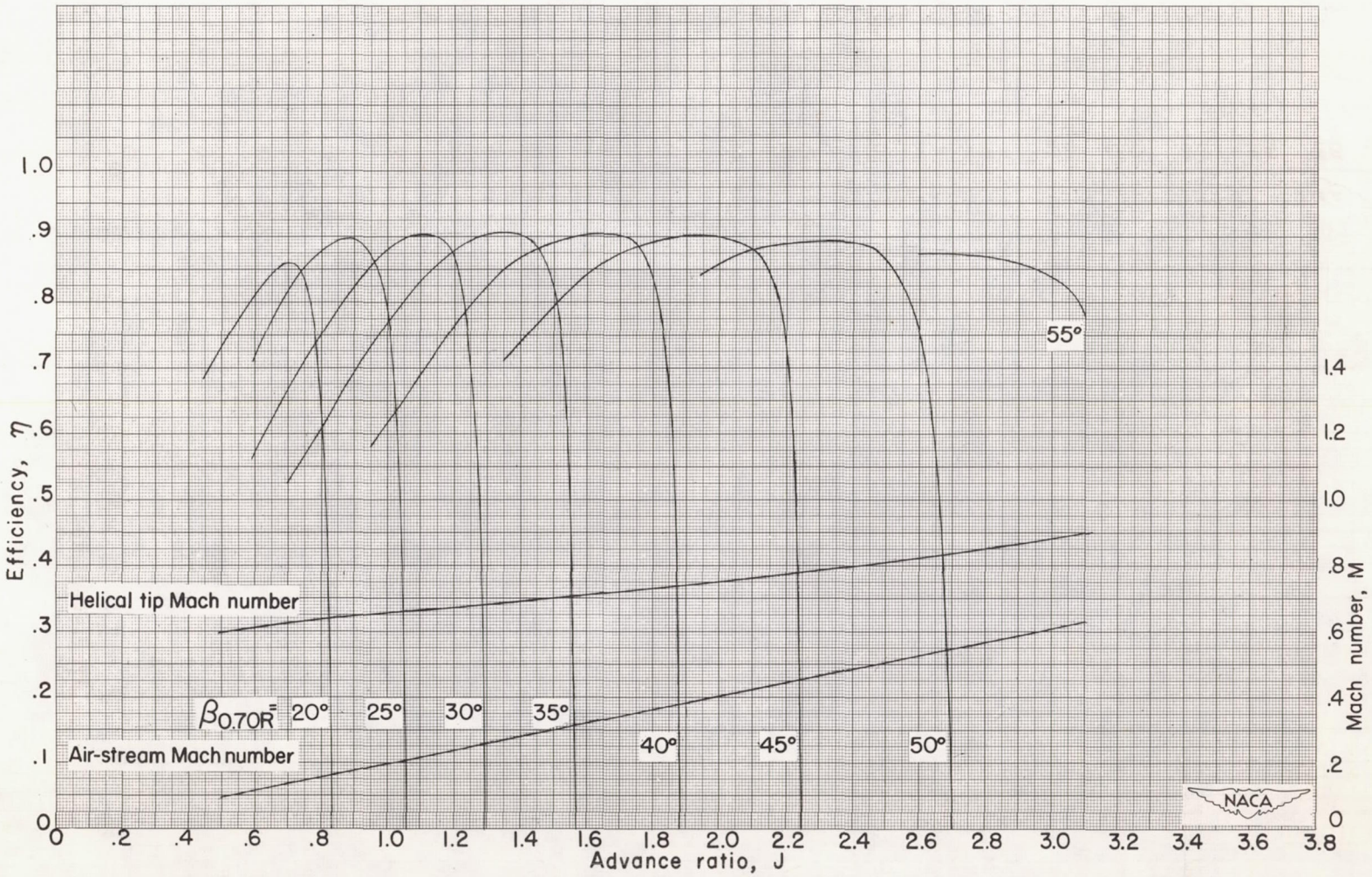

(c) Efficiency.

Figure 5.- Concluded. 1350 rpm.

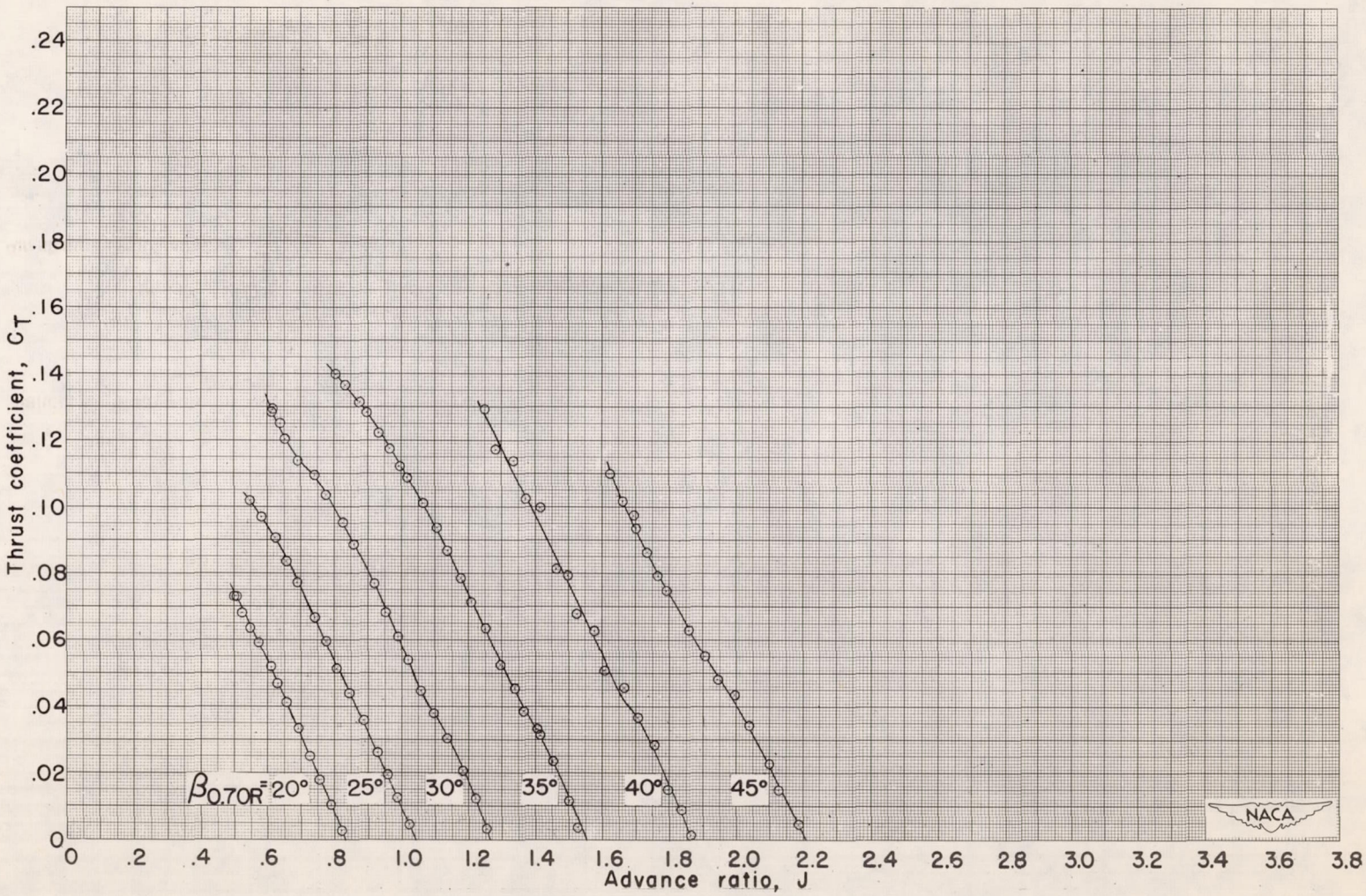

(a) Thrust coefficient.

Figure 6.- Characteristics of NACA 10-(1.7)(062)-057-27 propeller; 1600 rpm.

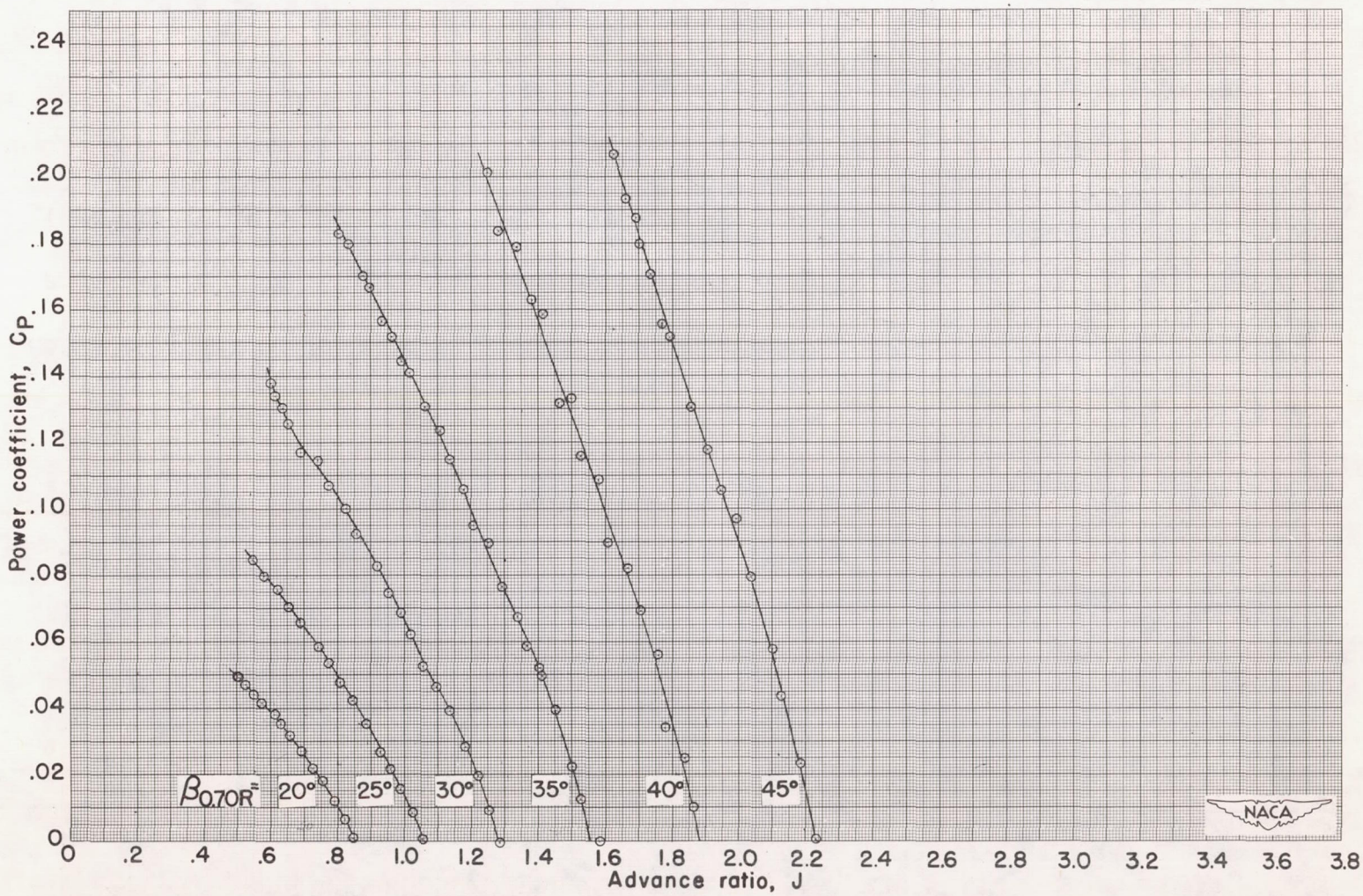

(b) Power coefficient.

Figure 6.- Continued. 1600 rpm.

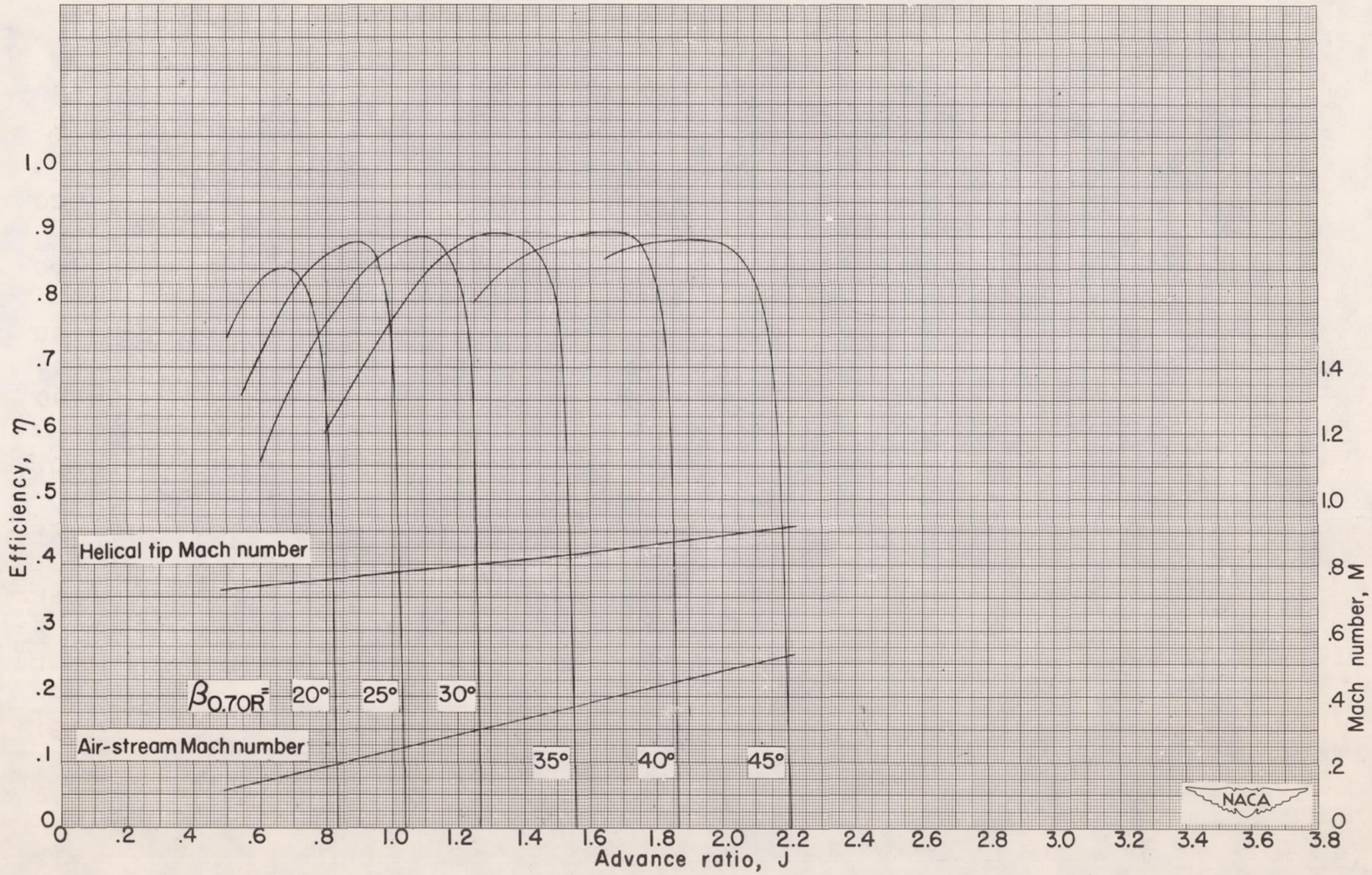

(c) Efficiency.

Figure 6.- Concluded. 1600 rpm.

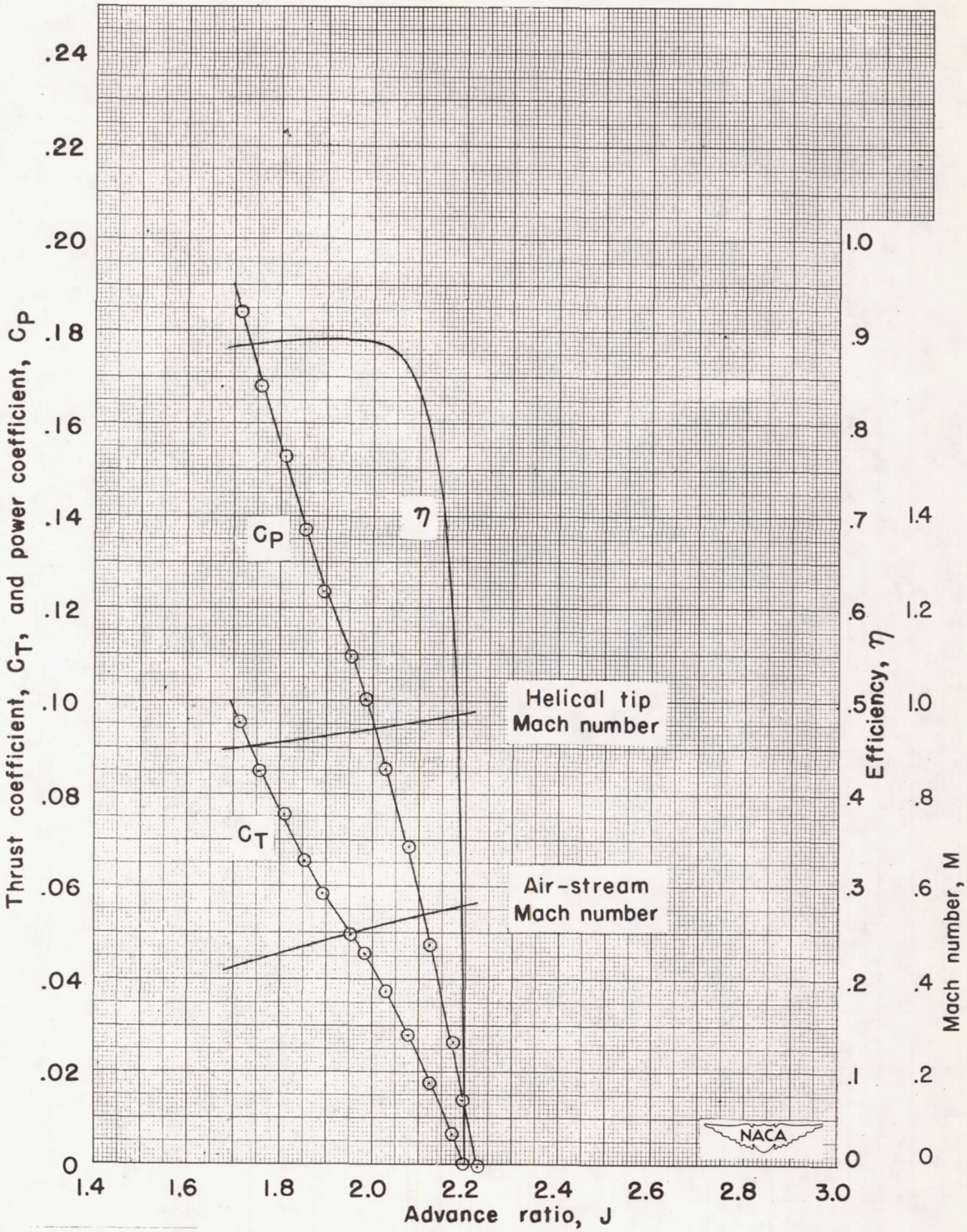

Figure 7.- Characteristics of NACA 10-(1.7)(062)-057-27 propeller; 1680 rpm; $\beta_{0.70R} = 45^{\circ}$.

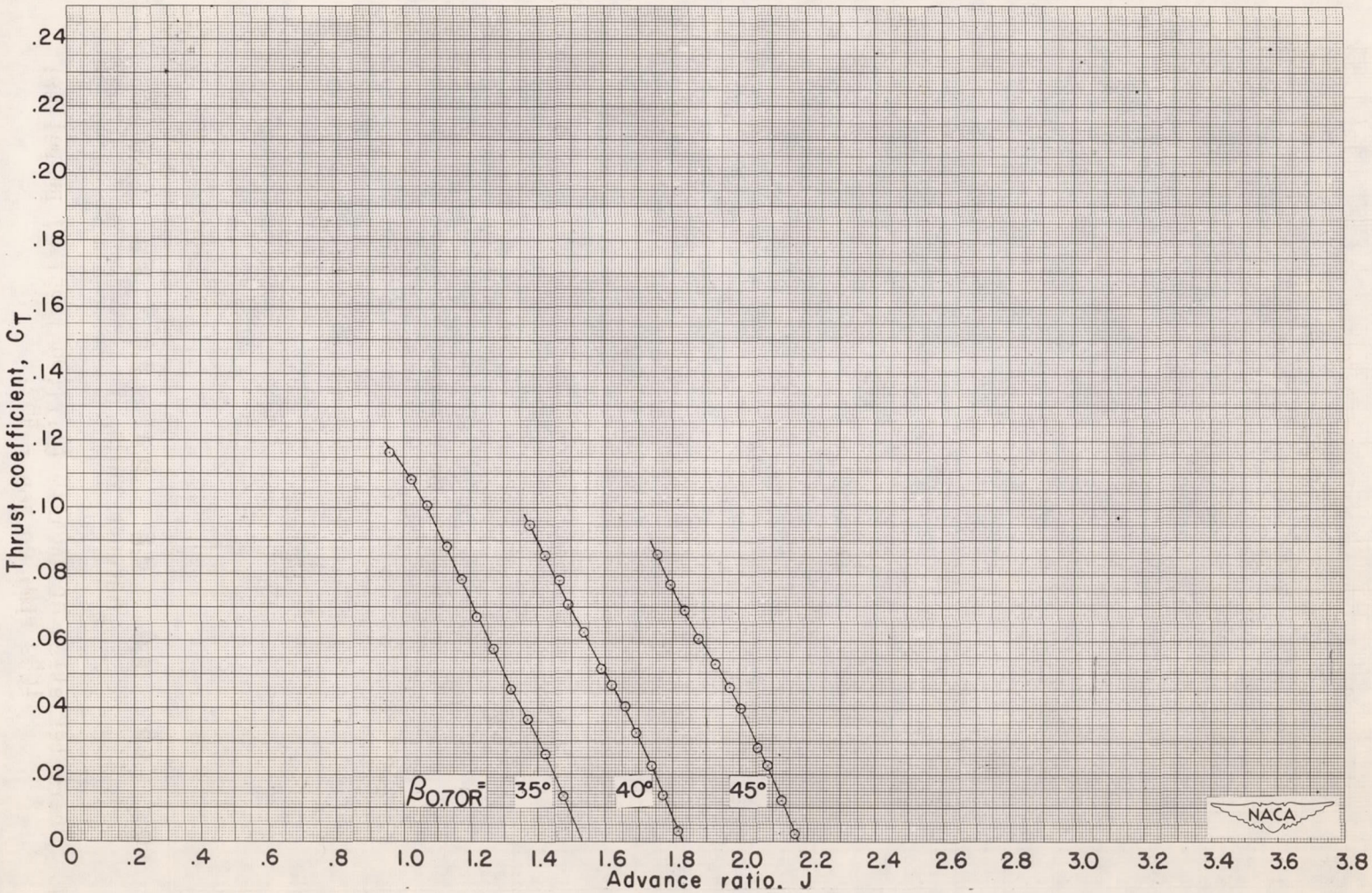

(a) Thrust coefficient.

Figure 8.- Characteristics of NACA 10-(1.7)(062)-057-27 propeller; 1800 rpm.

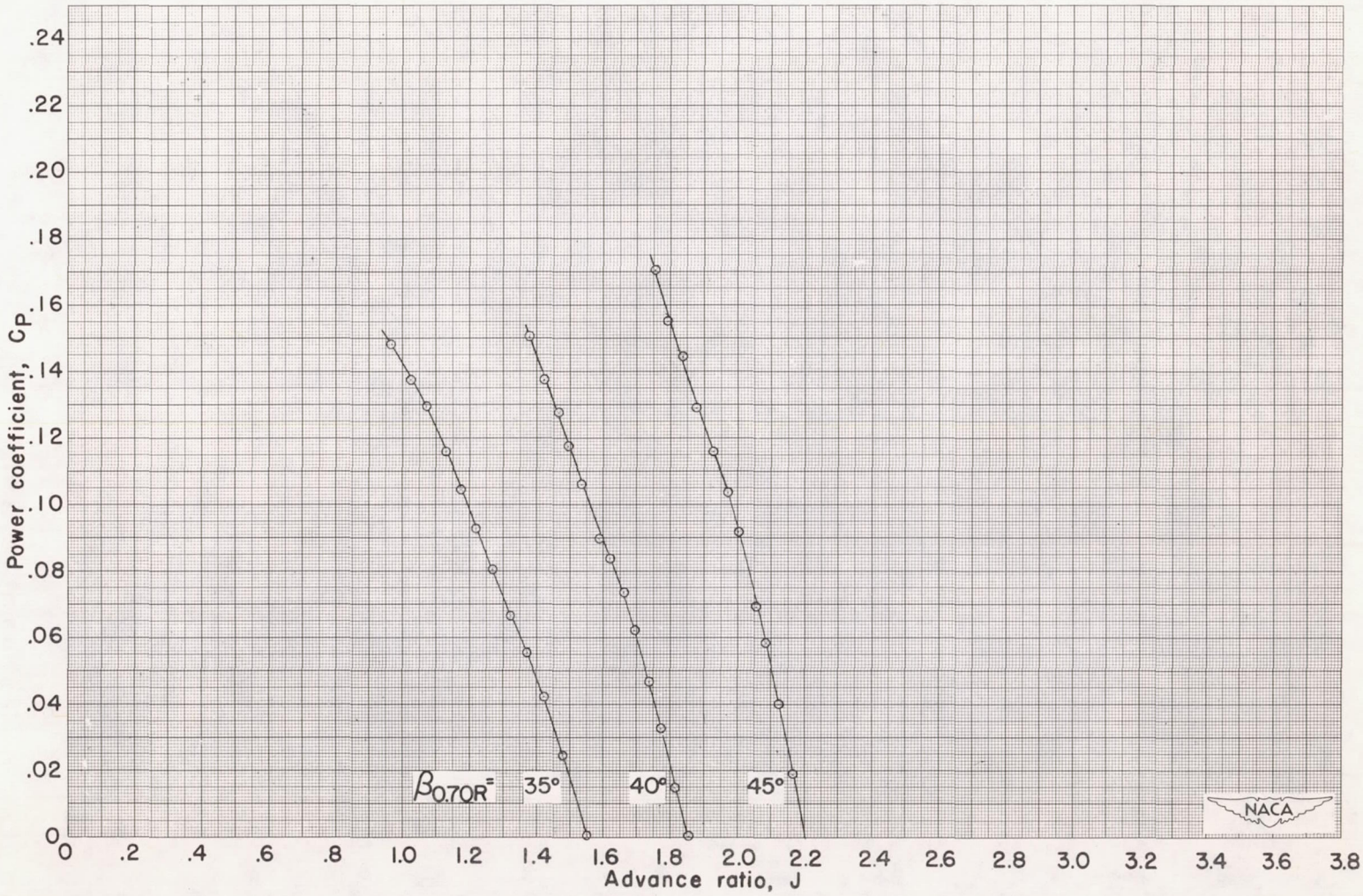

(b) Power coefficient.

Figure 8.- Continued. 1800 rpm.

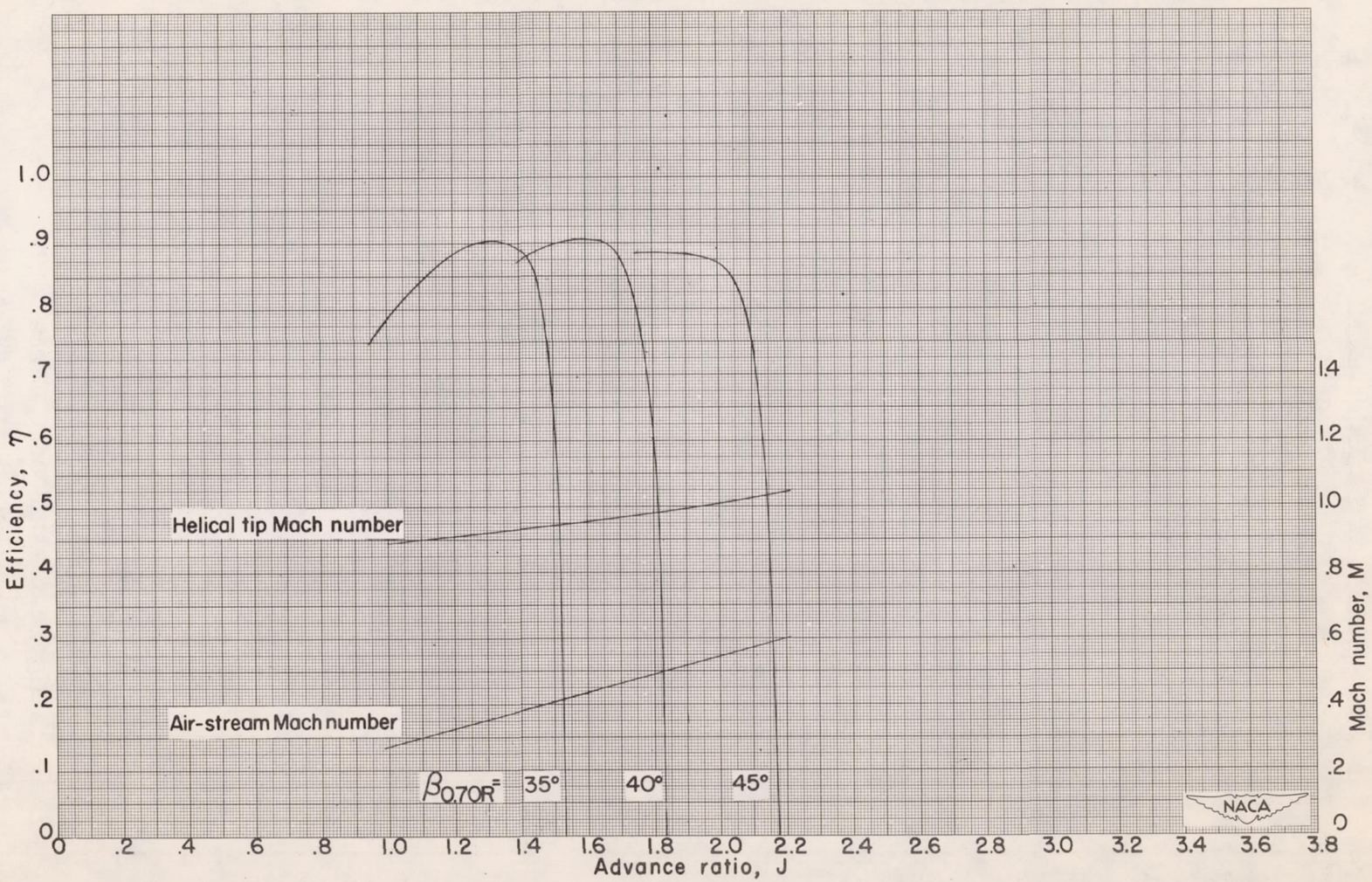

(c) Efficiency.

Figure 8.- Concluded. 1800 rpm.

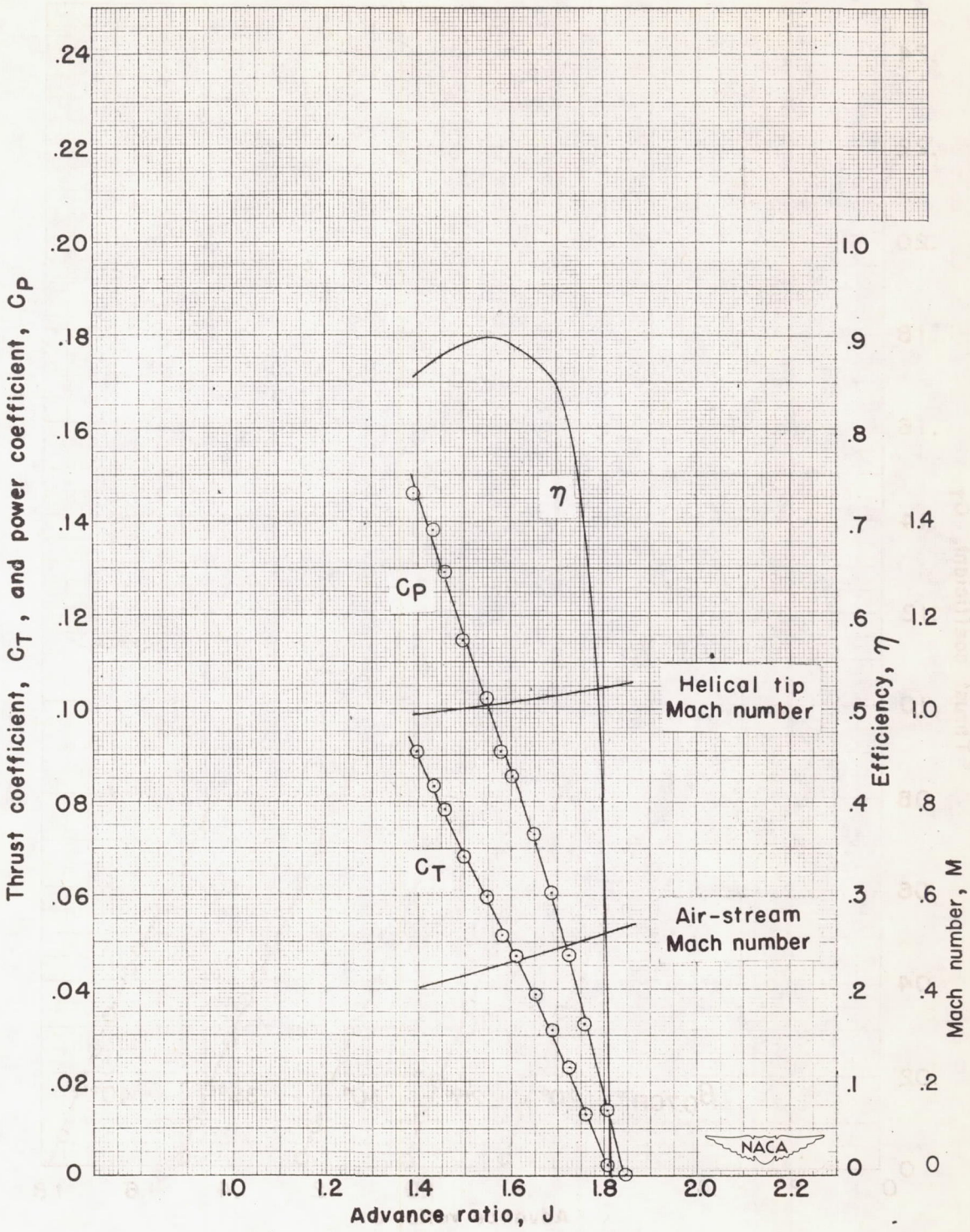

Figure 9.- Characteristics of NACA 10-(1.7)(062)-057-27 propeller; 1900 rpm; $\beta_{0.70R} = 40^{\circ}$.

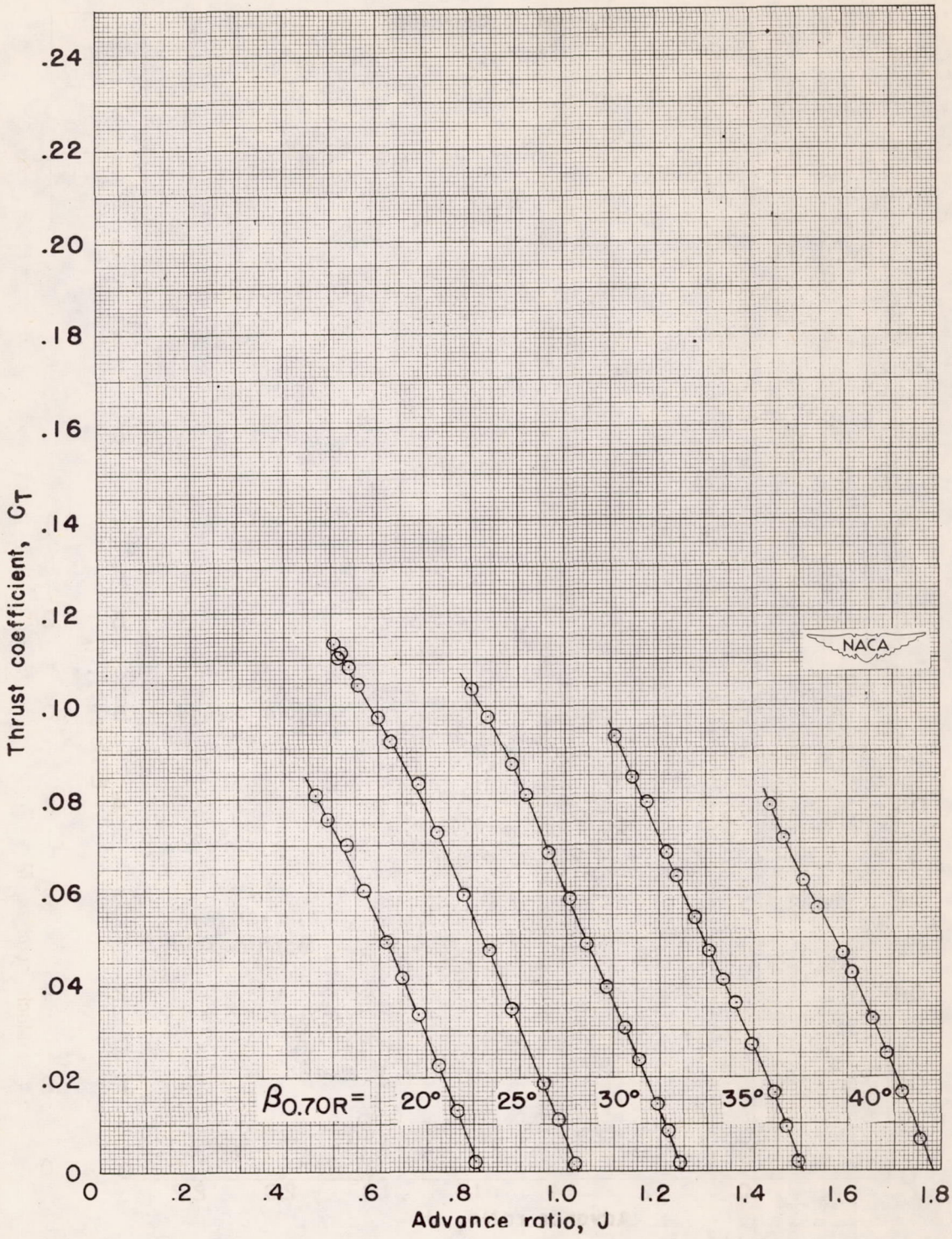

(a) Thrust coefficient.

Figure 10.- Characteristics of NACA 10-(1.7)(062)-057-27 propeller; 2000 rpm.

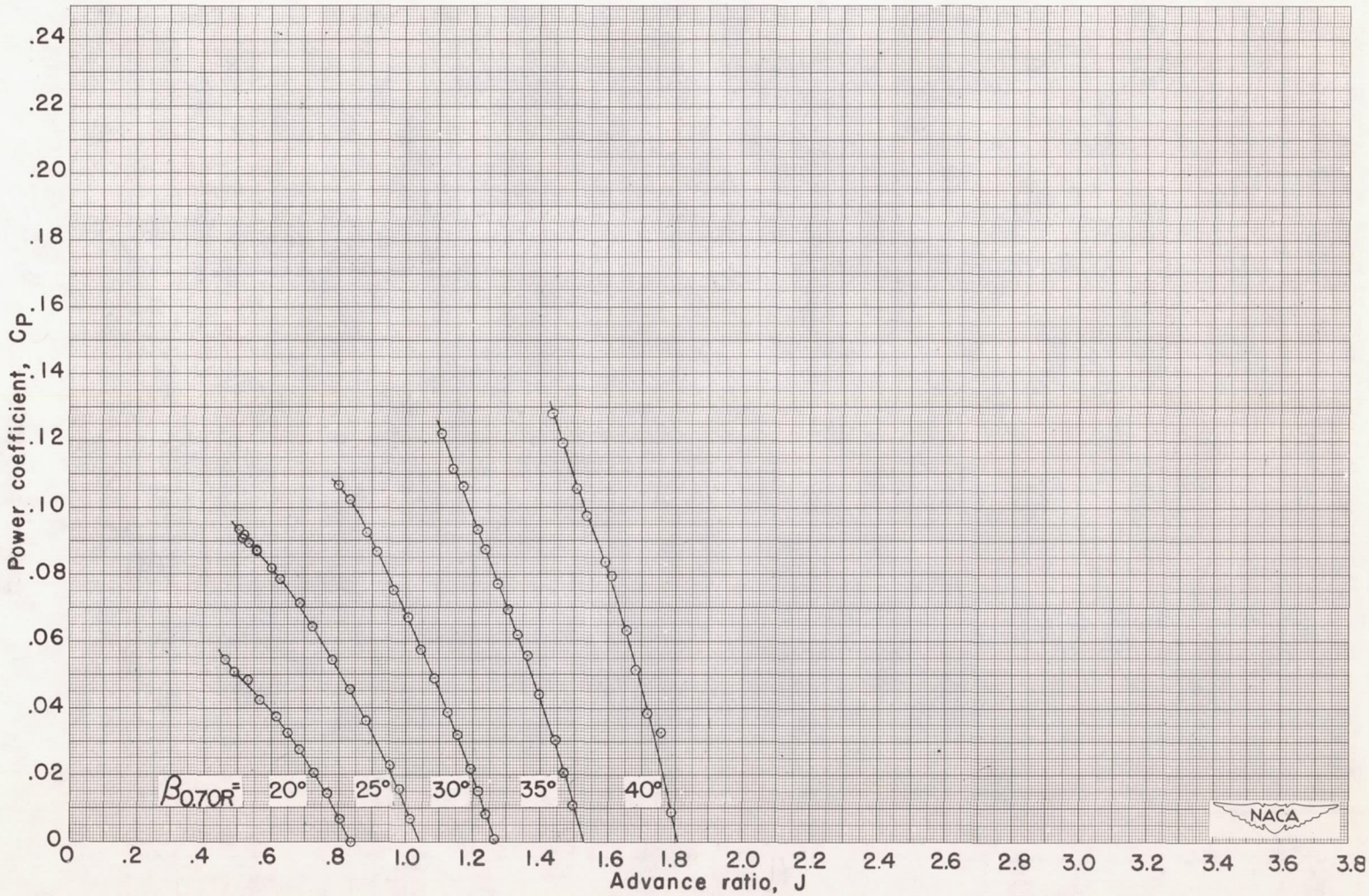

(b) Power coefficient.

Figure 10.- Continued. 2000 rpm.

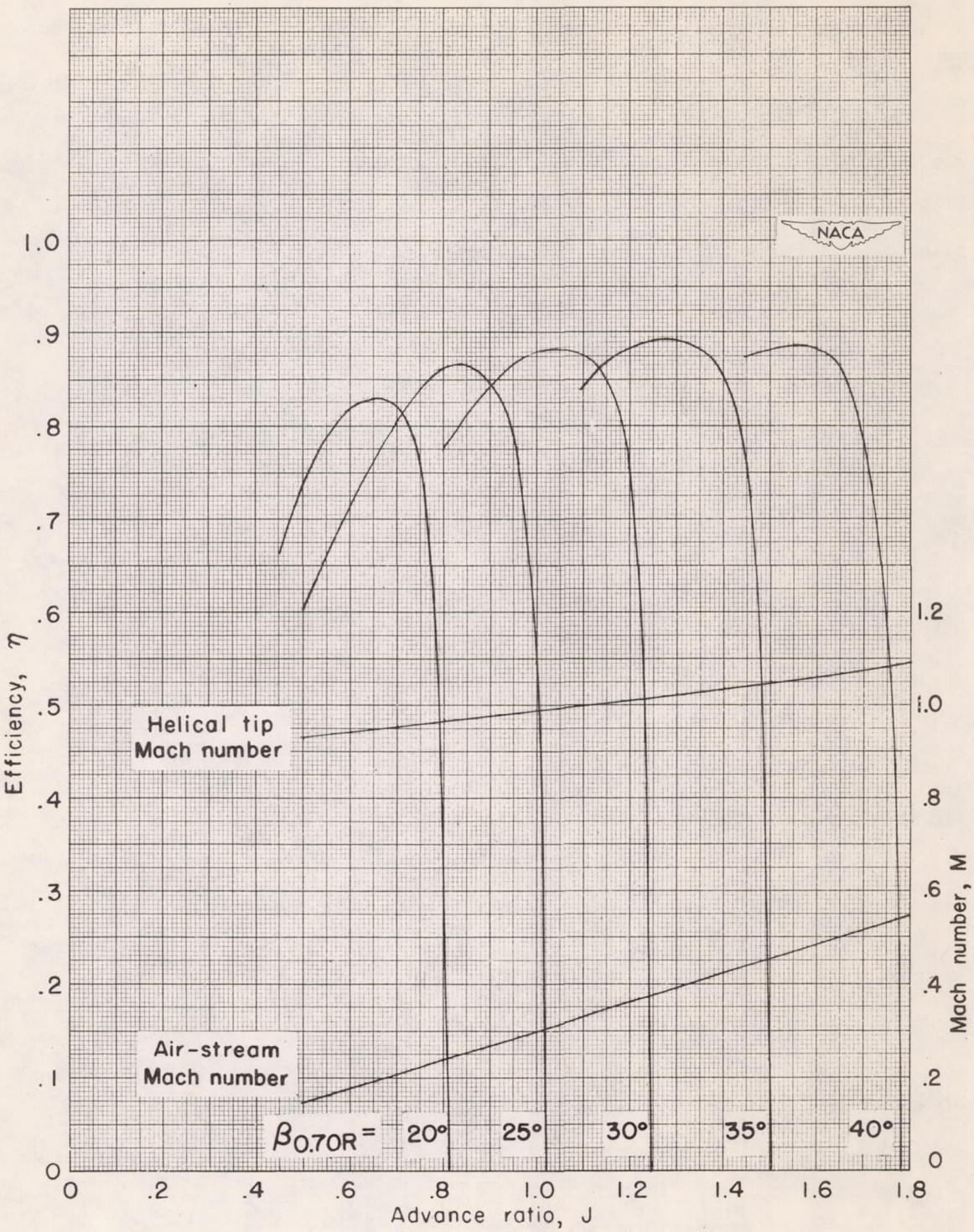

(c) Efficiency.

Figure 10.- Concluded. 2000 rpm.

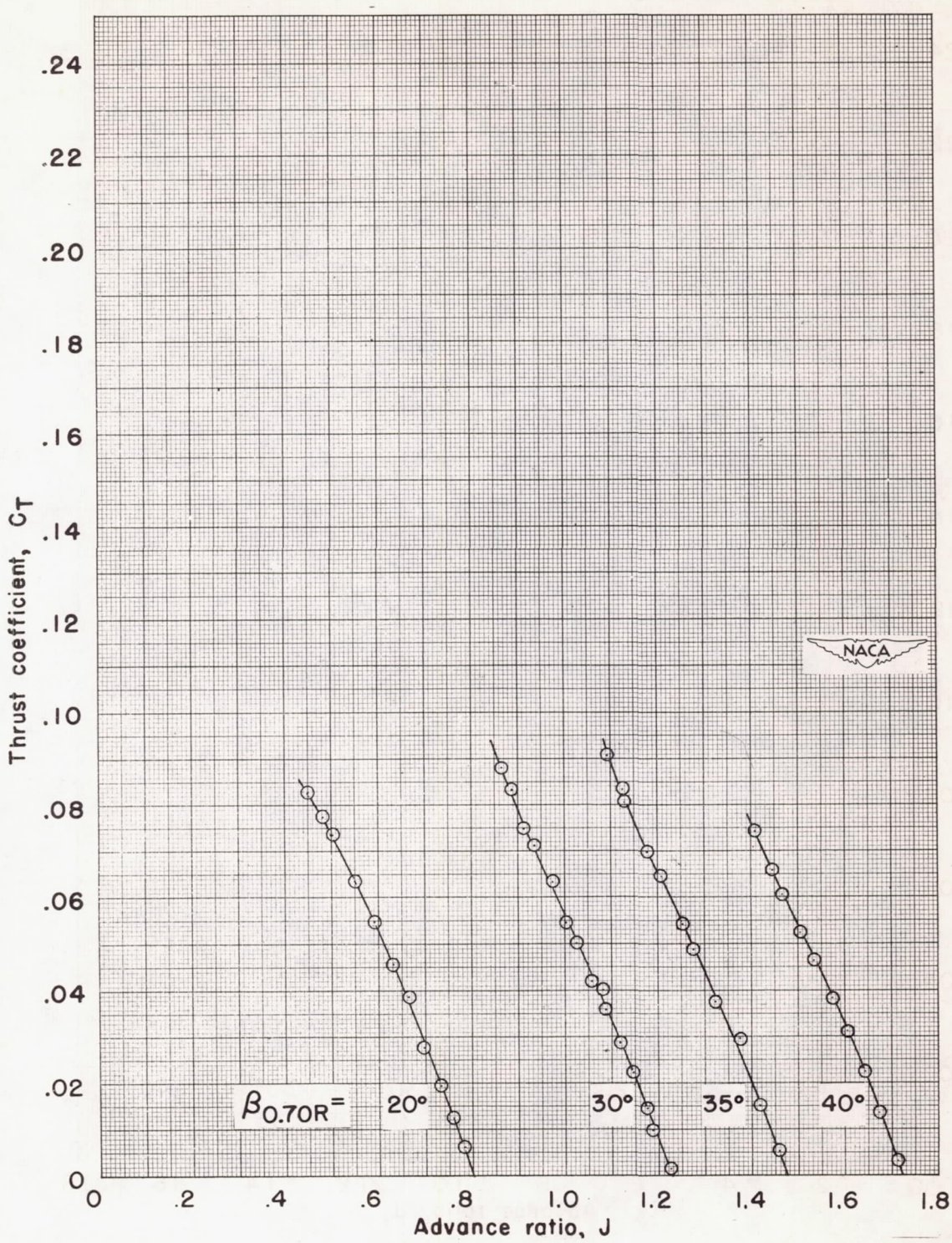

(a) Thrust coefficient.

Figure 11.- Characteristics of NACA 10-(1.7)(062)-057-27 propeller; 2100 rpm.

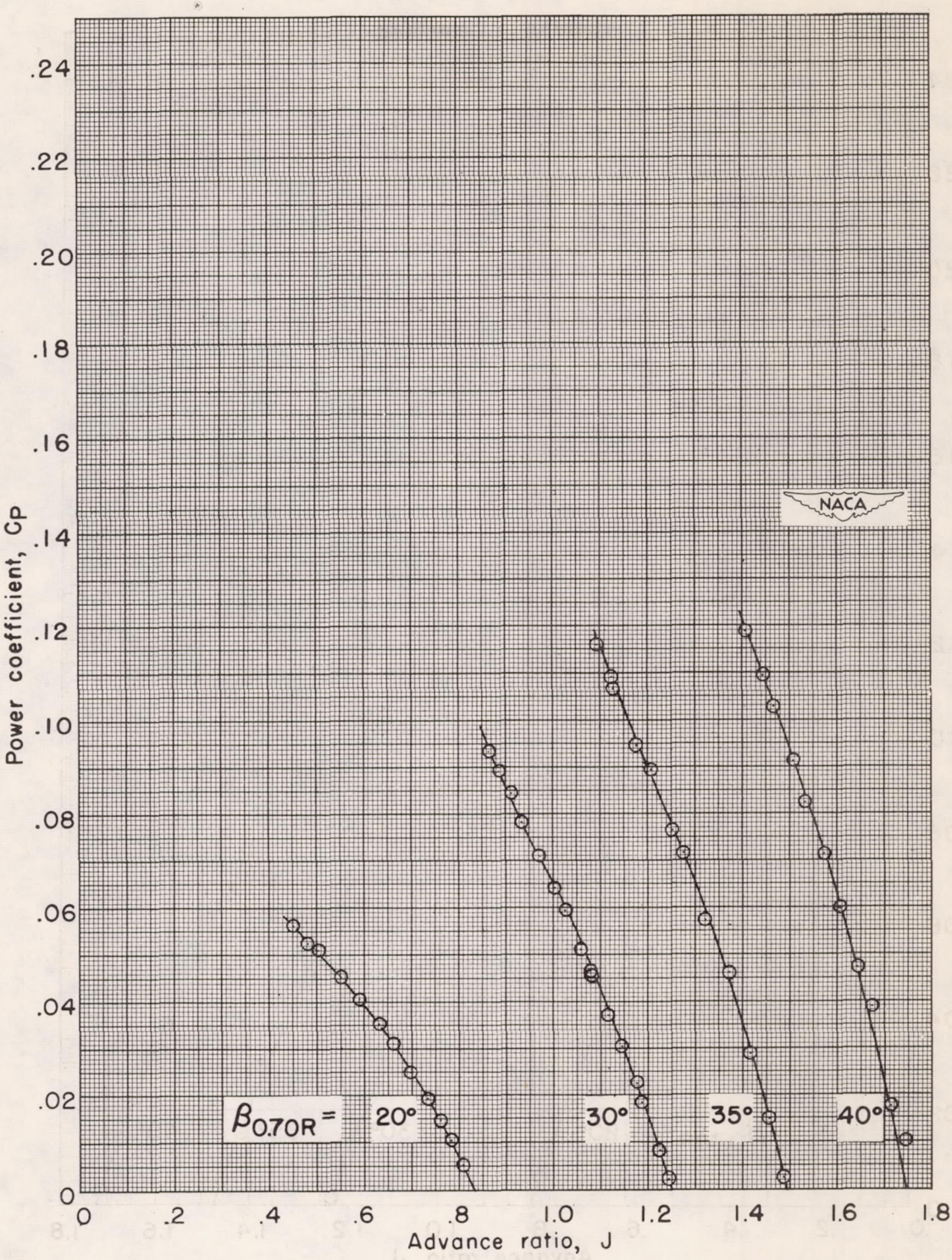

(b) Power coefficient.

Figure 11.- Continued. 2100 rpm.

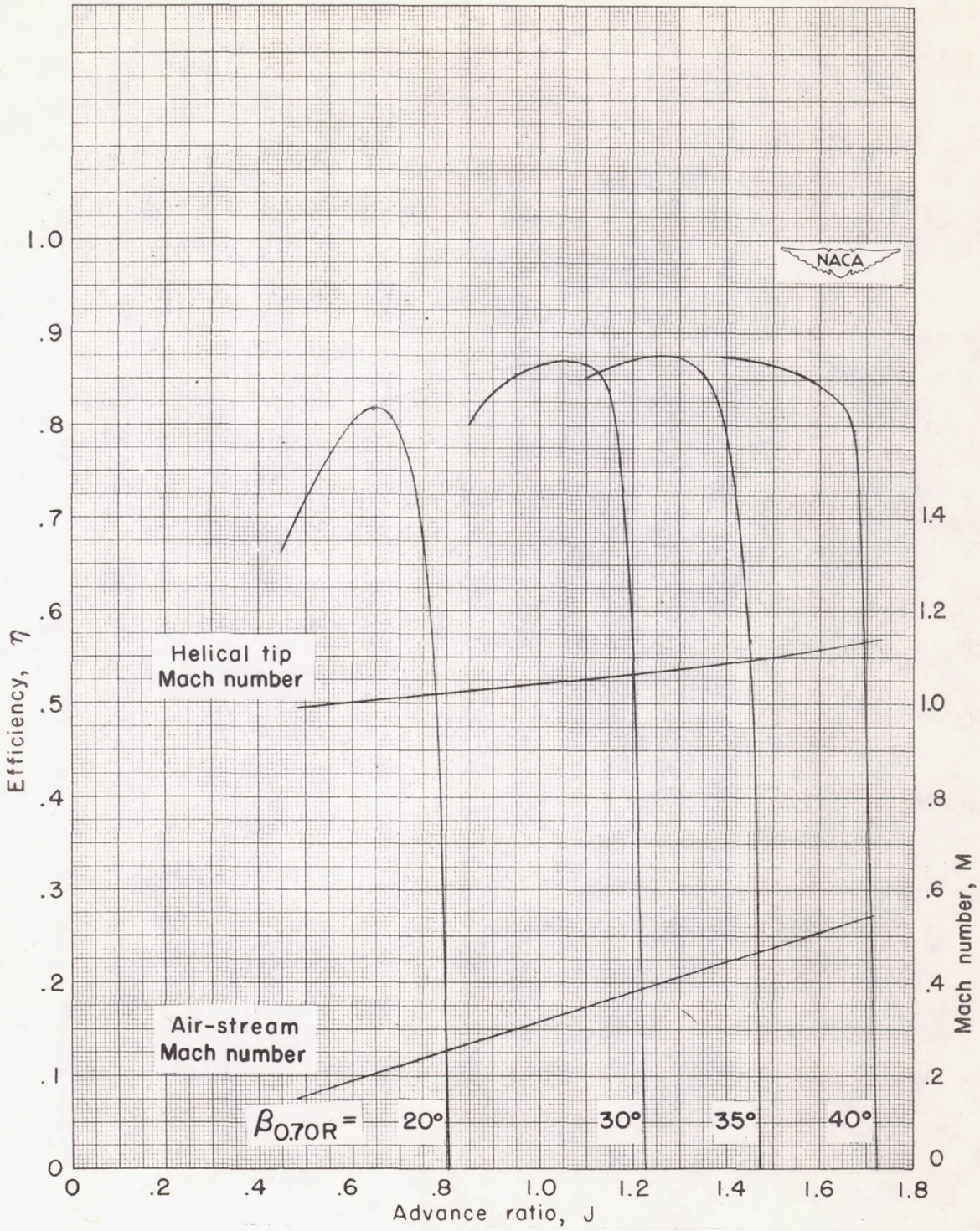

(c) Efficiency.

Figure 11.- Concluded. 2100 rpm.

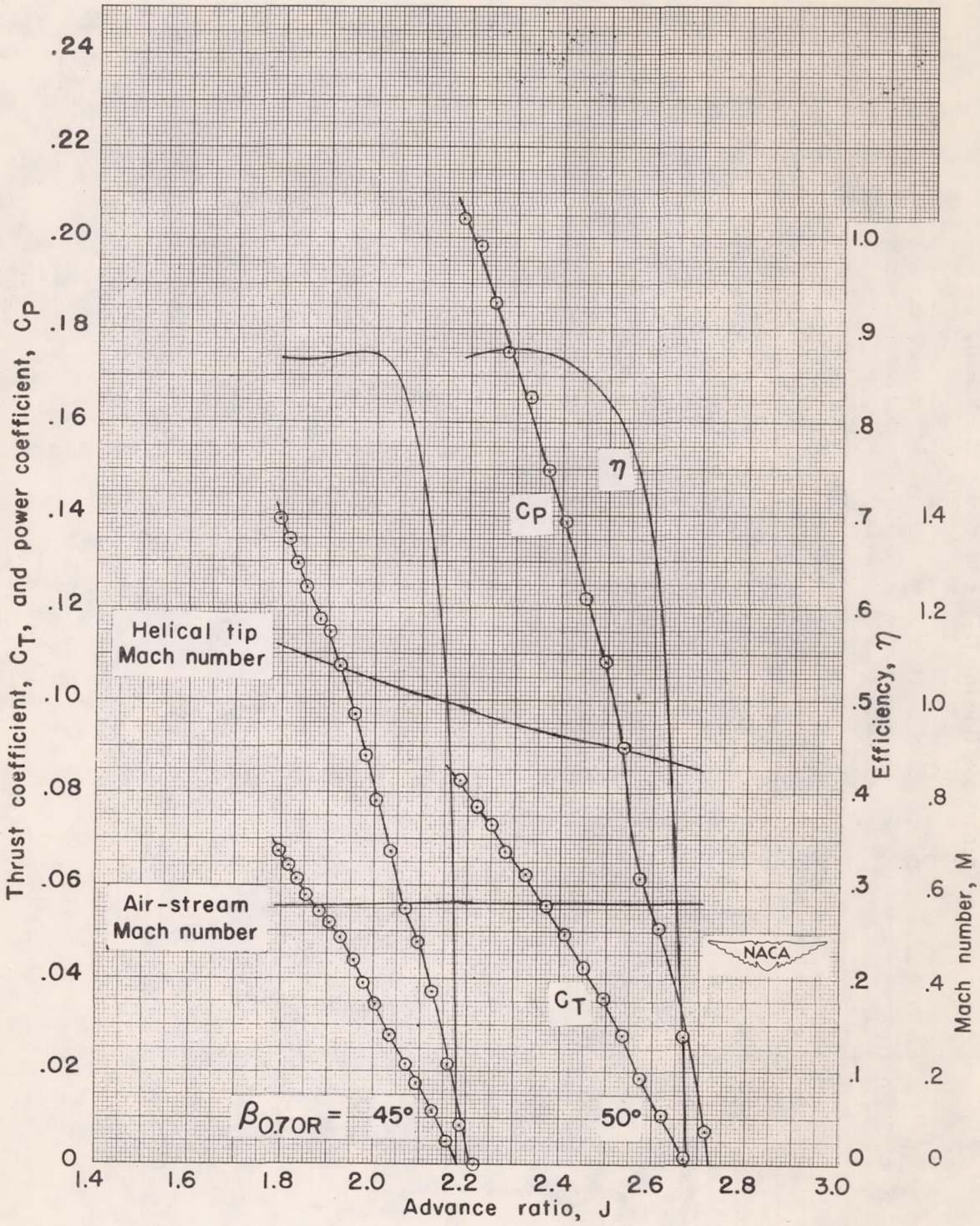

Figure 12.- Characteristics of NACA 10-(1.7)(062)-057-27 propeller; M = 0.56.

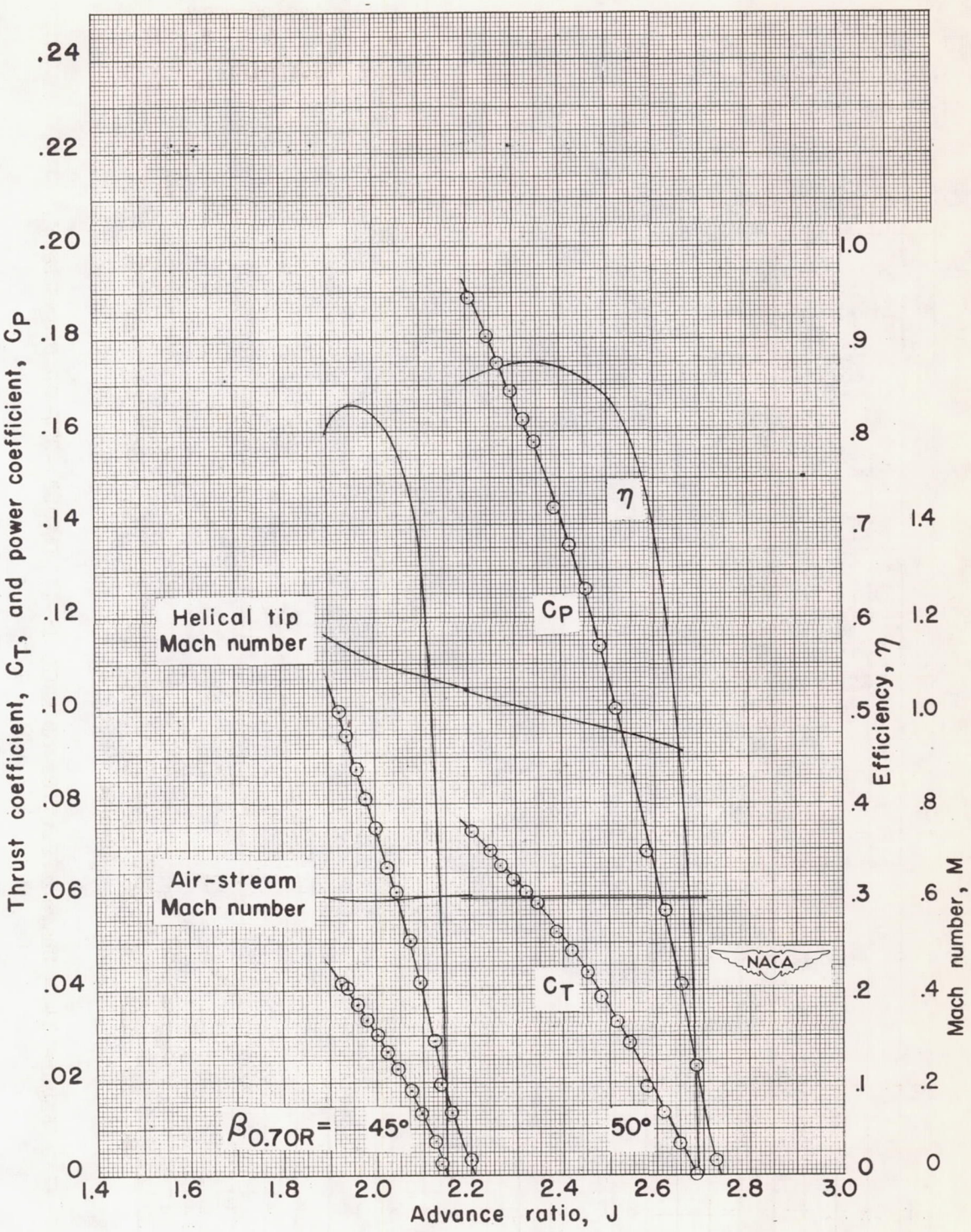

Figure 13.- Characteristics of NACA 10-(1.7)(062)-057-27 propeller; M = 0.60.

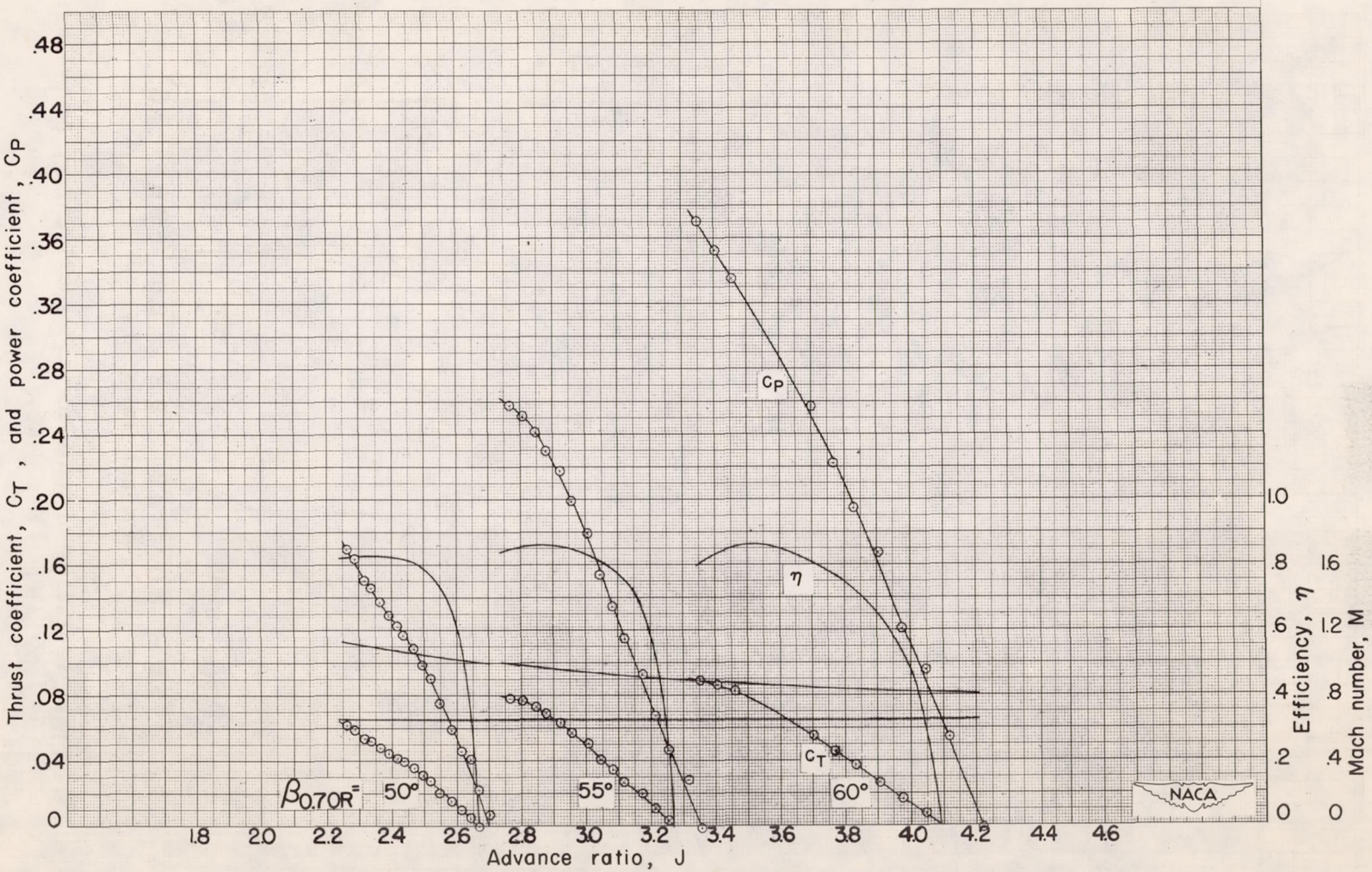

Figure 14.- Characteristics of NACA 10-(1.7)(062)-057-27 propeller; M = 0.65.

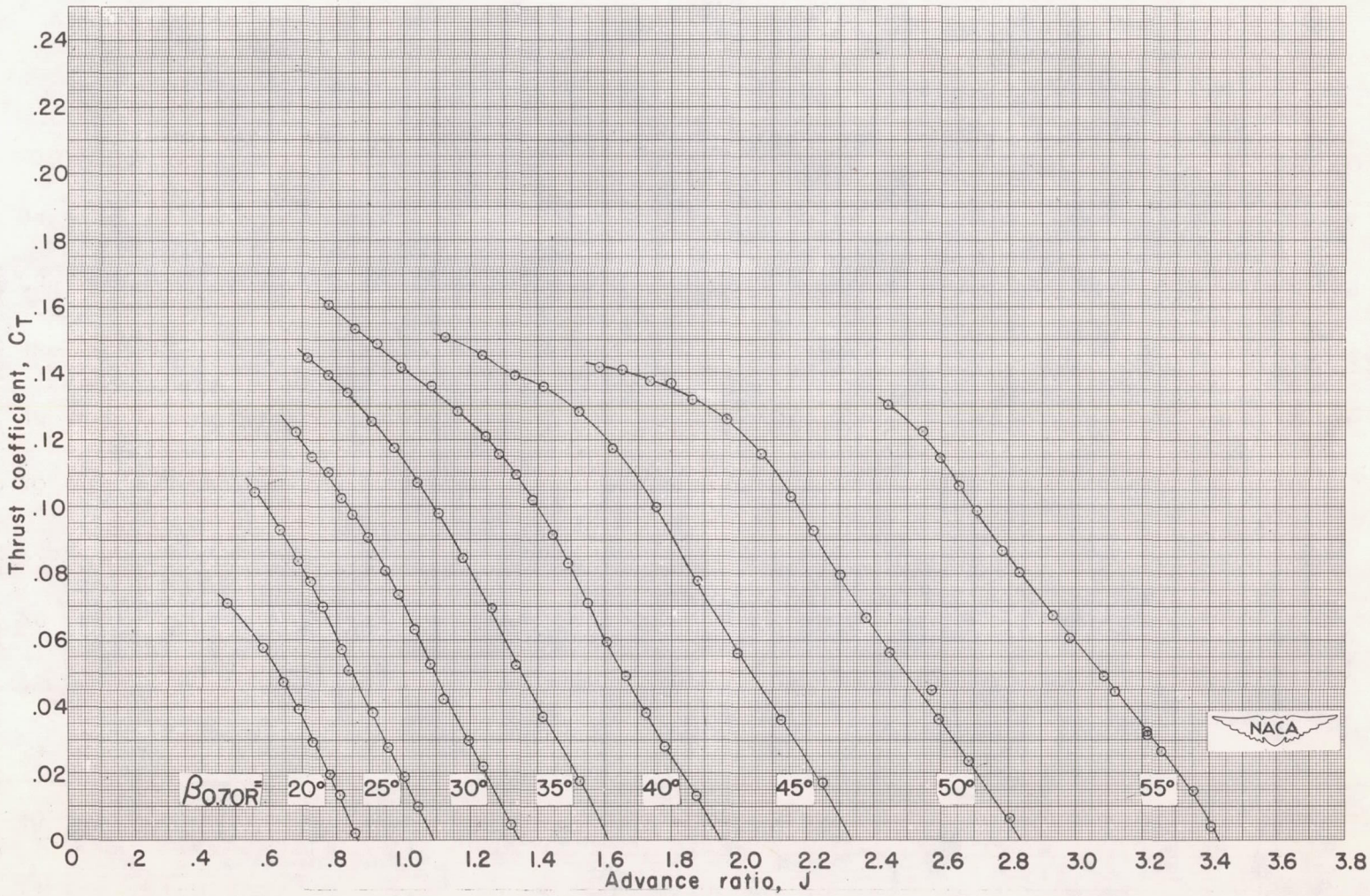

(a) Thrust coefficient.

Figure 15.- Characteristics of NACA 10-(1.7)(062)-051 propeller; 1140 rpm.

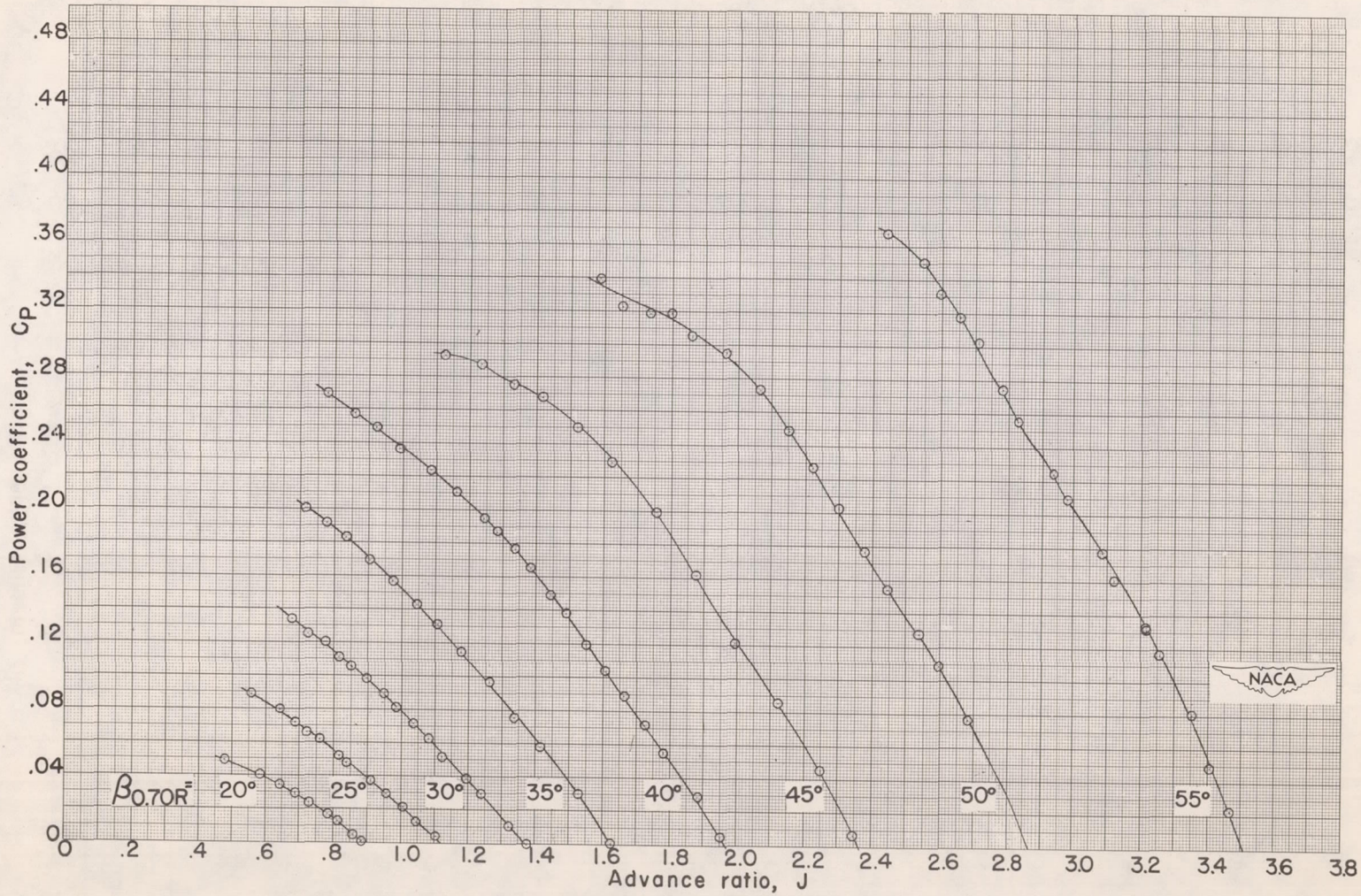

(b) Power coefficient.

Figure 15.- Continued. 1140 rpm.

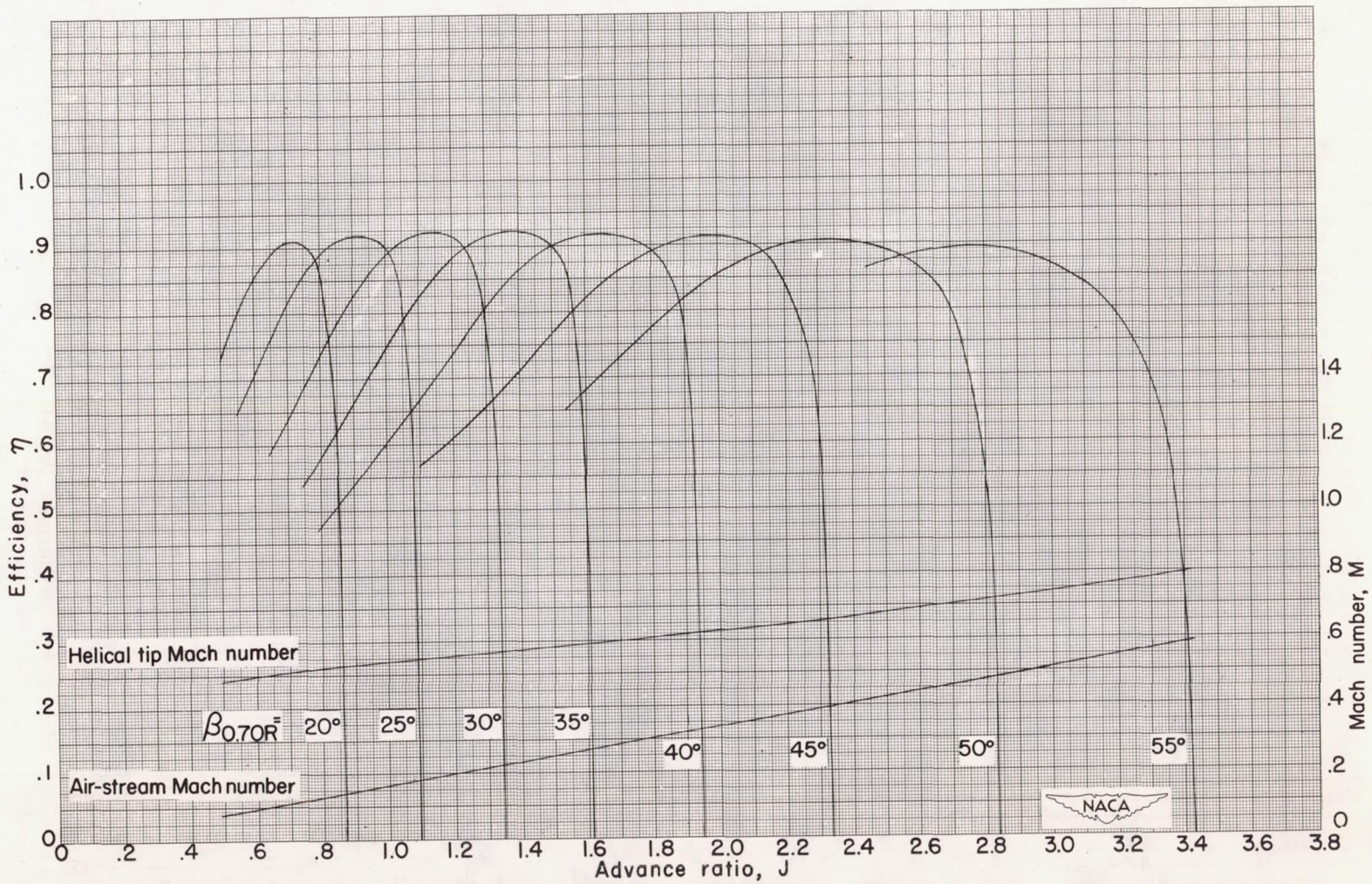

(c) Efficiency.

Figure 15.- Concluded. 1140 rpm.

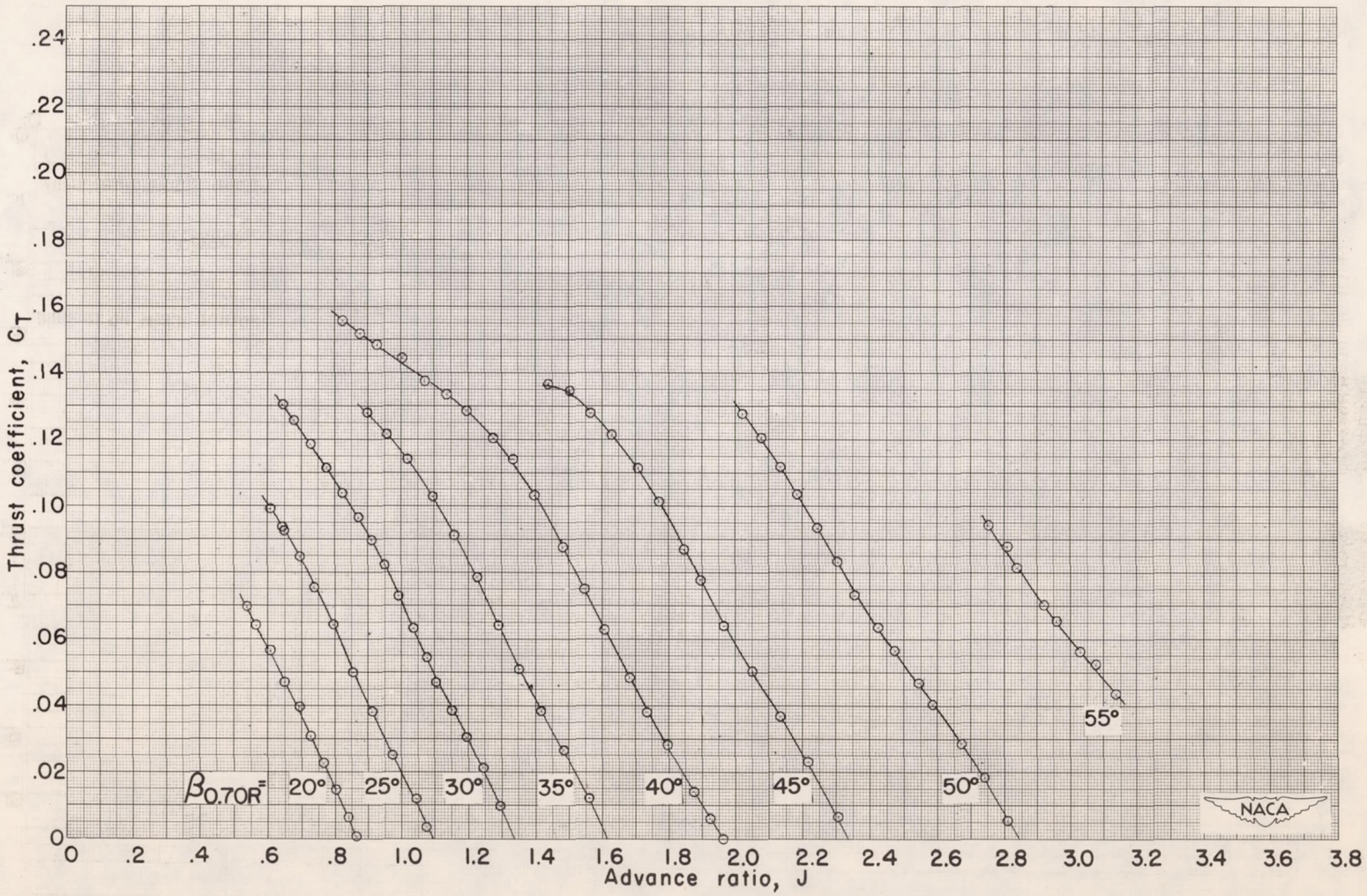

(a) Thrust coefficient.

Figure 16.- Characteristics of NACA 10-(1.7)(062)-051 propeller; 1350 rpm.

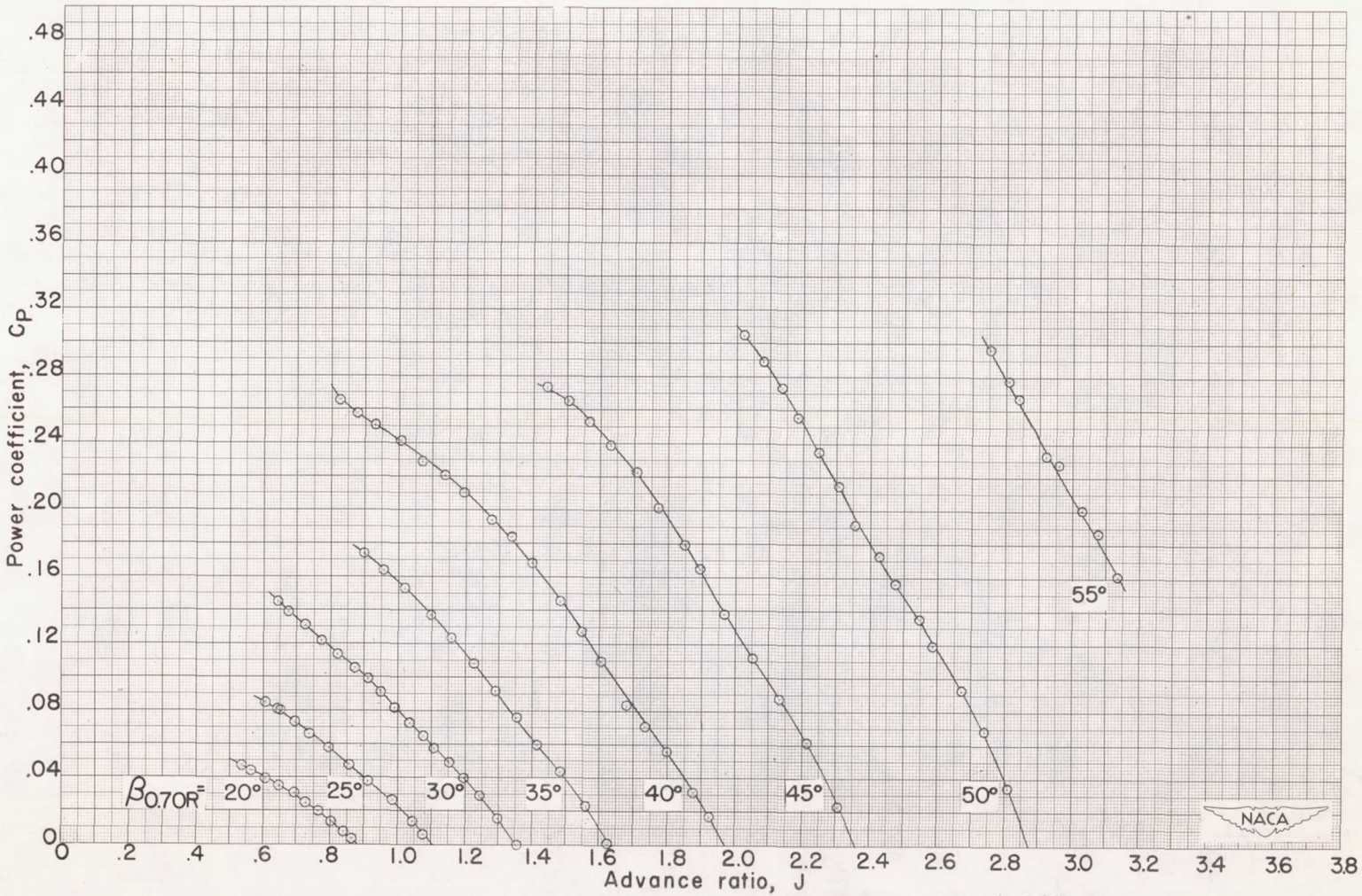

(b) Power coefficient.

Figure 16.- Continued. 1350 rpm.

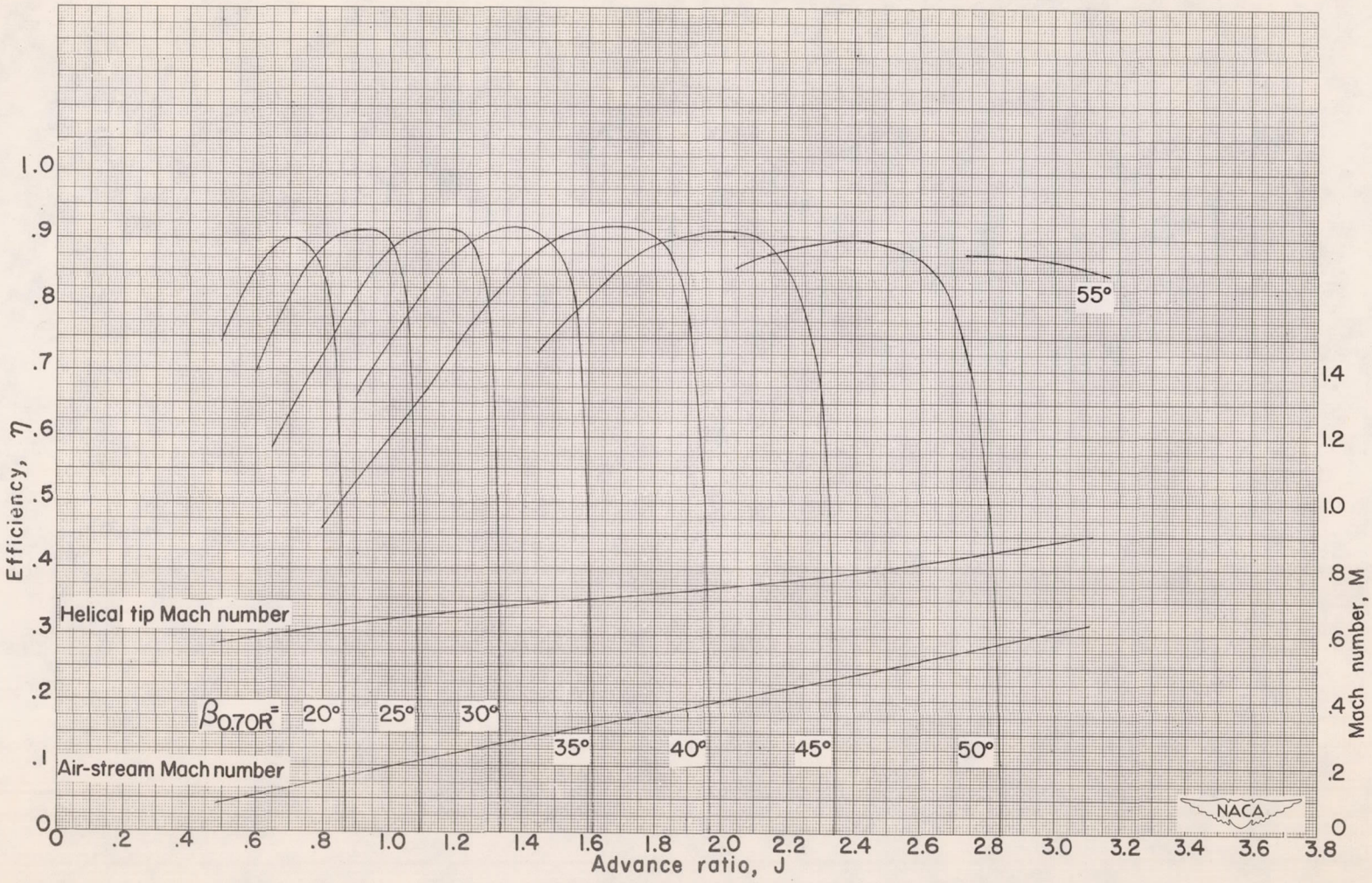

(c) Efficiency.

Figure 16.- Concluded. 1350 rpm.

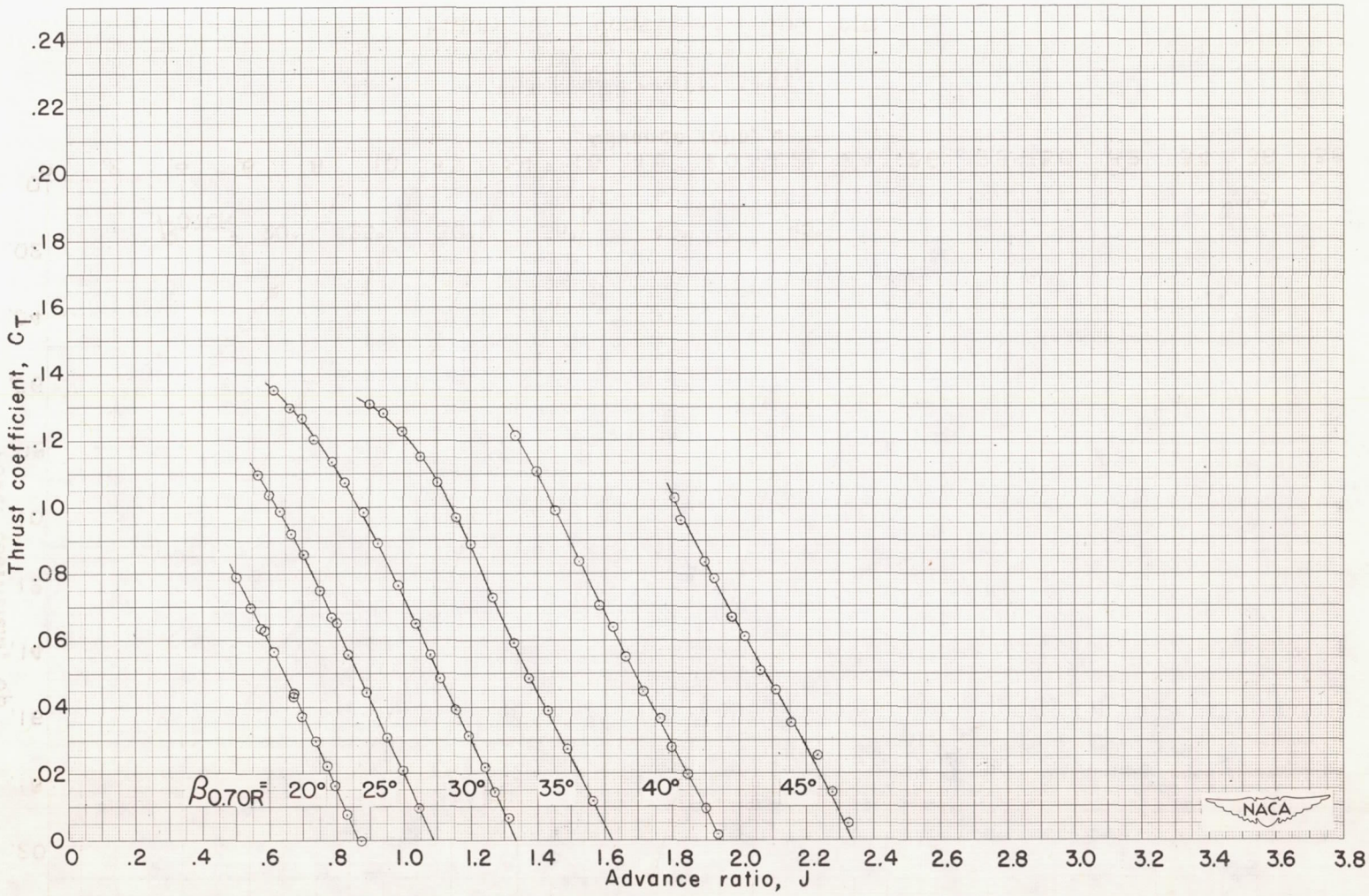

(a) Thrust coefficient.

Figure 17.- Characteristics of NACA 10-(1.7)(062)-051 propeller; 1600 rpm.

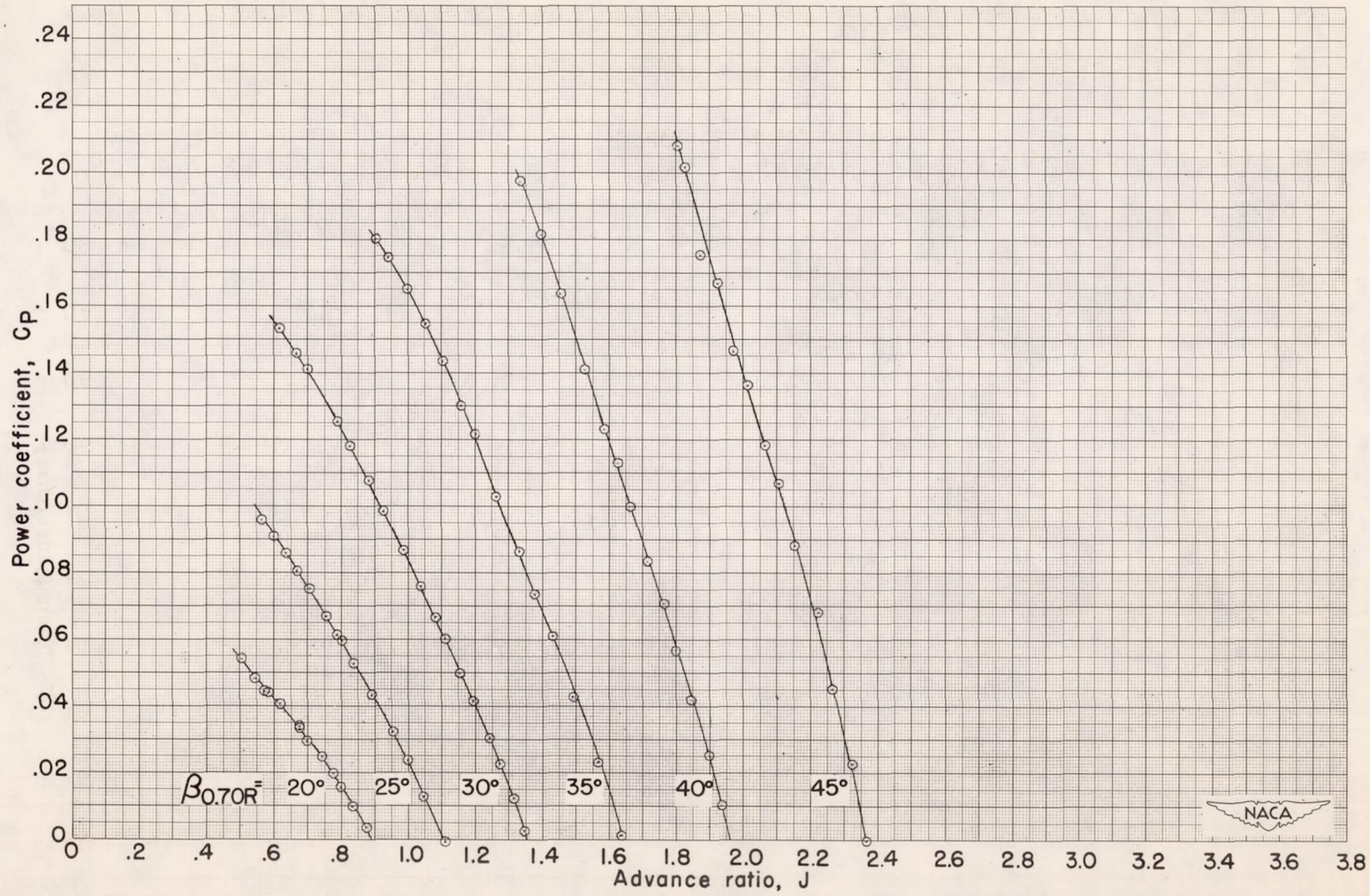

(b) Power coefficient.

Figure 17.- Continued. 1600 rpm.

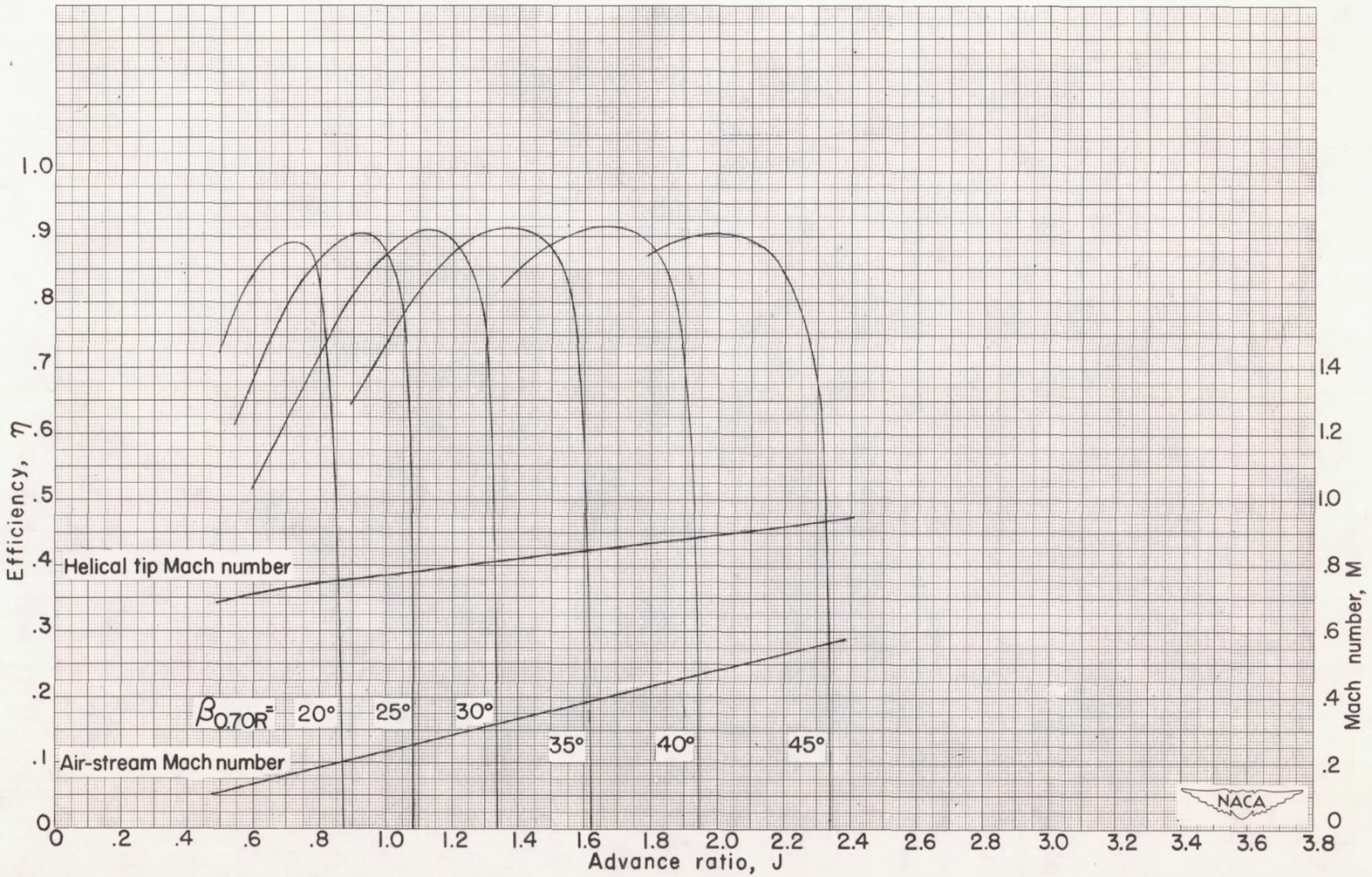

(c) Efficiency.

Figure 17.- Concluded. 1600 rpm.

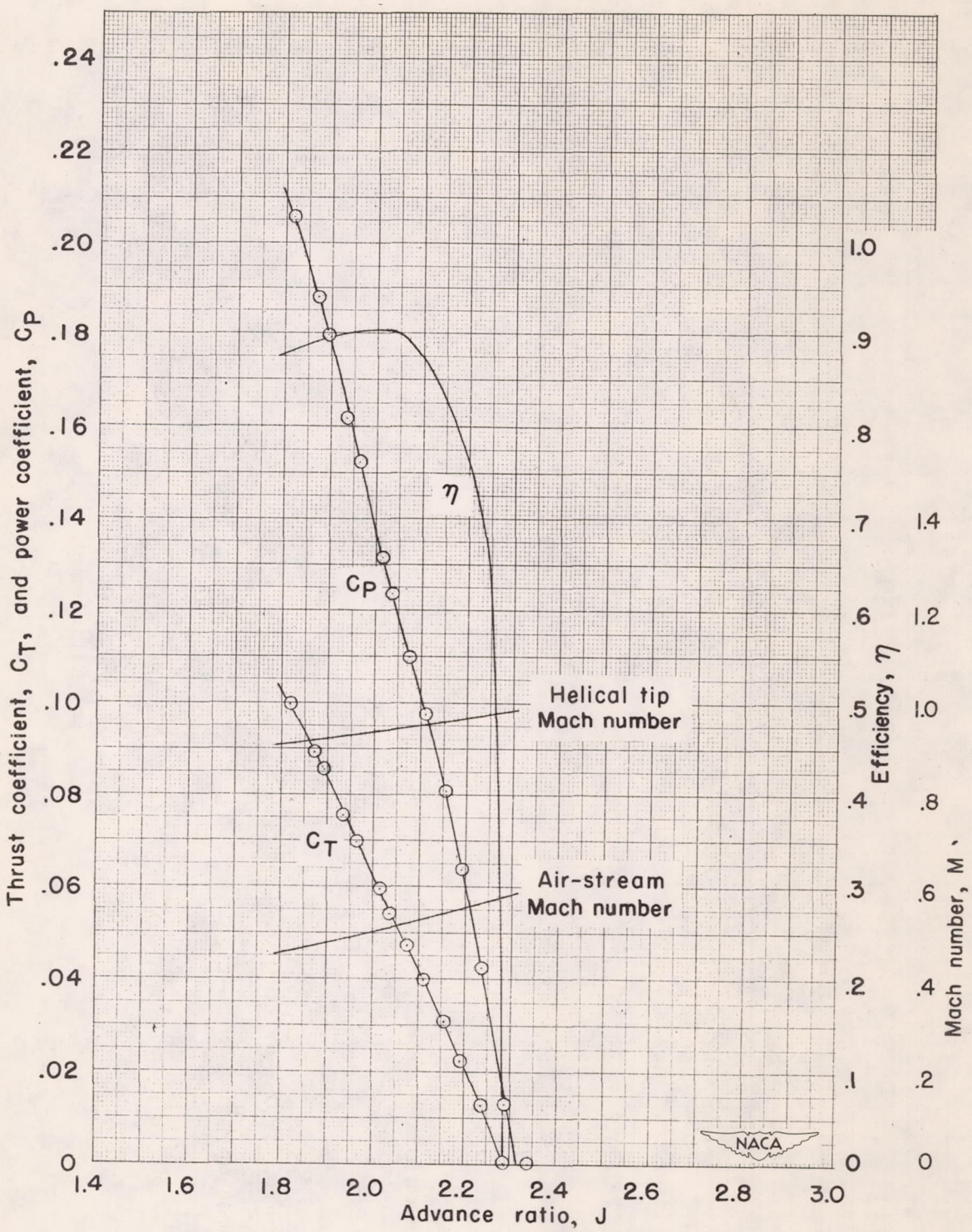

Figure 18.- Characteristics of NACA 10-(1.7)(062)-051 propeller; 1680 rpm; $\beta_{0.70R} = 45^{\circ}$.

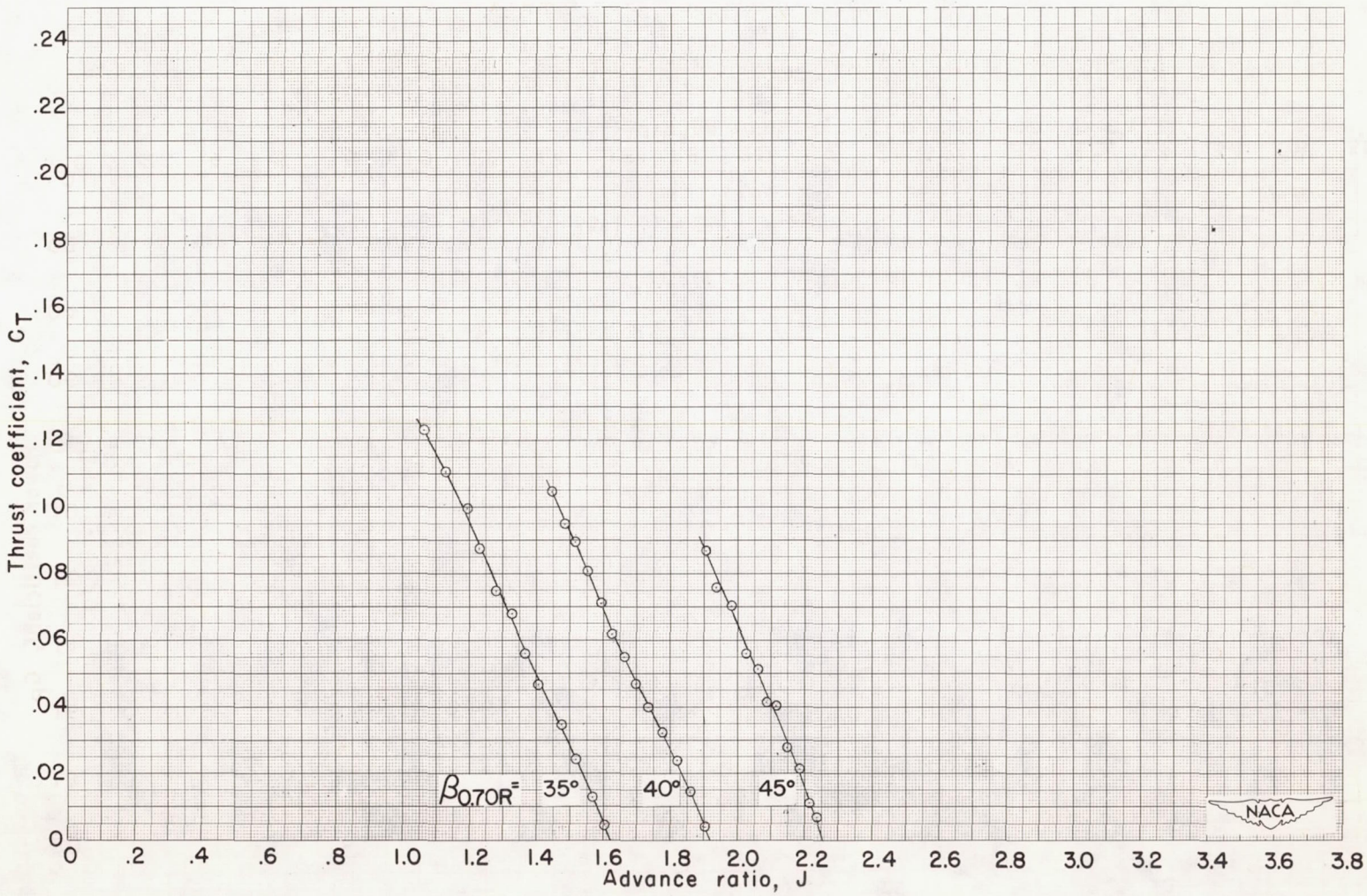

(a) Thrust coefficient.

Figure 19.- Characteristics of NACA 10-(1.7)(062)-051 propeller; 1800 rpm.

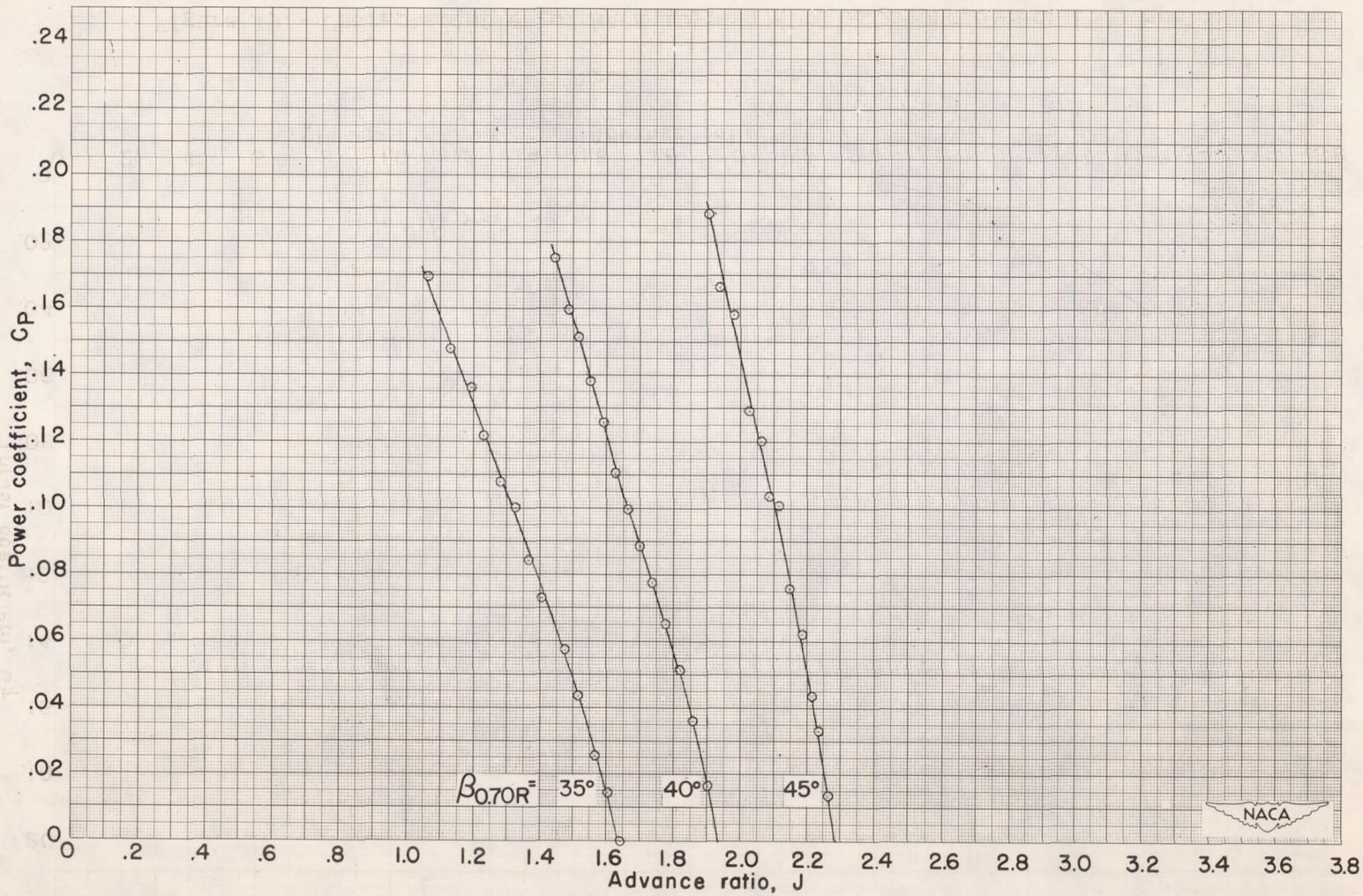

(b) Power coefficient.

Figure 19.- Continued. 1800 rpm.

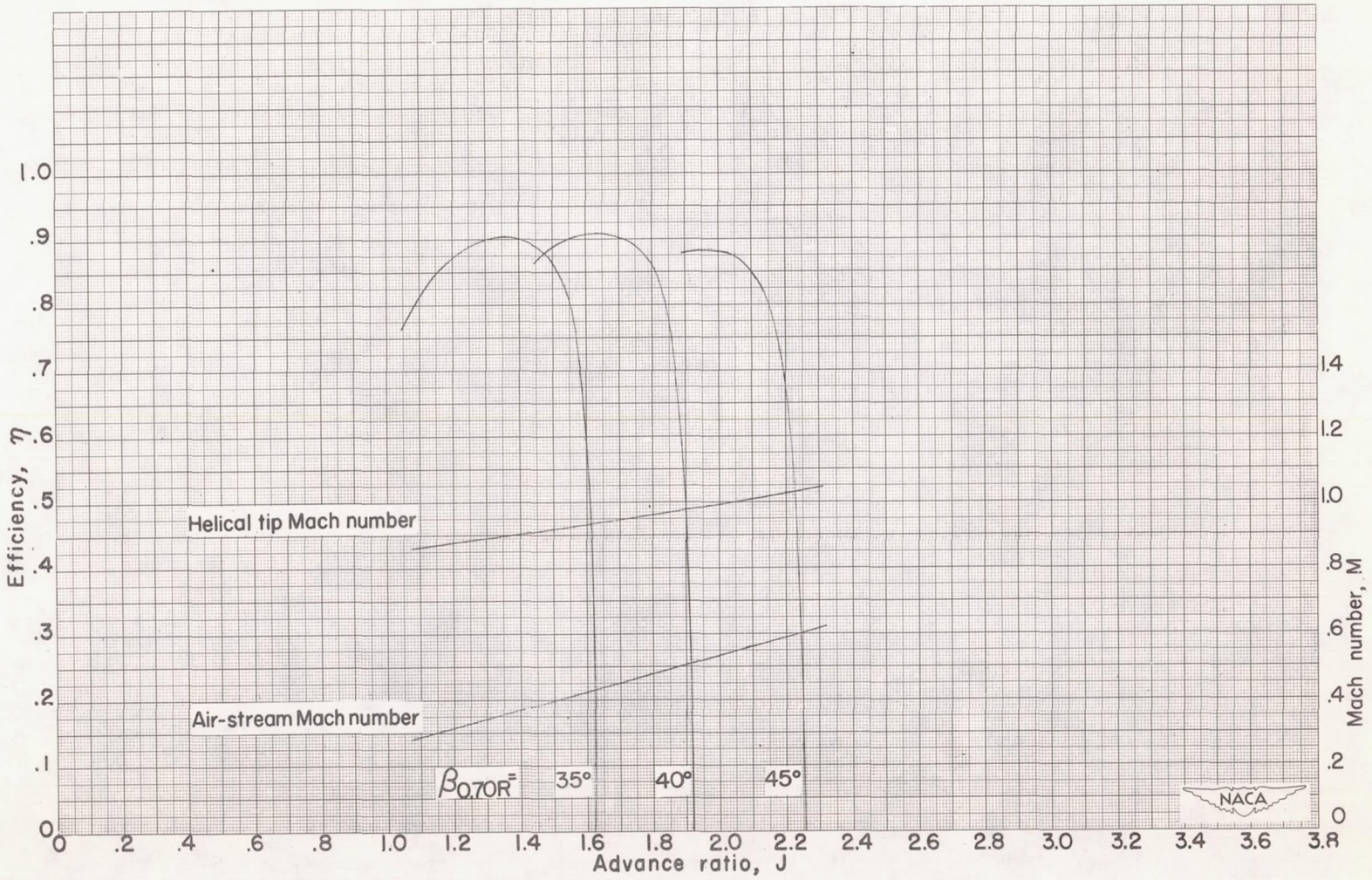

(c) Efficiency.

Figure 19.- Concluded. 1800 rpm.

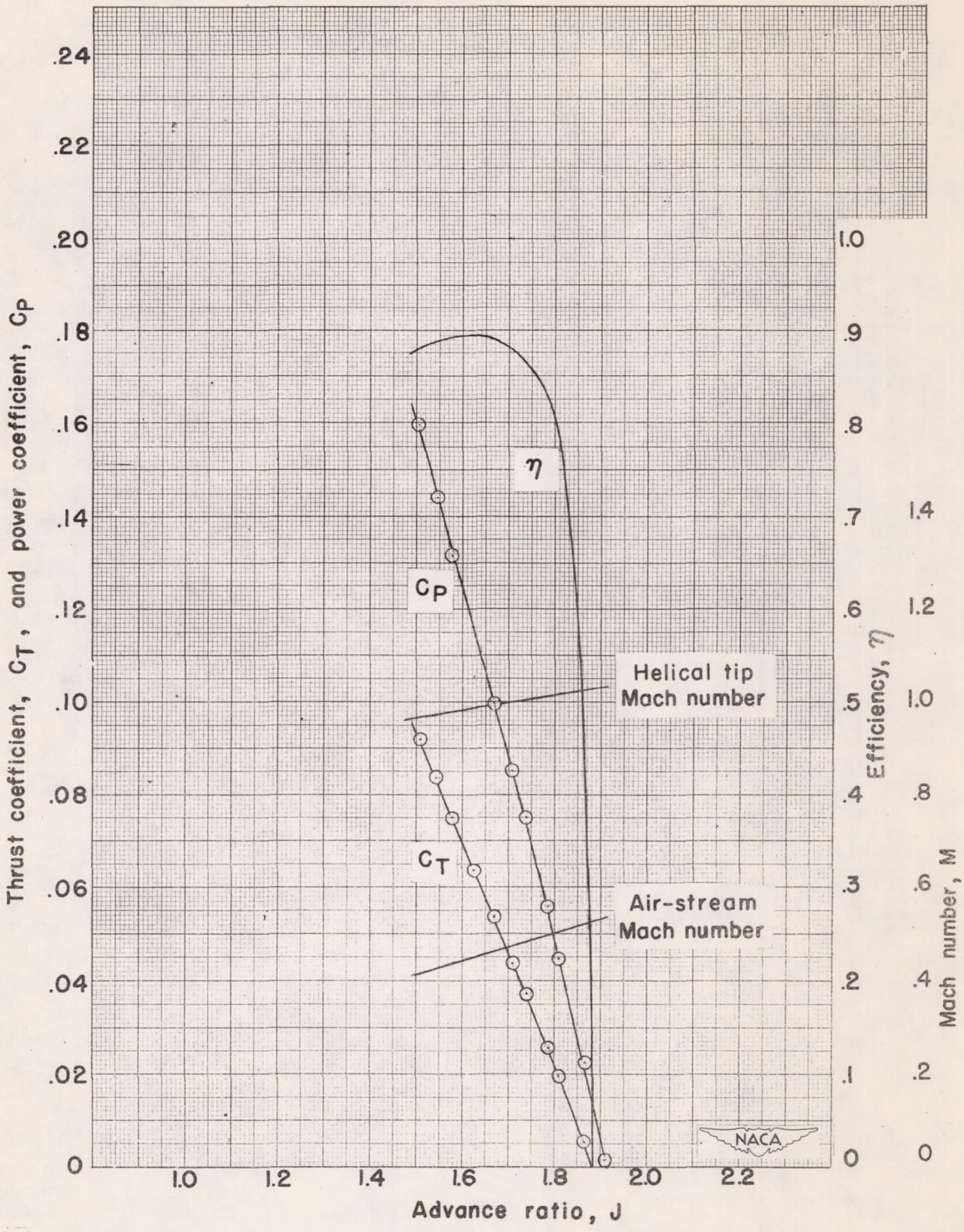

Figure 20.- Characteristics of NACA 10-(1.7)(062)-051 propeller; 1900 rpm; $\beta_{0.70R} = 40^{\circ}$.

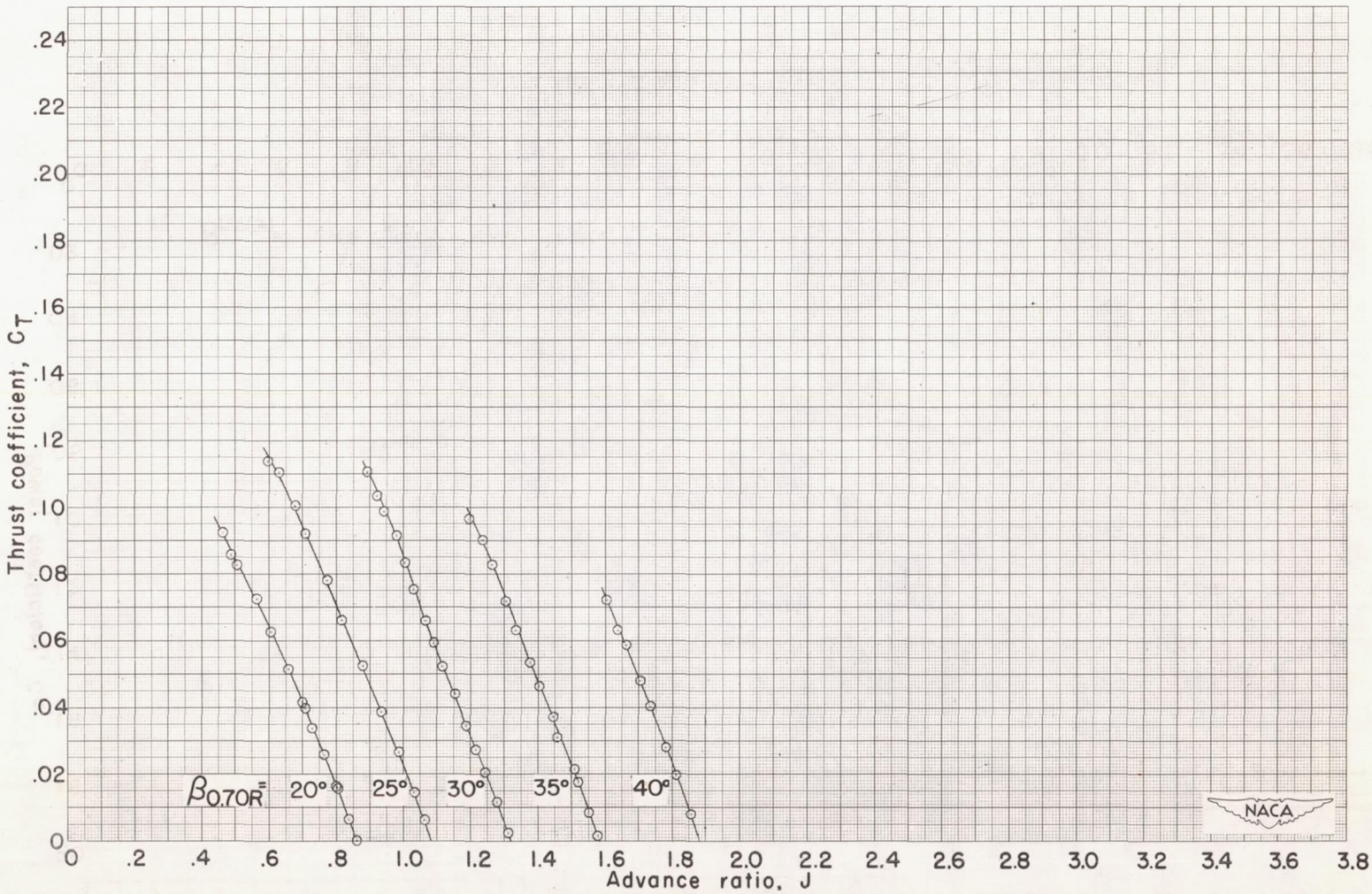

(a) Thrust coefficient.

Figure 21.- Characteristics of NACA 10-(1.7)(062)-051 propeller; 2000 rpm.

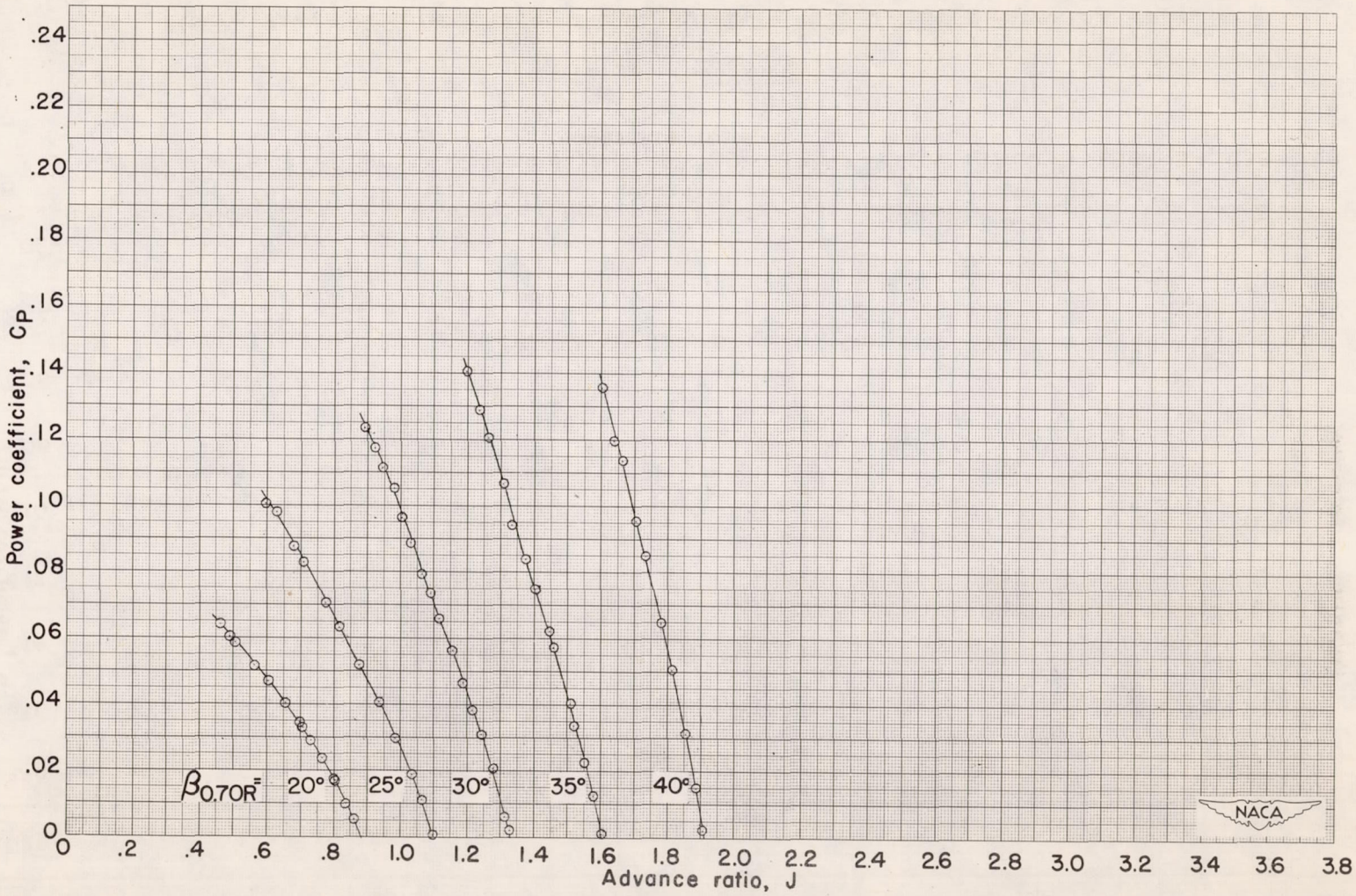

(b) Power coefficient.

Figure 21.- Continued. 2000 rpm.

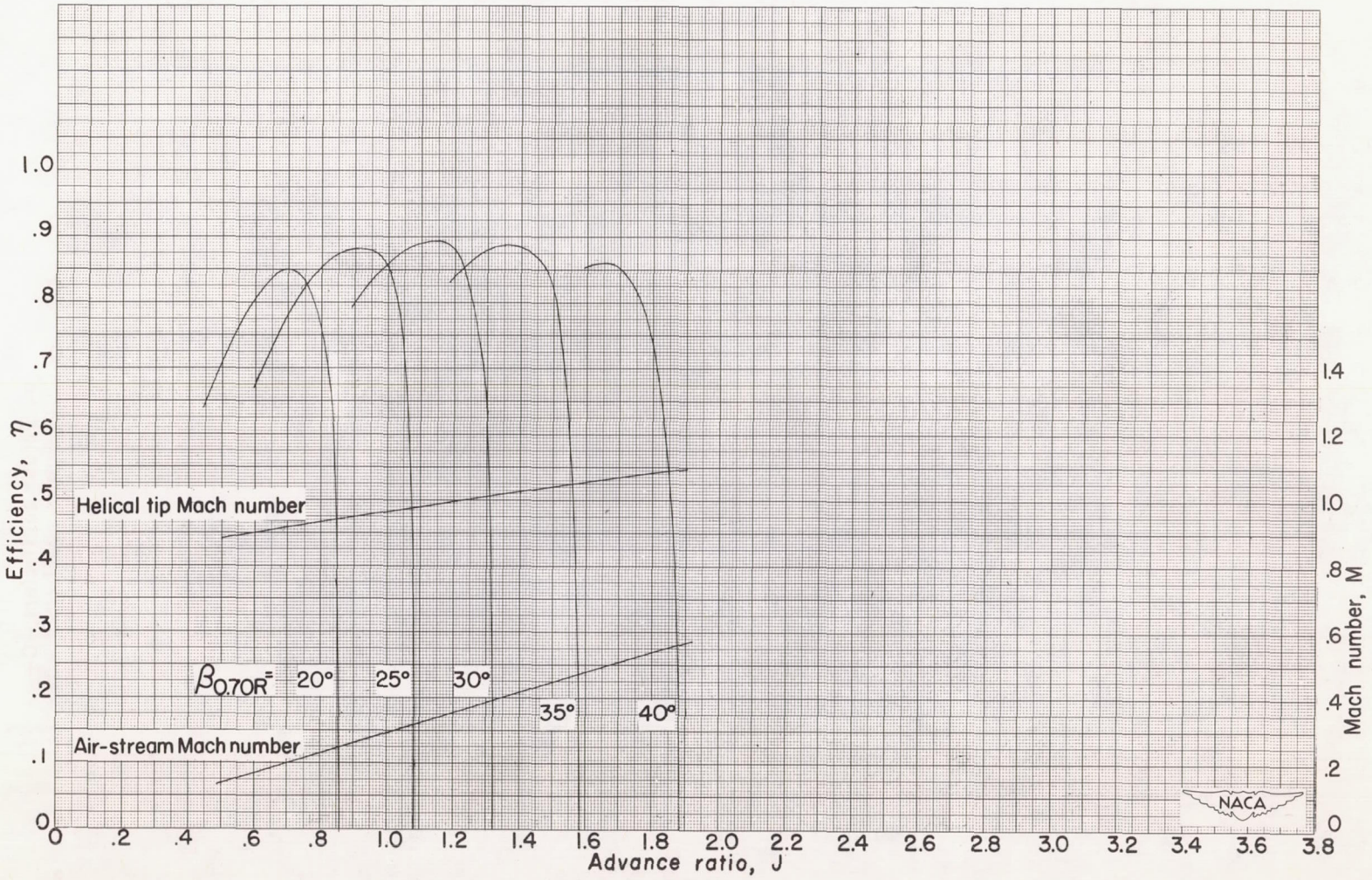

(c) Efficiency.

Figure 21.- Concluded. 2000 rpm.

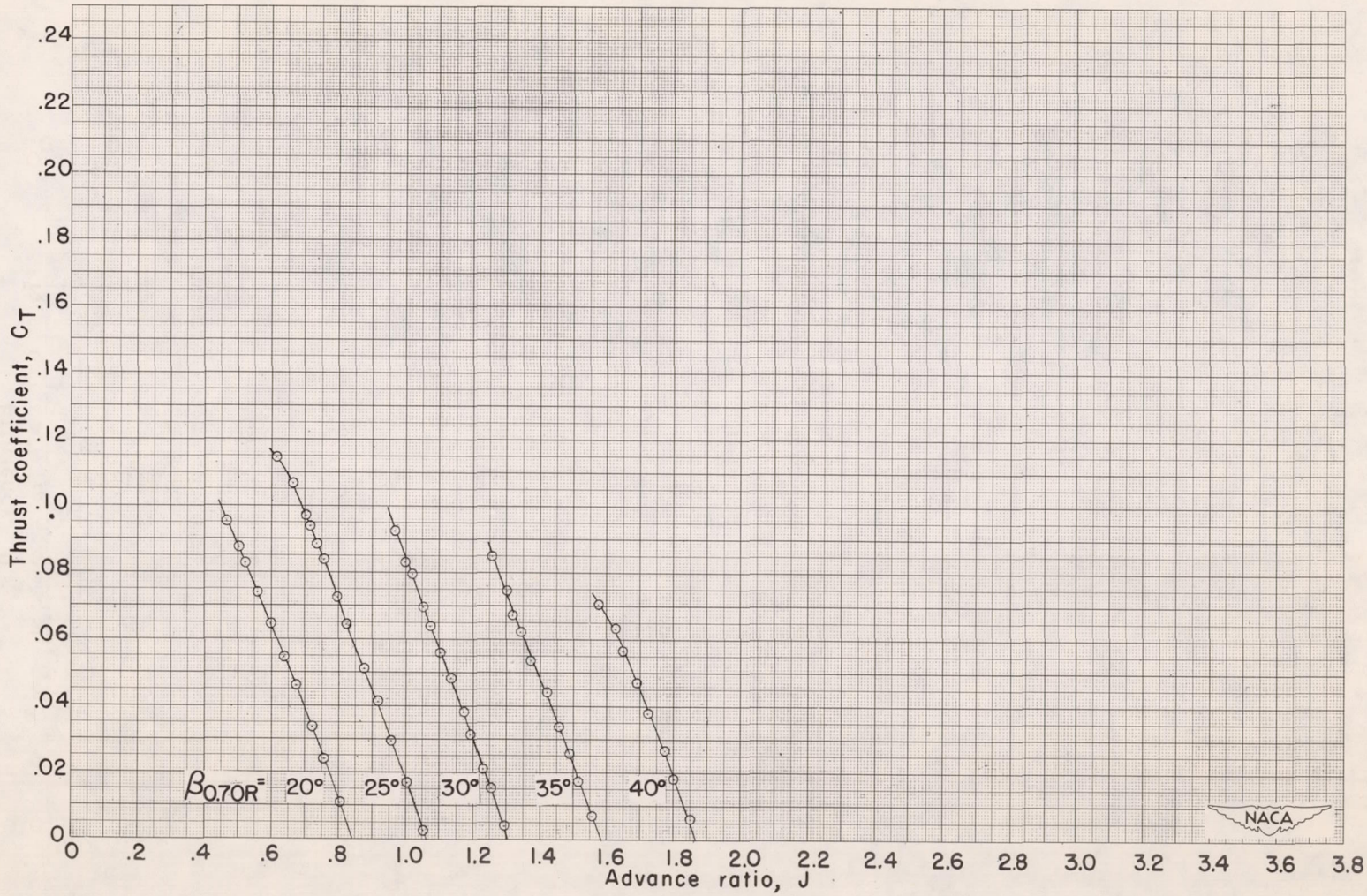

(a) Thrust coefficient.

Figure 22.- Characteristics of NACA 10-(1.7)(062)-051 propeller; 2100 rpm.

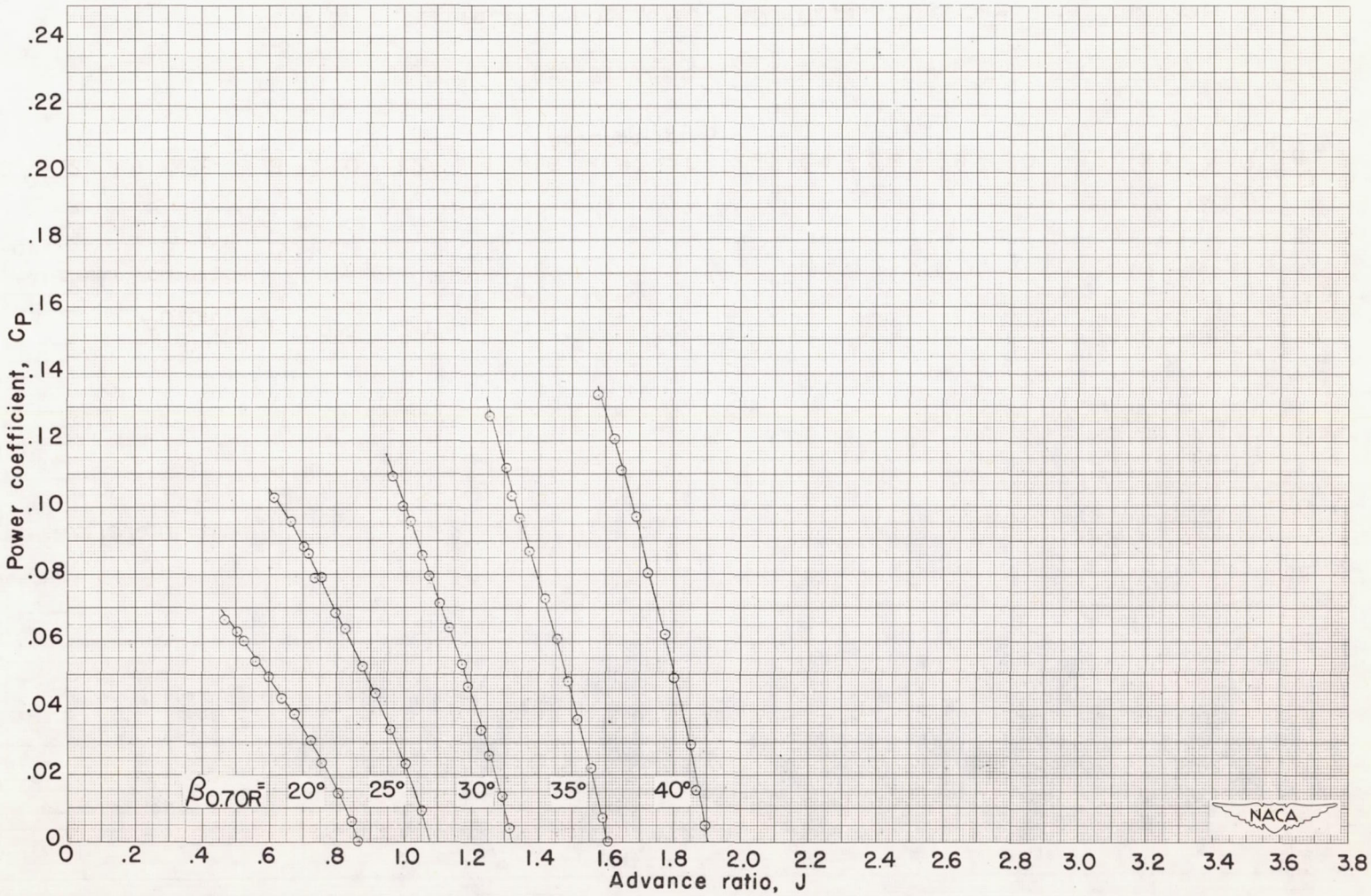

(b) Power coefficient.

Figure 22.- Continued. 2100 rpm.

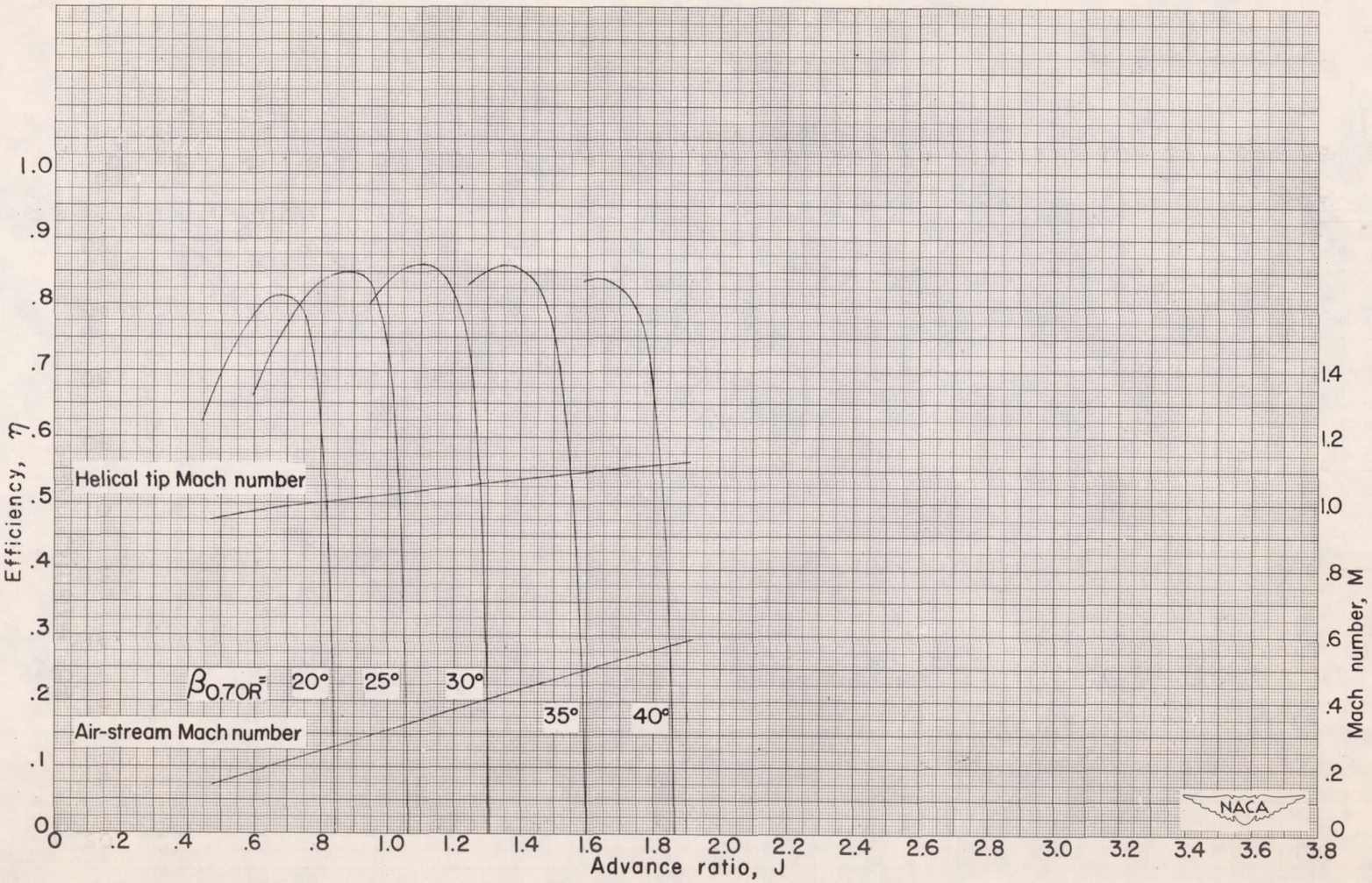

(c) Efficiency.

Figure 22.- Concluded. 2100 rpm.

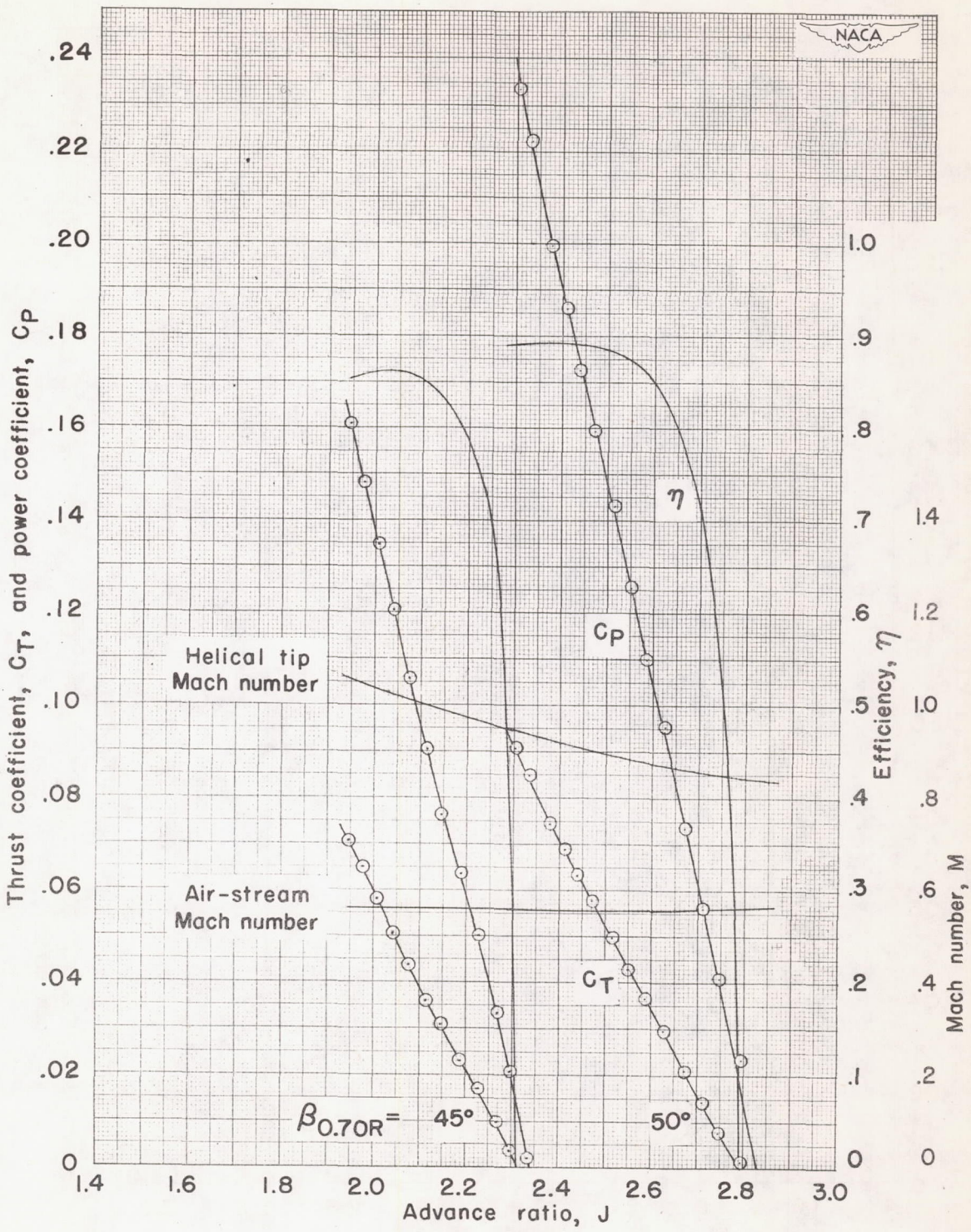

Figure 23.- Characteristics of NACA 10-(1.7)(062)-051 propeller; M = 0.56.

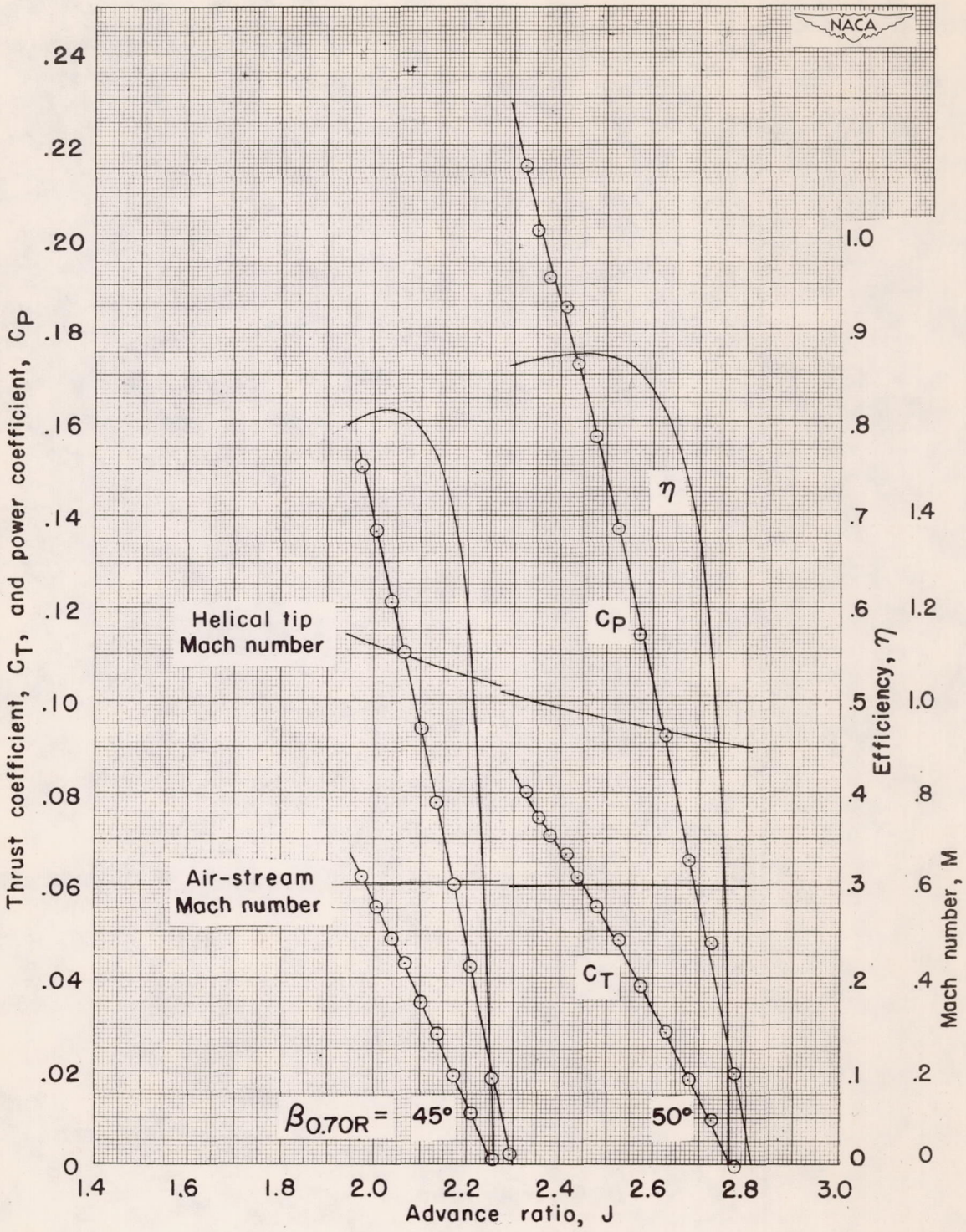

Figure 24.- Characteristics of NACA 10-(1.7)(062)-051 propeller; M = 0.60.

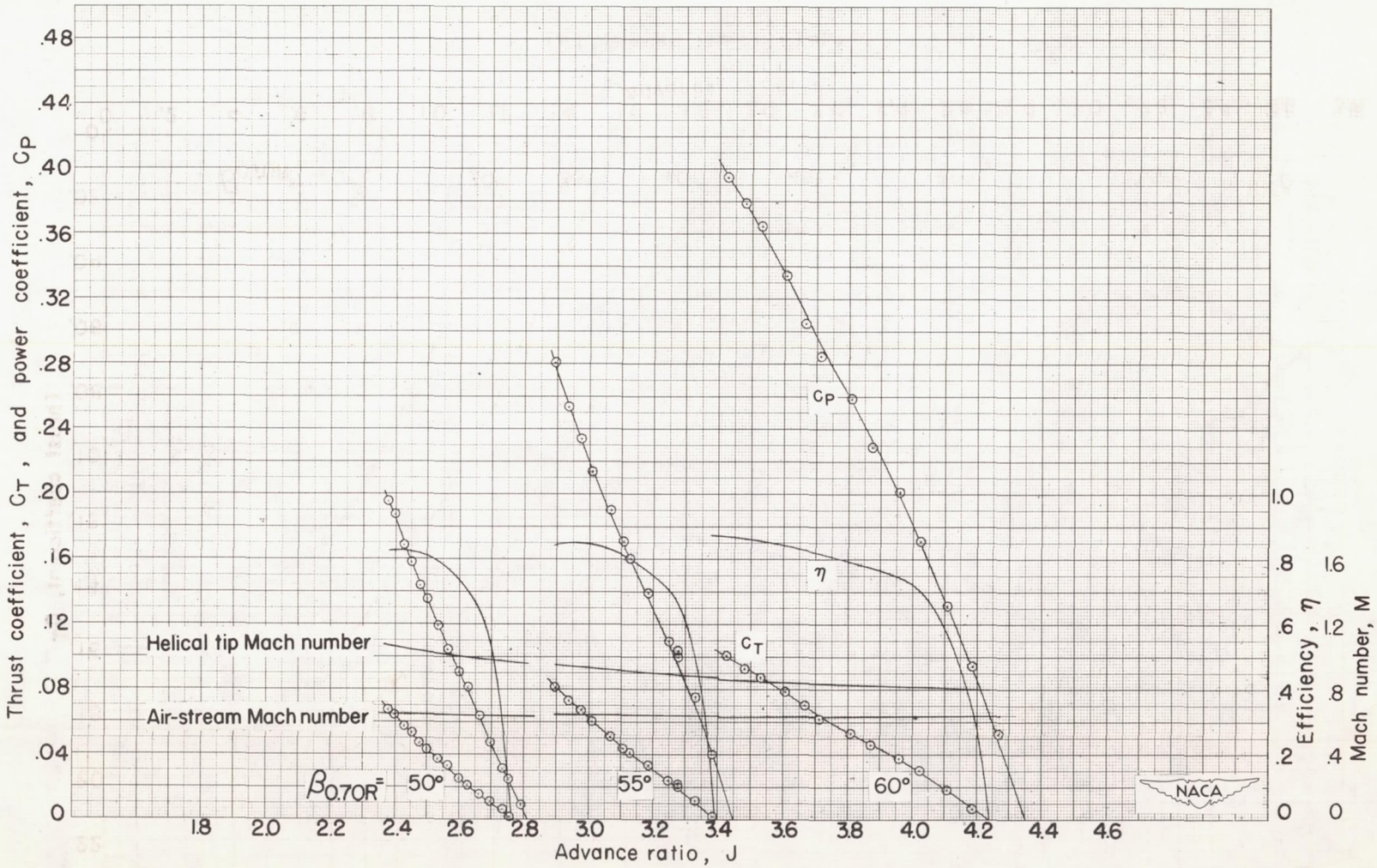

Figure 25.- Characteristics of NACA 10-(1.7)(062)-051 propeller; M = 0.65.

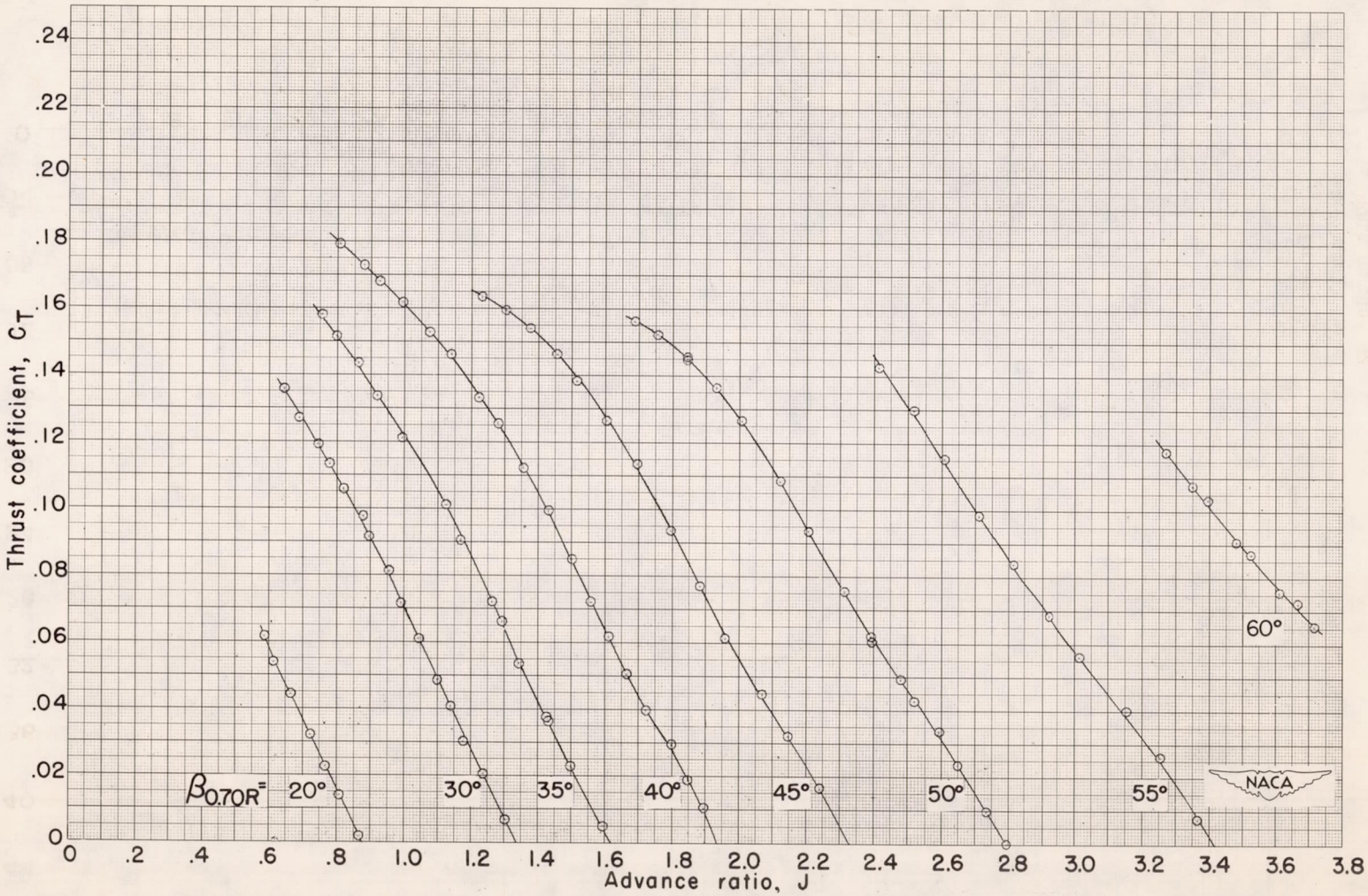

(a) Thrust coefficient.

Figure 26.- Characteristics of NACA 10-(1.5)(062)-057 propeller; 1140 rpm.

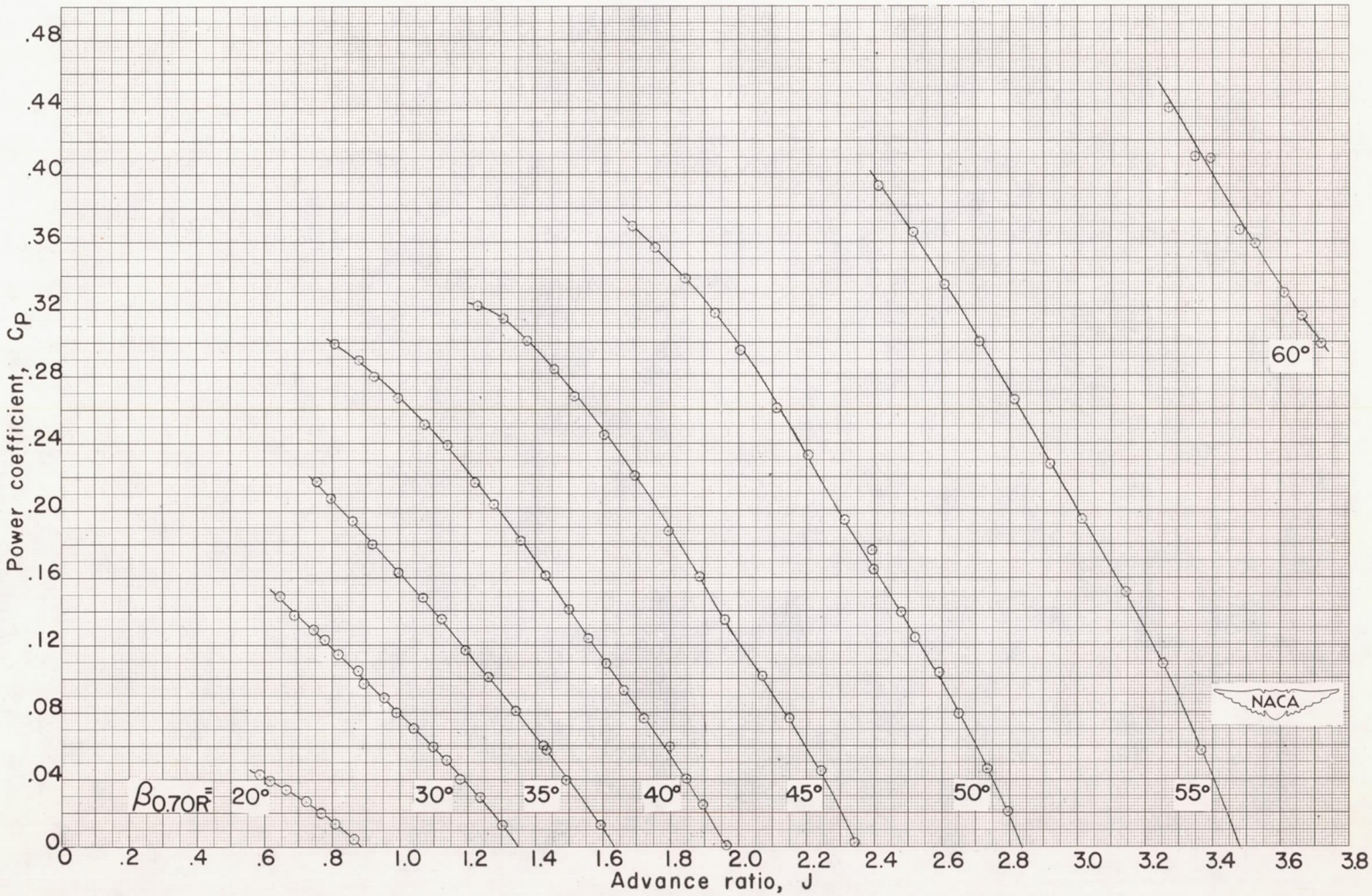

(b) Power coefficient.

Figure 26.- Continued. 1140 rpm.

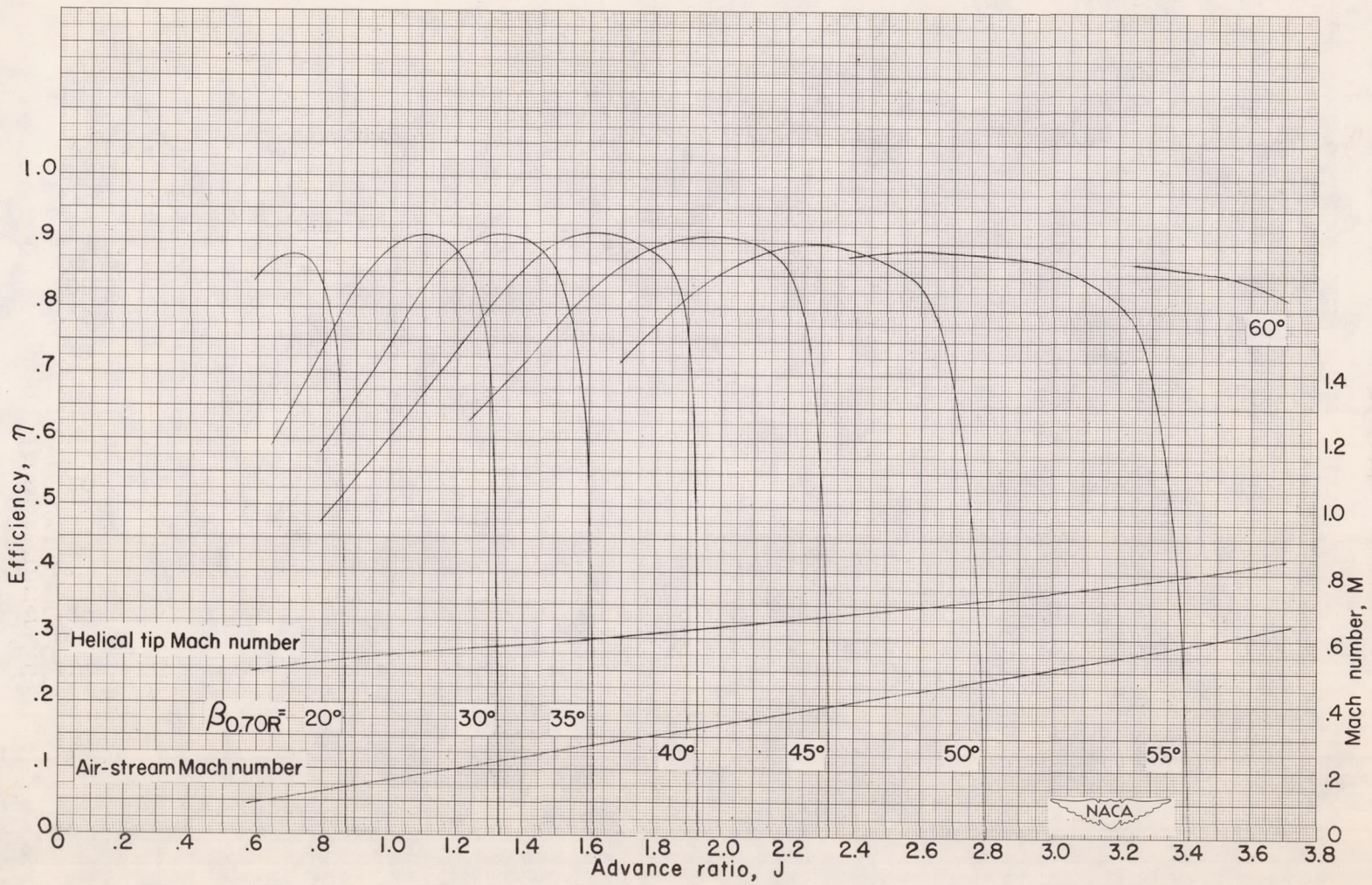

(c) Efficiency.

Figure 26.- Concluded. 1140 rpm.

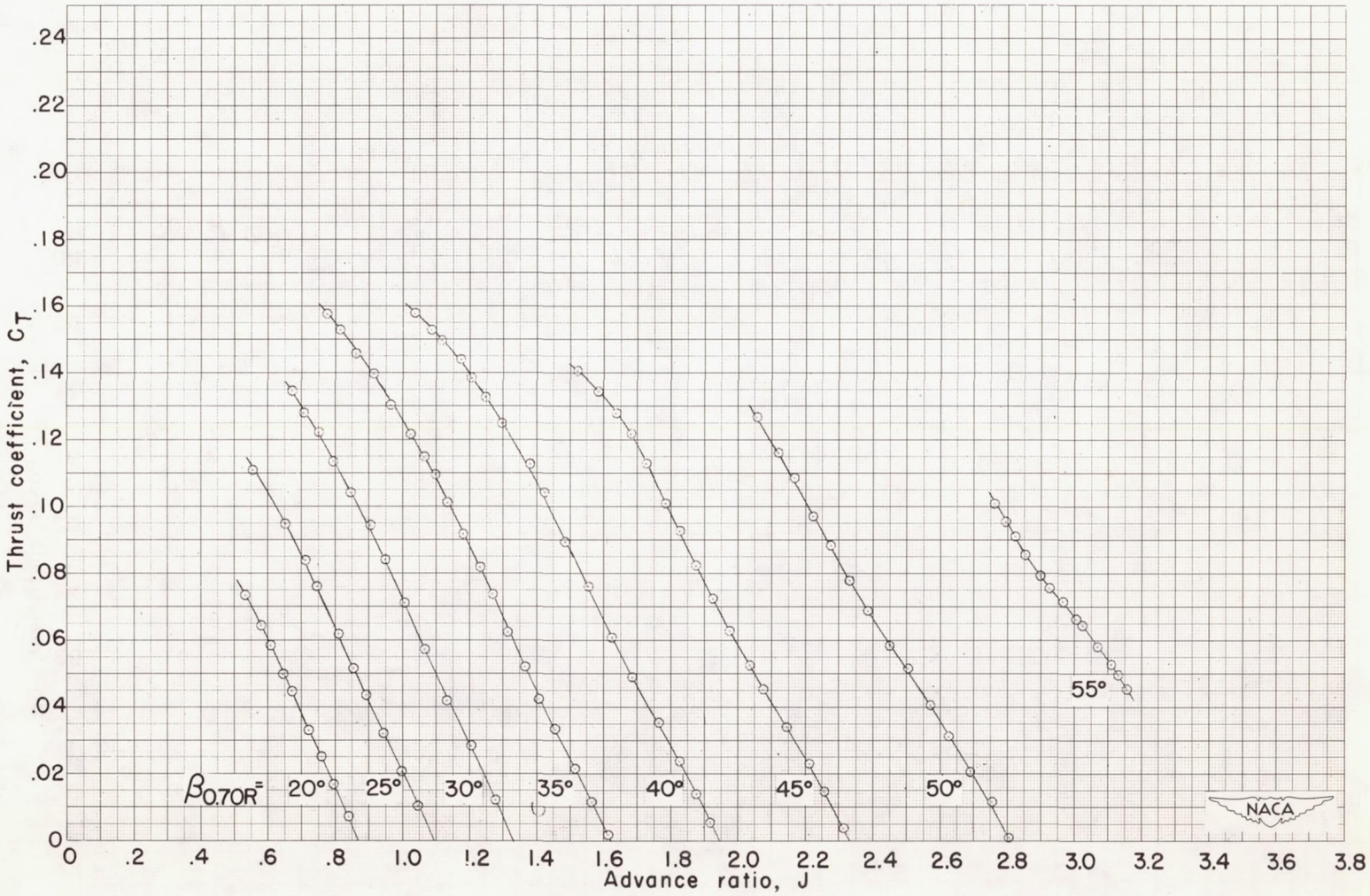

(a) Thrust coefficient.

Figure 27.- Characteristics of NACA 10-(1.5)(062)-057 propeller; 1350 rpm.

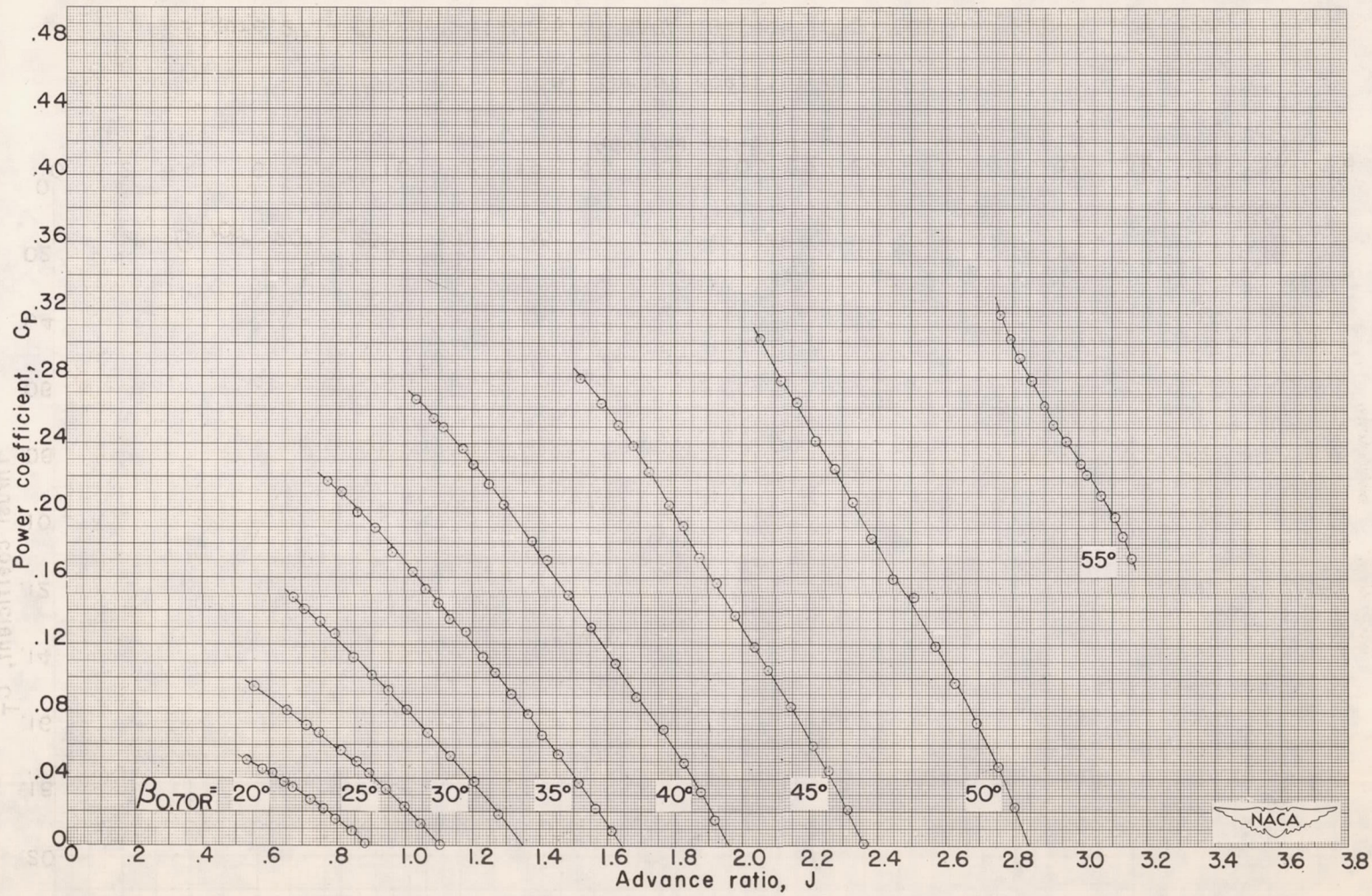

(b) Power coefficient.

Figure 27.- Continued. 1350 rpm.

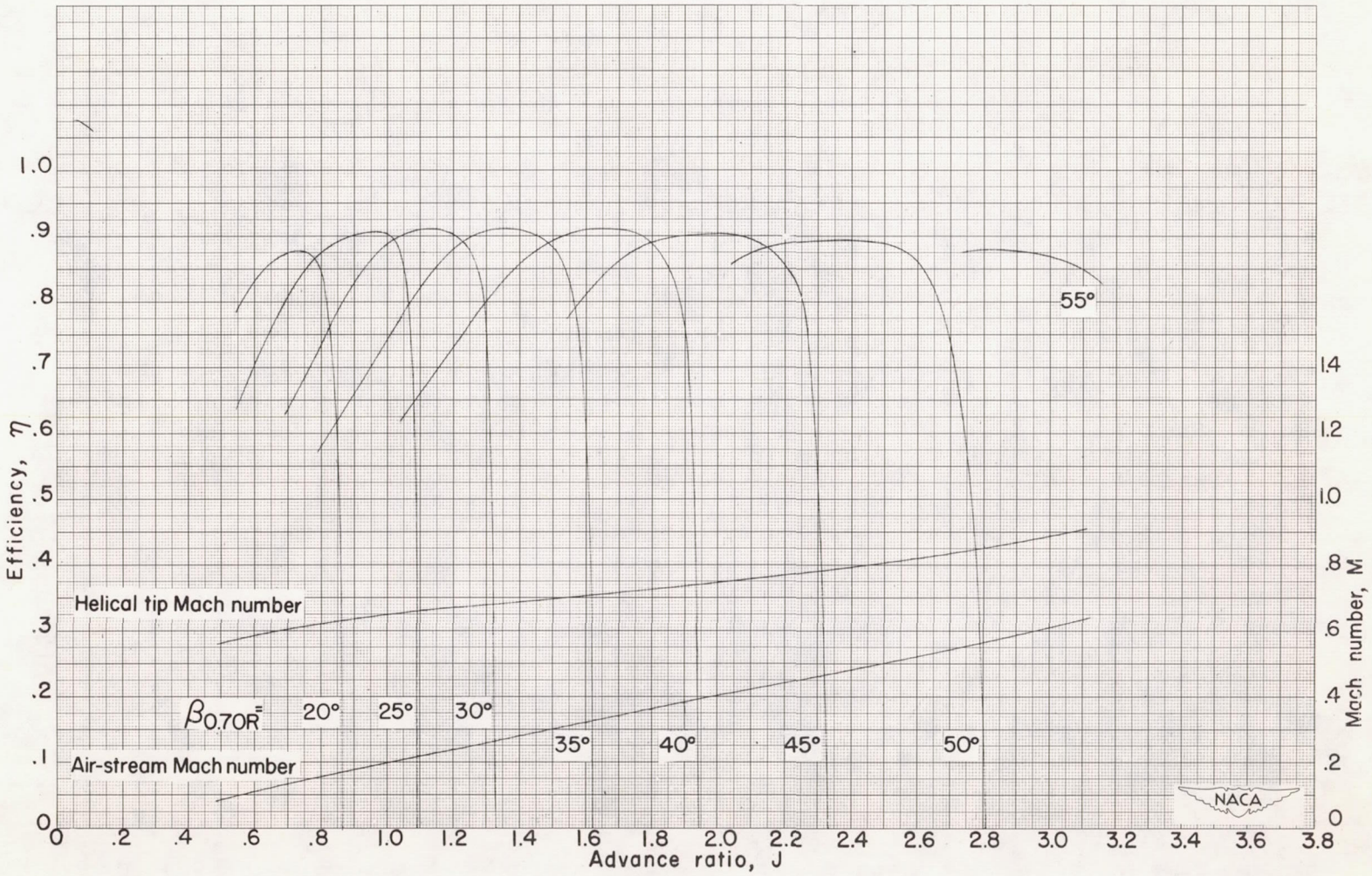

(c) Efficiency.

Figure 27.- Concluded. 1350 rpm.

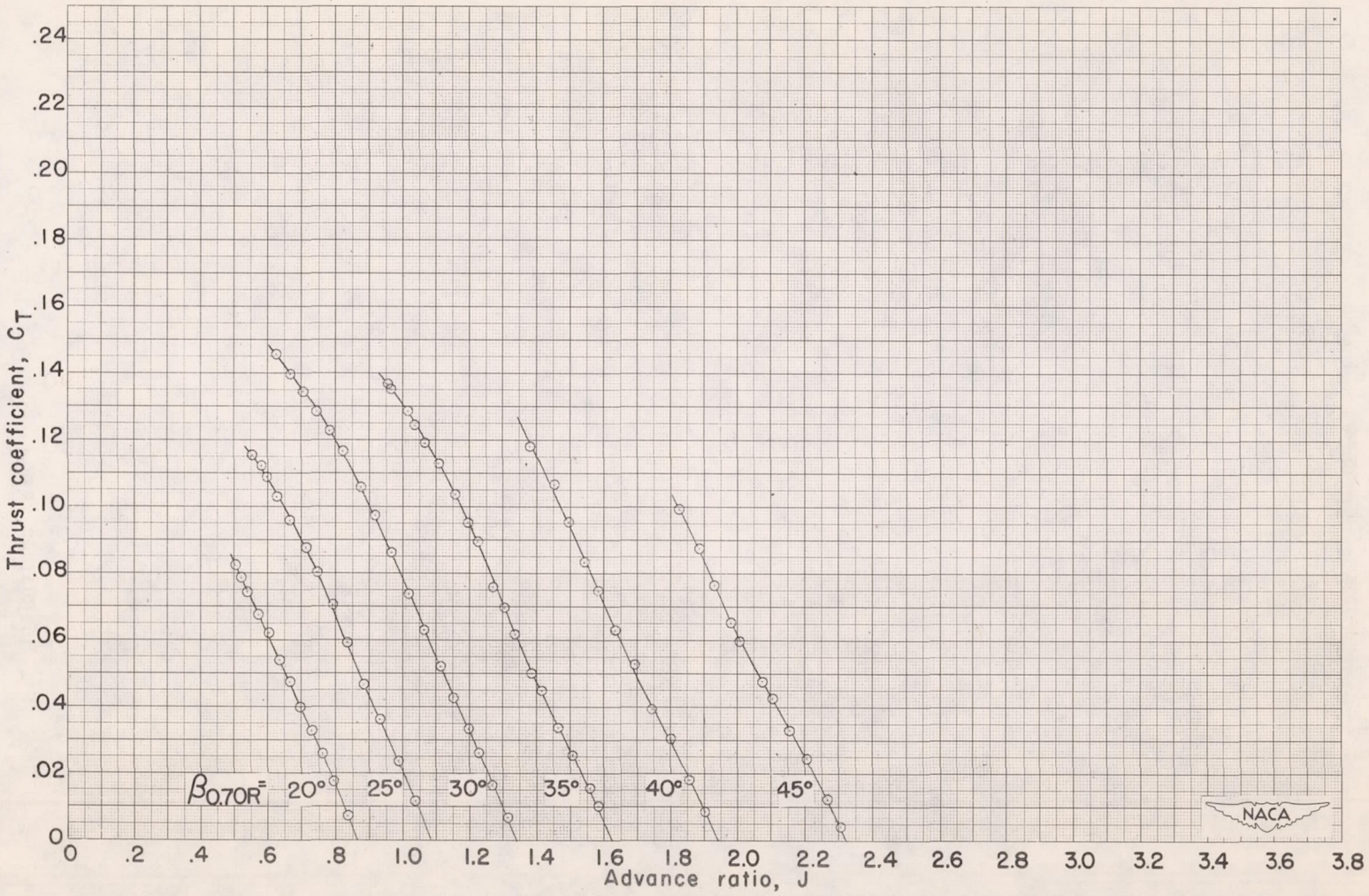

(a) Thrust coefficient.

Figure 28.- Characteristics of NACA 10-(1.5)(062)-057 propeller; 1600 rpm.

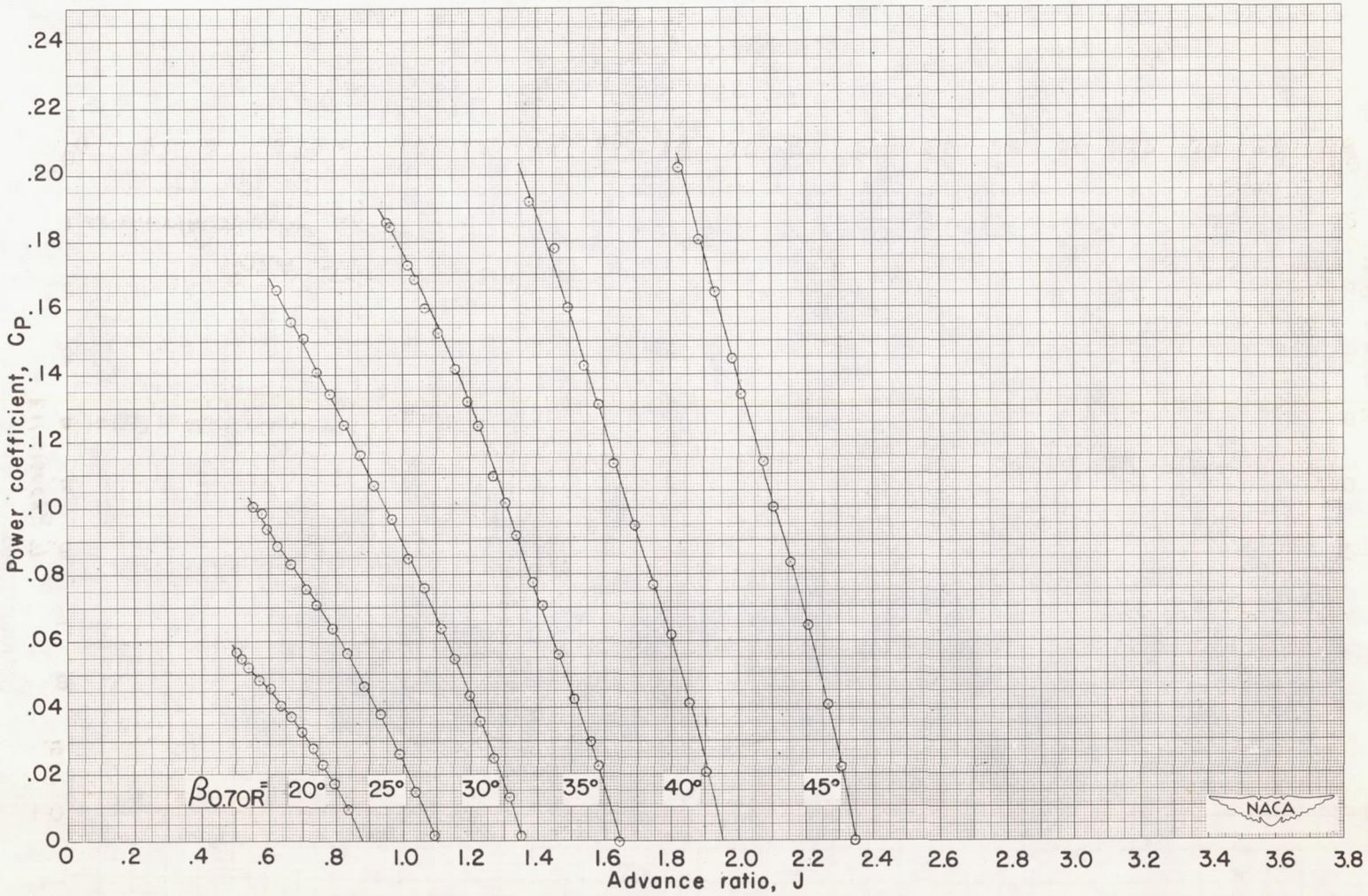

(b) Power coefficient.

Figure 28.- Continued. 1600 rpm.

(c) Efficiency.

Figure 28.- Concluded. 1600 rpm.

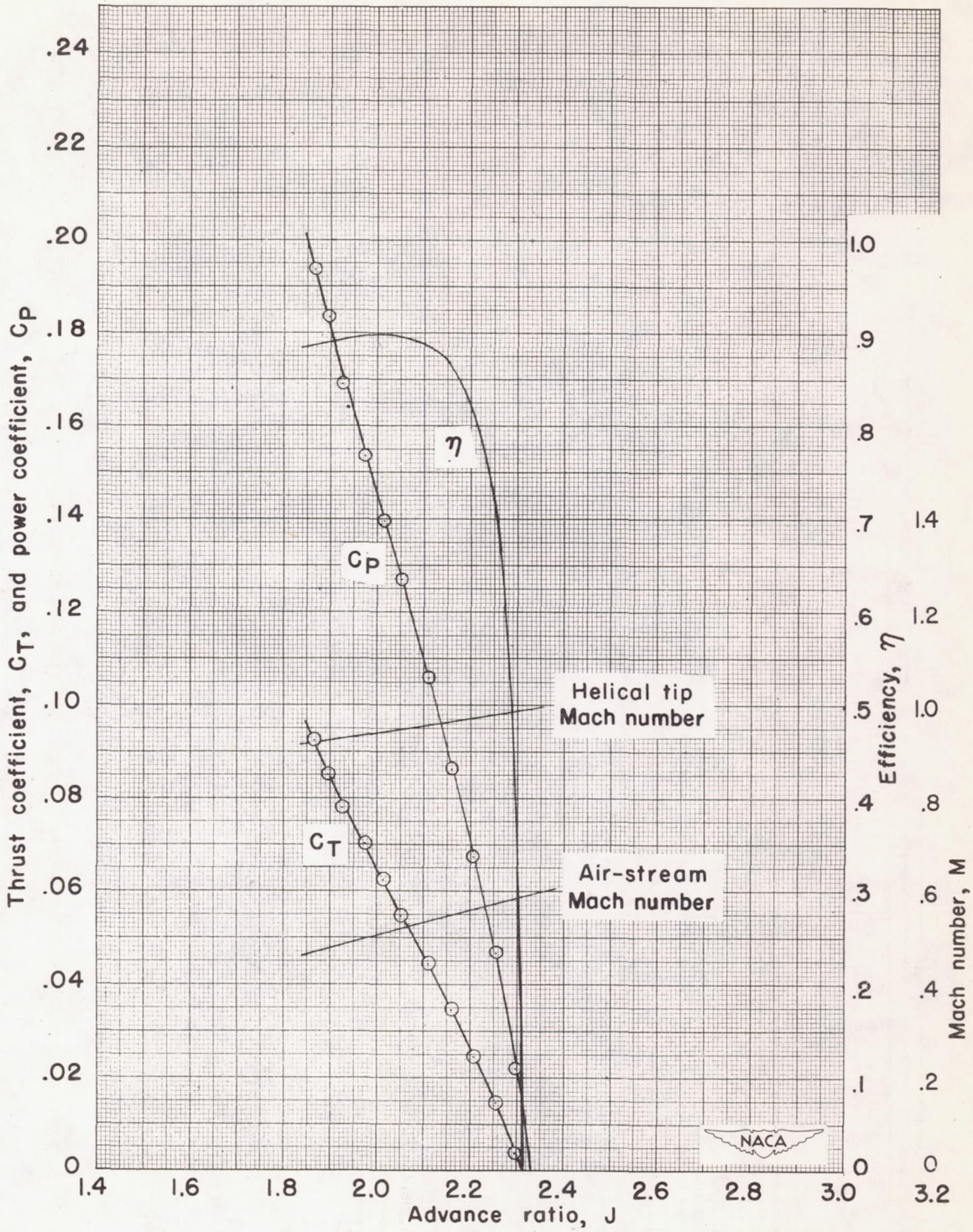

Figure 29.- Characteristics of NACA 10-(1.5)(062)-057 propeller; 1680 rpm; $\beta_{0.70R} = 45^{\circ}$.

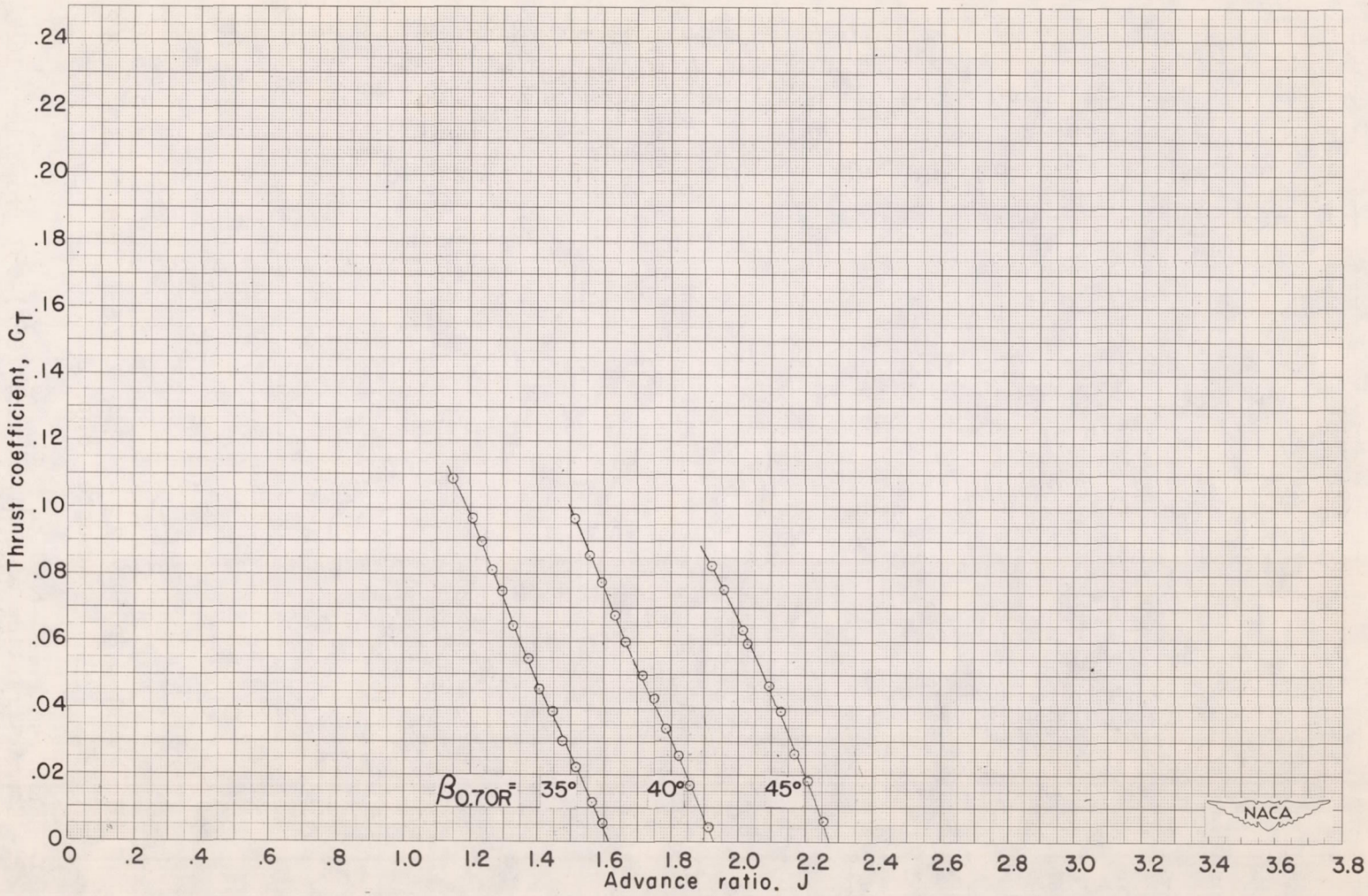

(a) Thrust coefficient.

Figure 30.- Characteristics of NACA 10-(1.5)(062)-057 propeller; 1800 rpm.

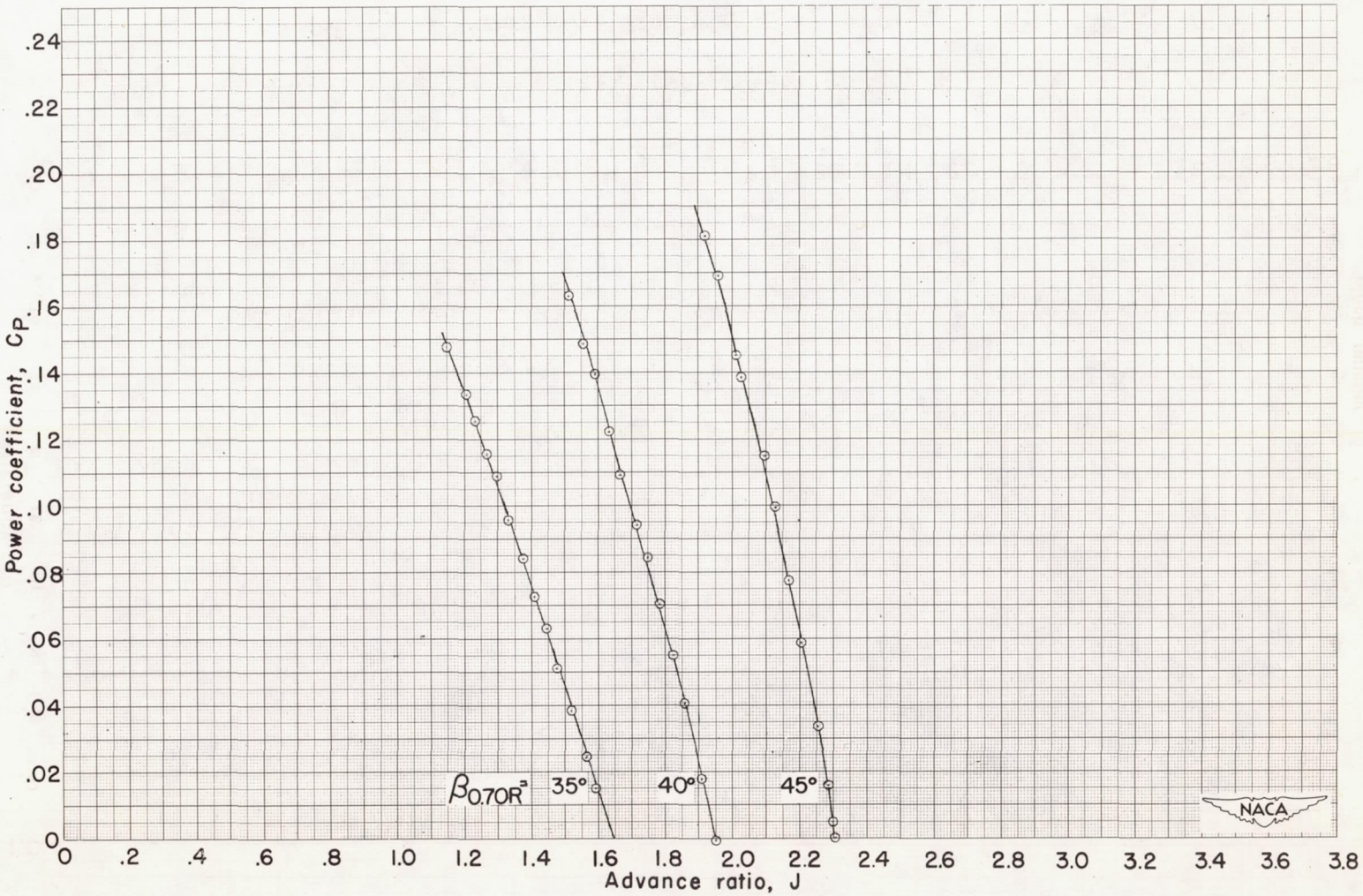

(b) Power coefficient.

Figure 30.- Continued. 1800 rpm.

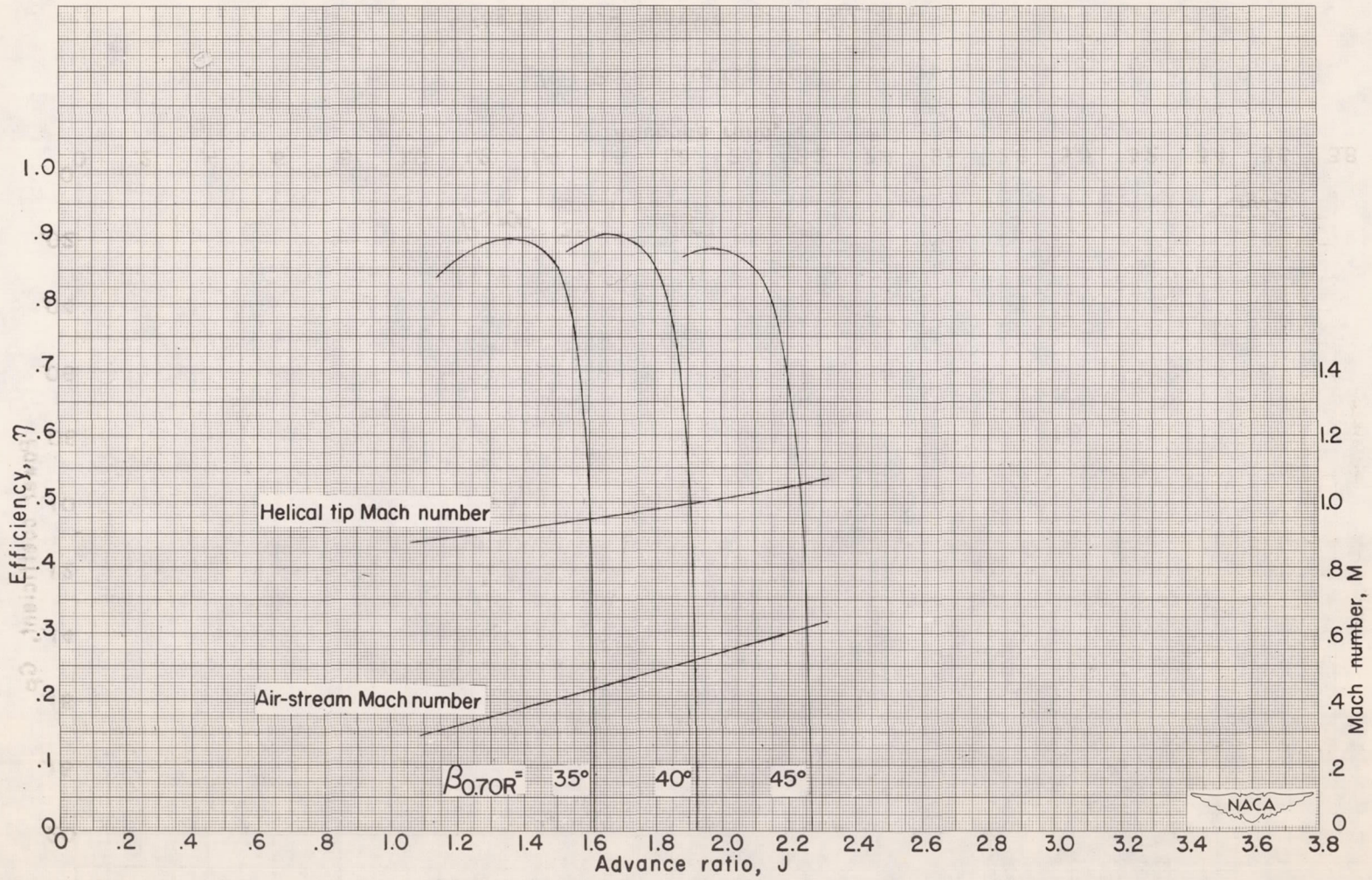

(c) Efficiency.

Figure 30.- Concluded. 1800 rpm.

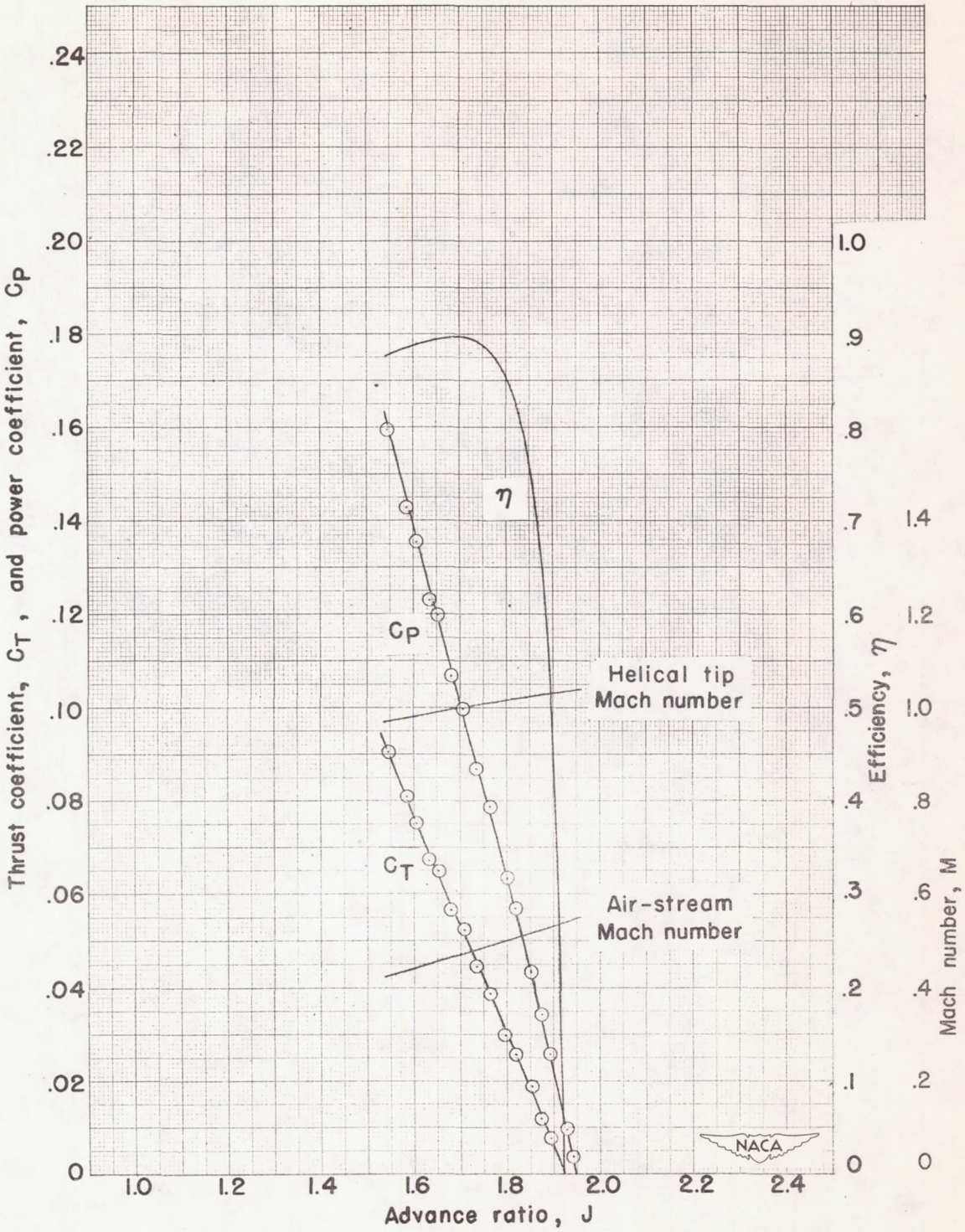

Figure 31.- Characteristics of NACA 10-(1.5)(062)-057 propeller; 1900 rpm; $\beta_{0.70R} = 40^{\circ}$.

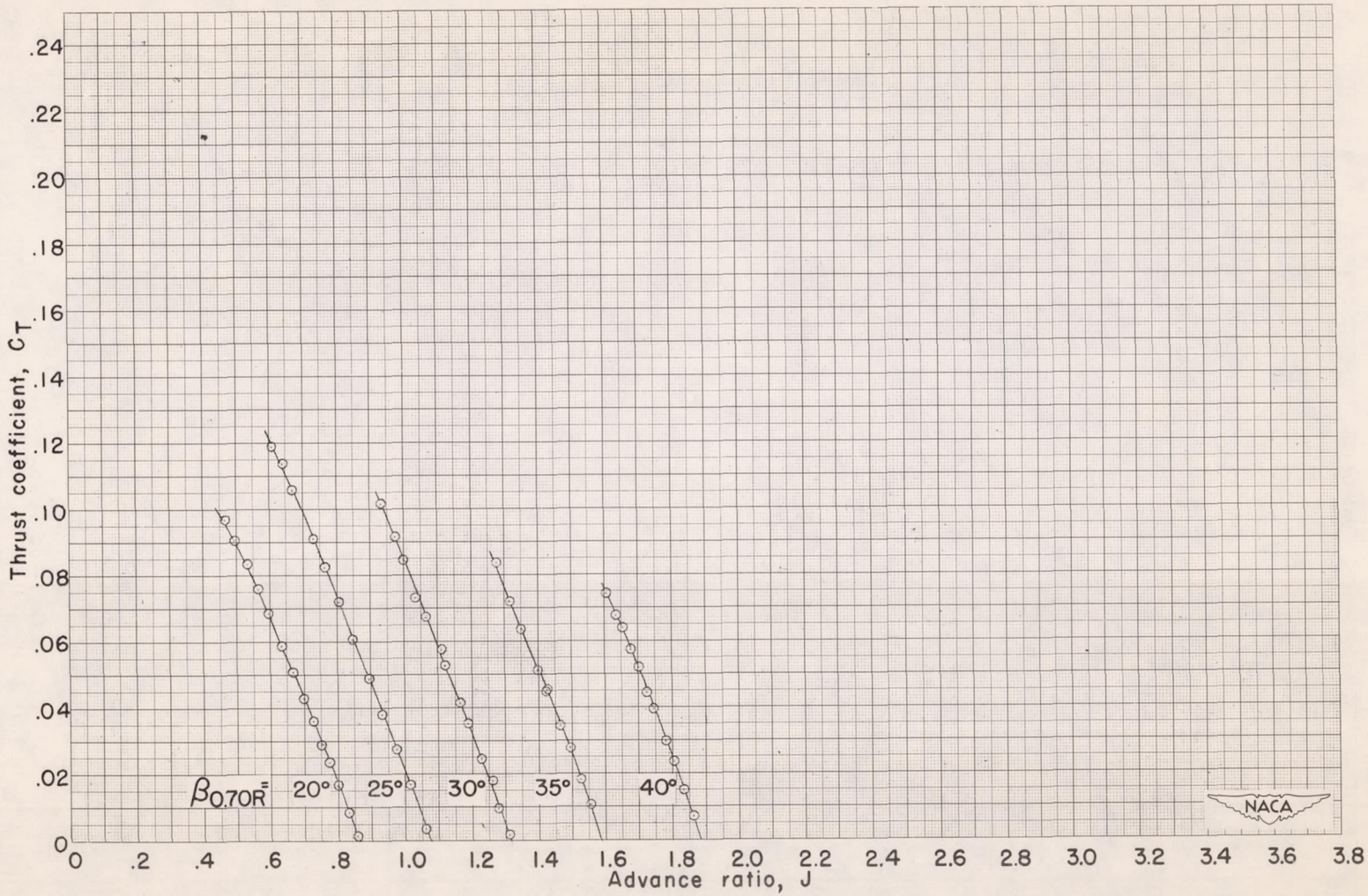

(a) Thrust coefficient.

Figure 32.- Characteristics of NACA 10-(1.5)(062)-057 propeller; 2000 rpm.

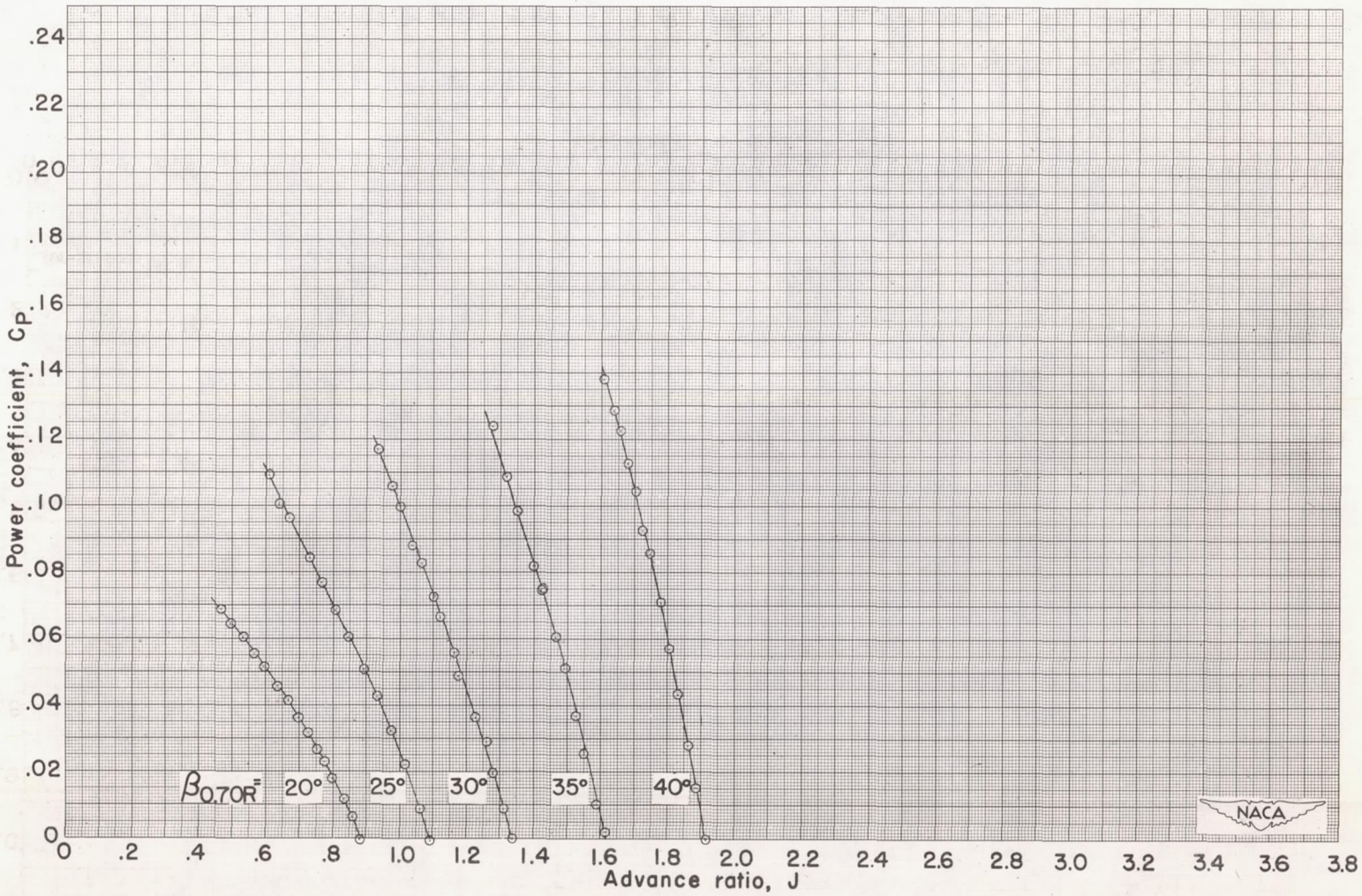

(b) Power coefficient.

Figure 32.- Continued. 2000 rpm.

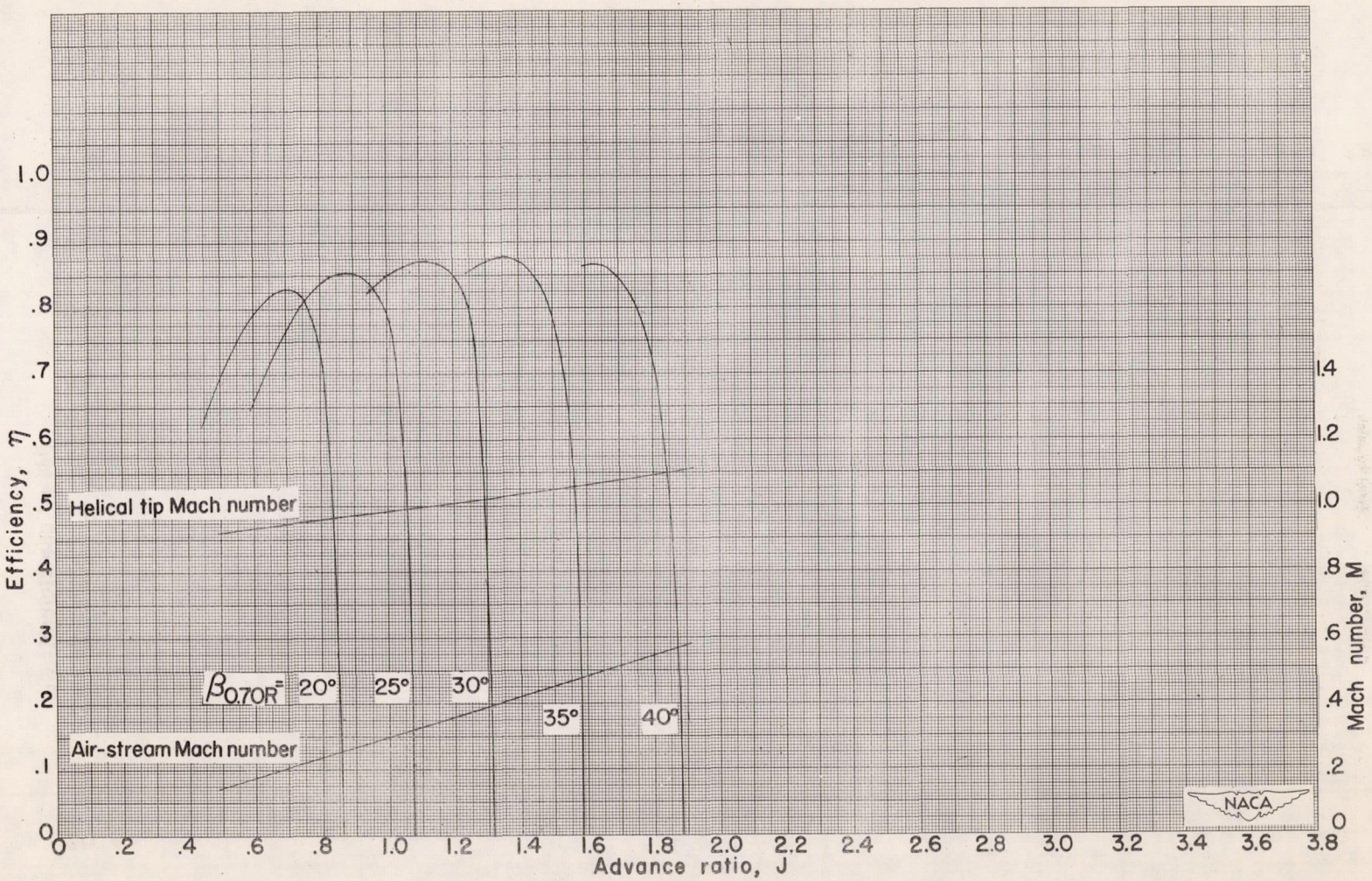

(c) Efficiency.

Figure 32.- Concluded. 2000 rpm.

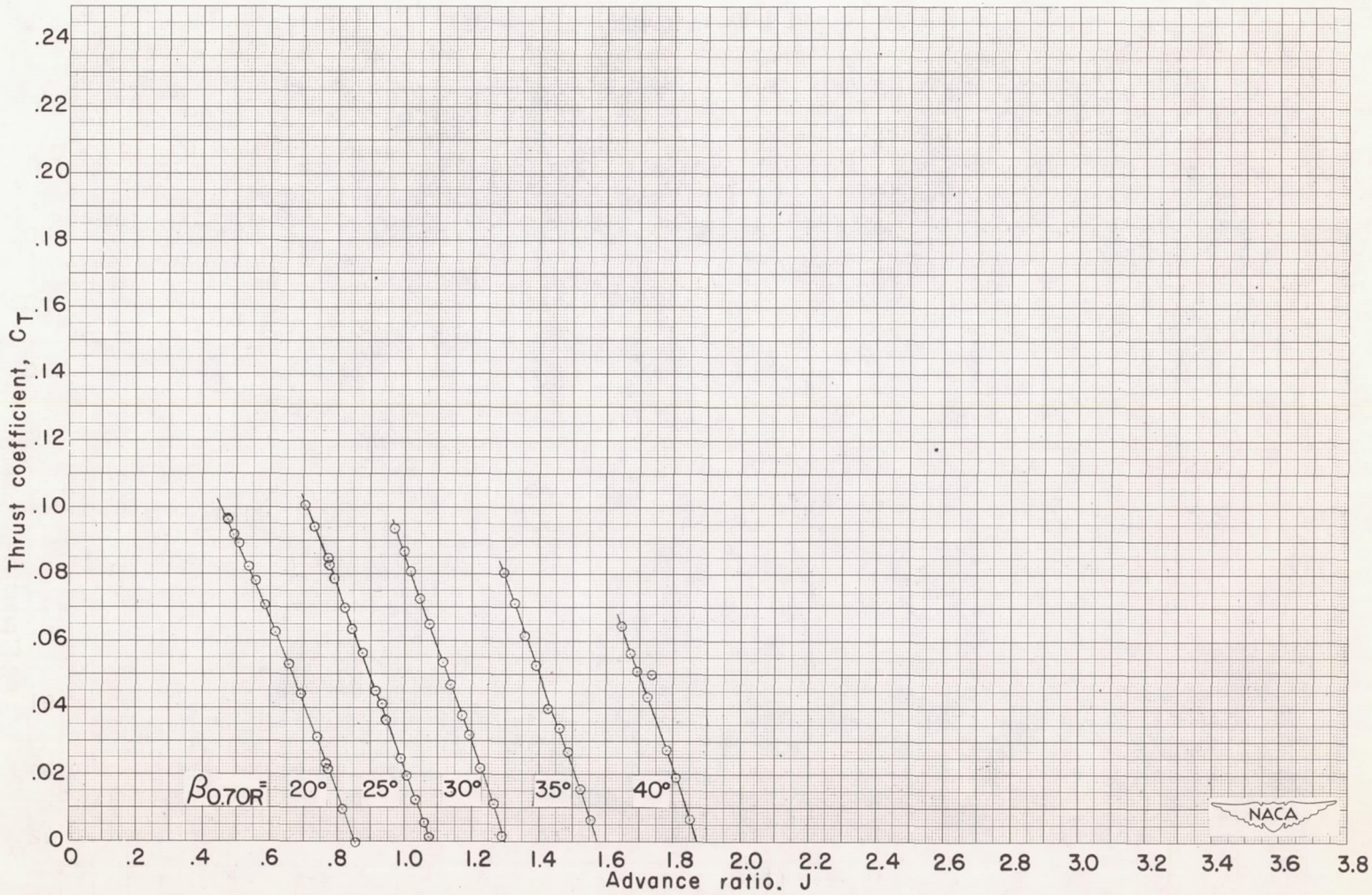

(a) Thrust coefficient.

Figure 33.- Characteristics of NACA 10-(1.5)(062)-057 propeller; 2100 rpm.

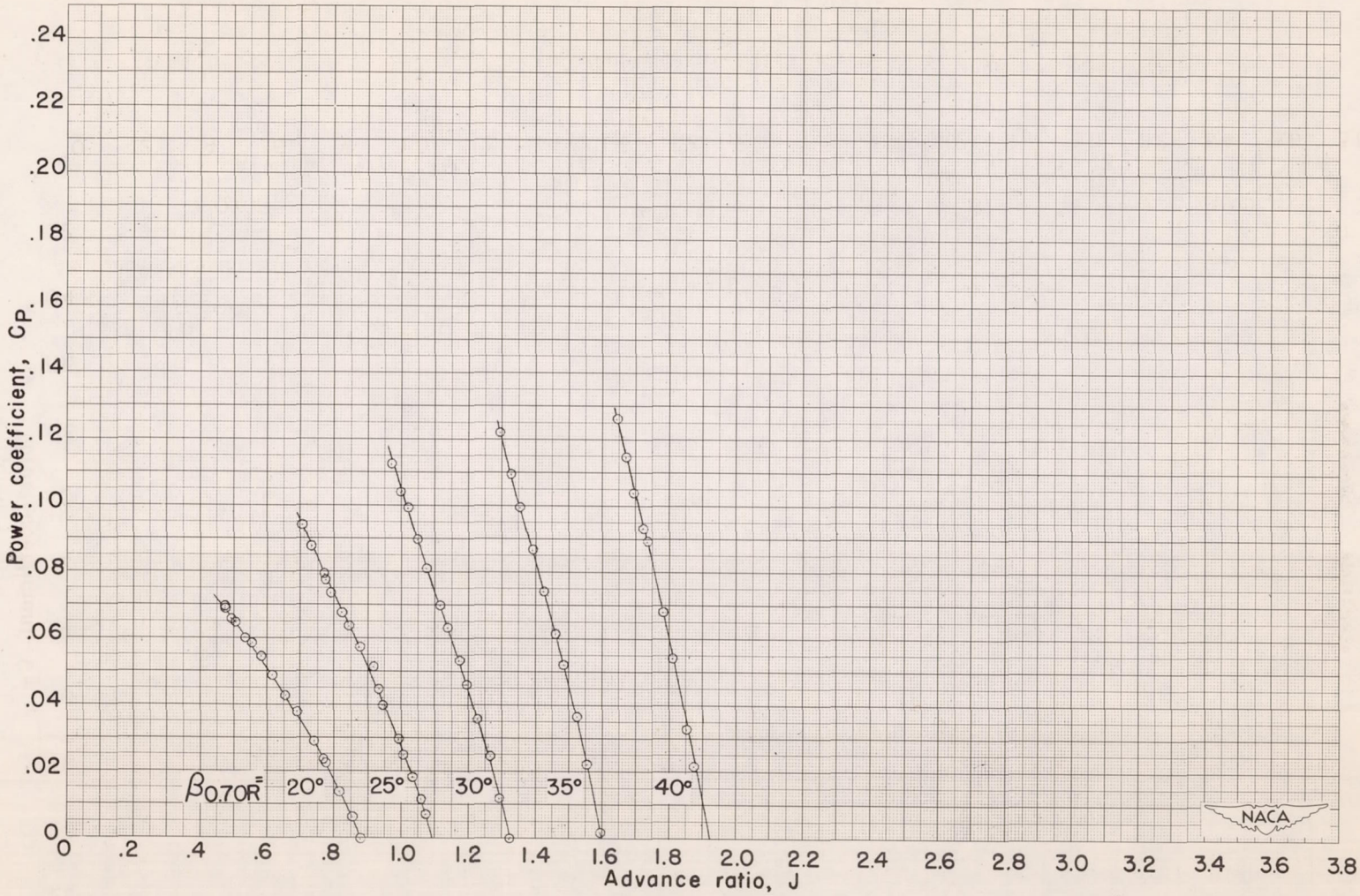

(b) Power coefficient.

Figure 33.- Continued. 2100 rpm.

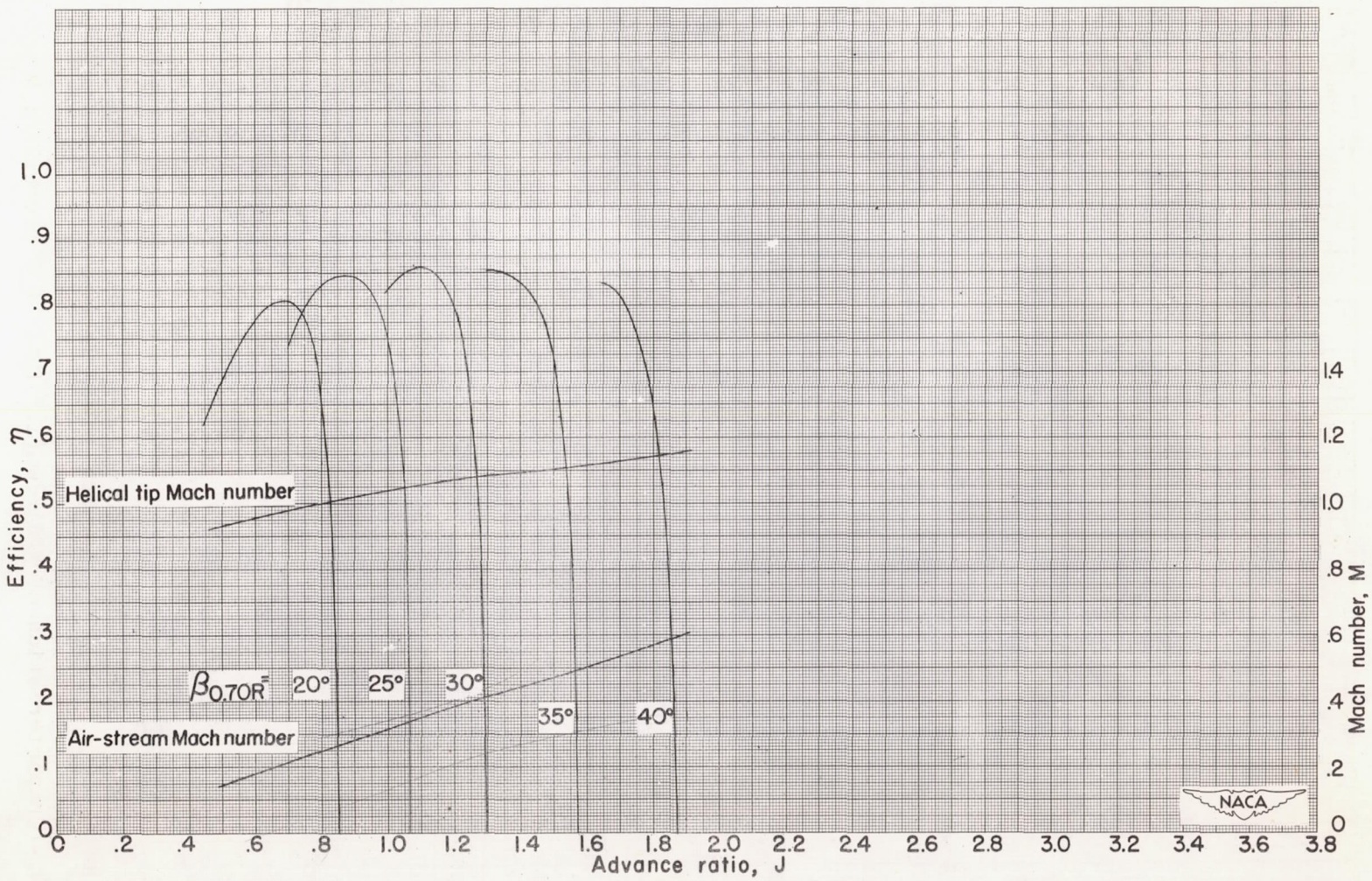

(c) Efficiency.

Figure 33.- Concluded. 2100 rpm.

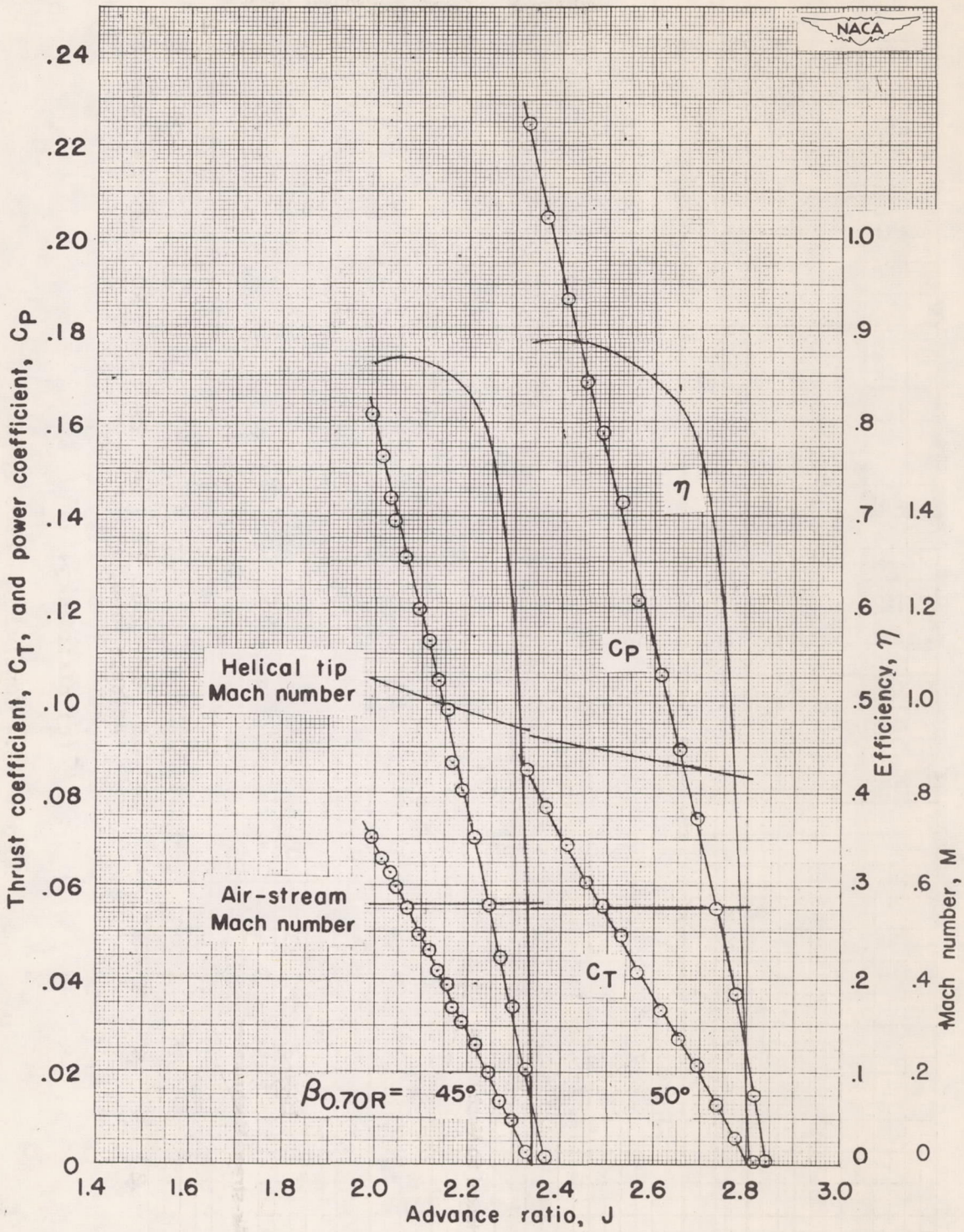

Figure 34.- Characteristics of NACA 10-(1.5)(062)-057 propeller; M = 0.56.

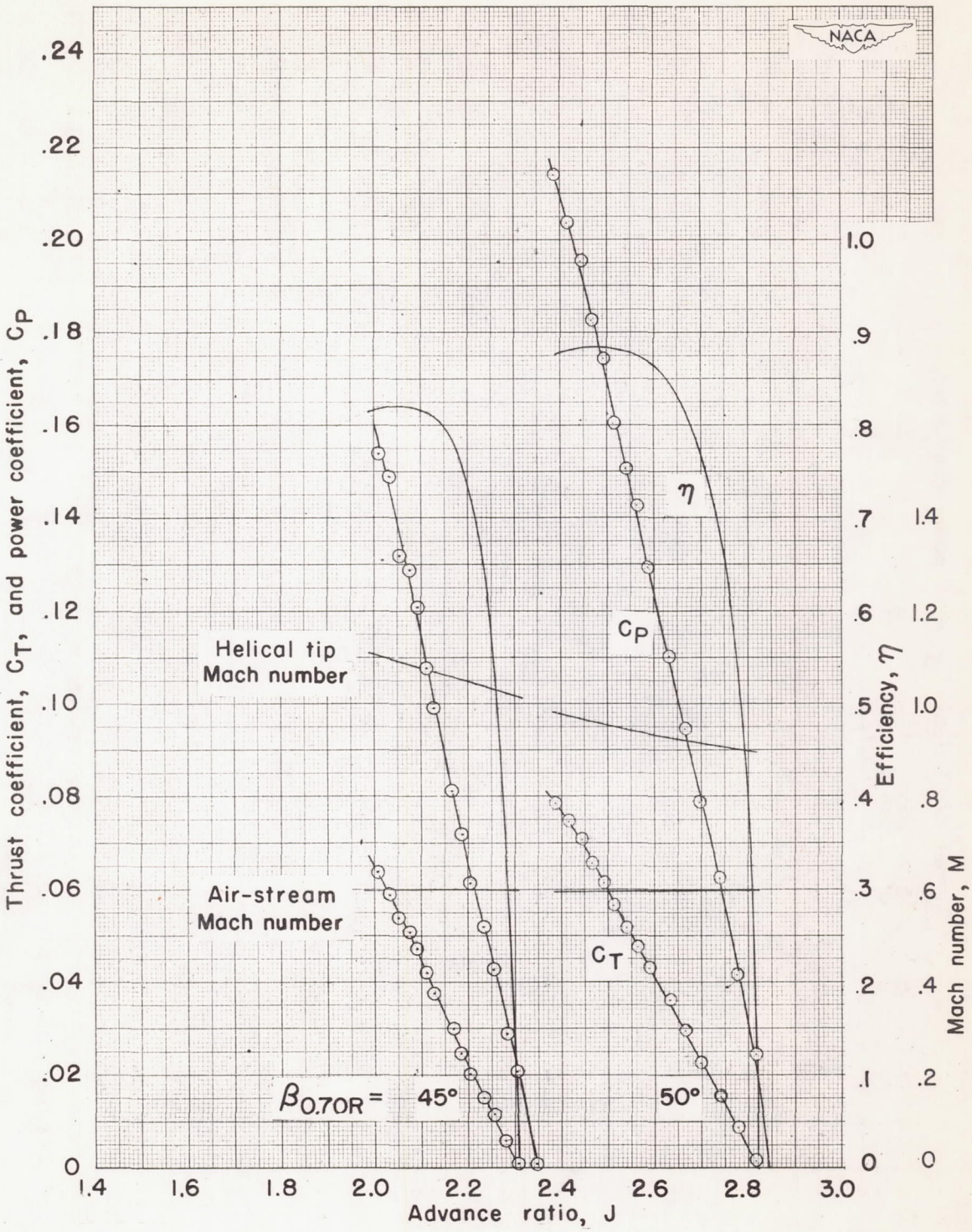

Figure 35.- Characteristics of NACA 10-(1.5)(062)-057 propeller; M = 0.60.

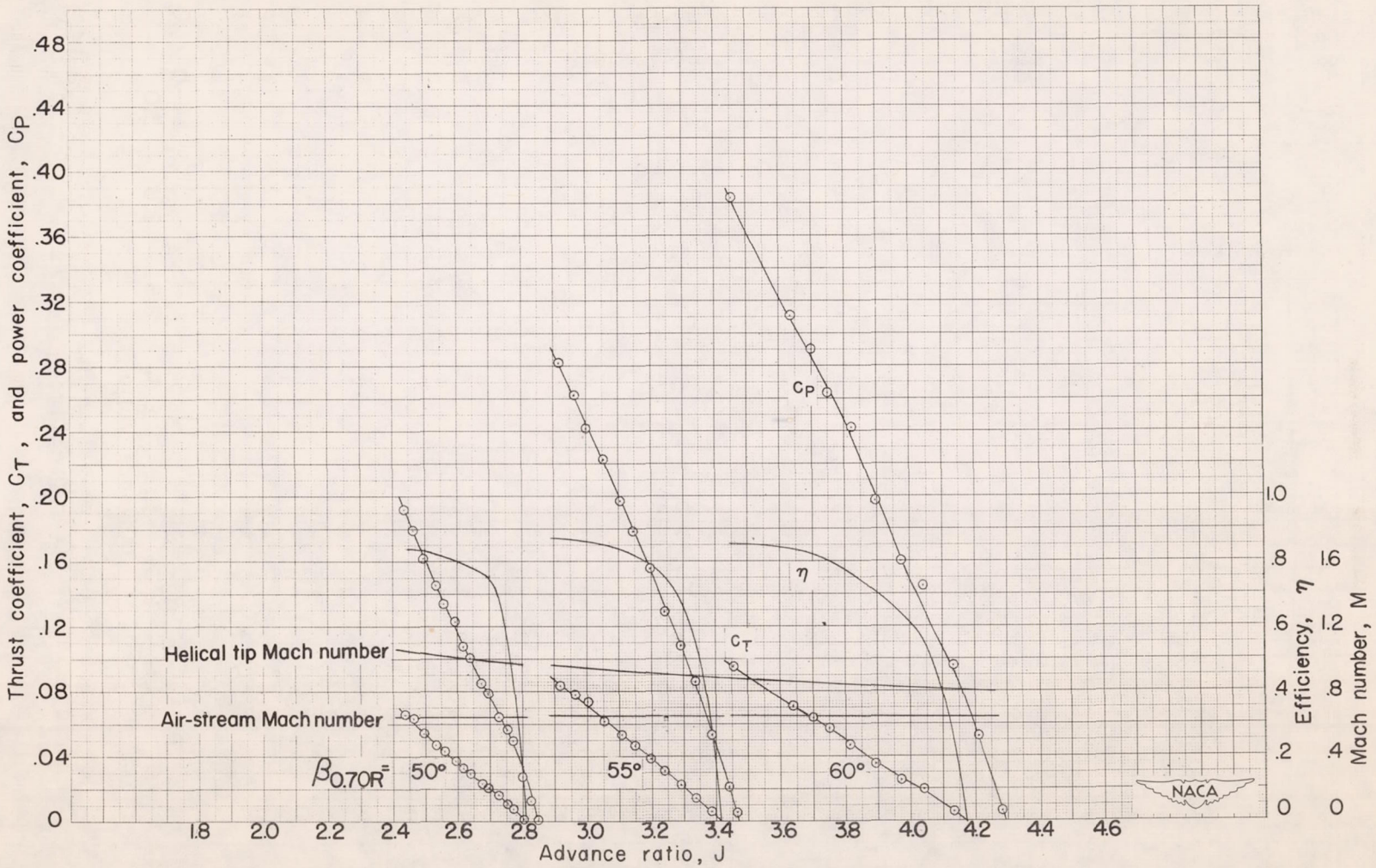

Figure 36.- Characteristics of NACA 10-(1.5)(062)-057 propeller; M = 0.65.

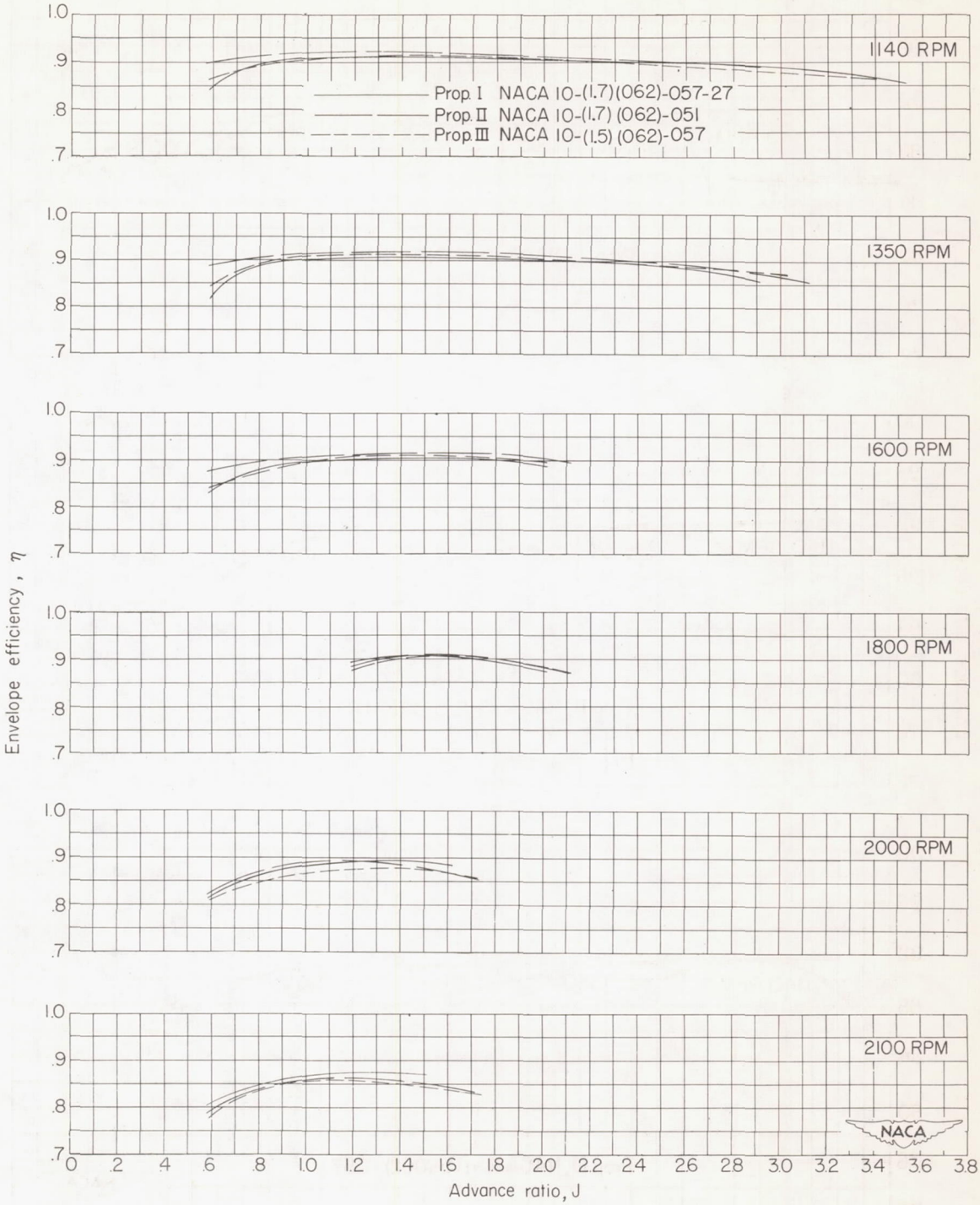

Figure 37.- Comparison of envelope efficiency curves for swept and unswept propellers.

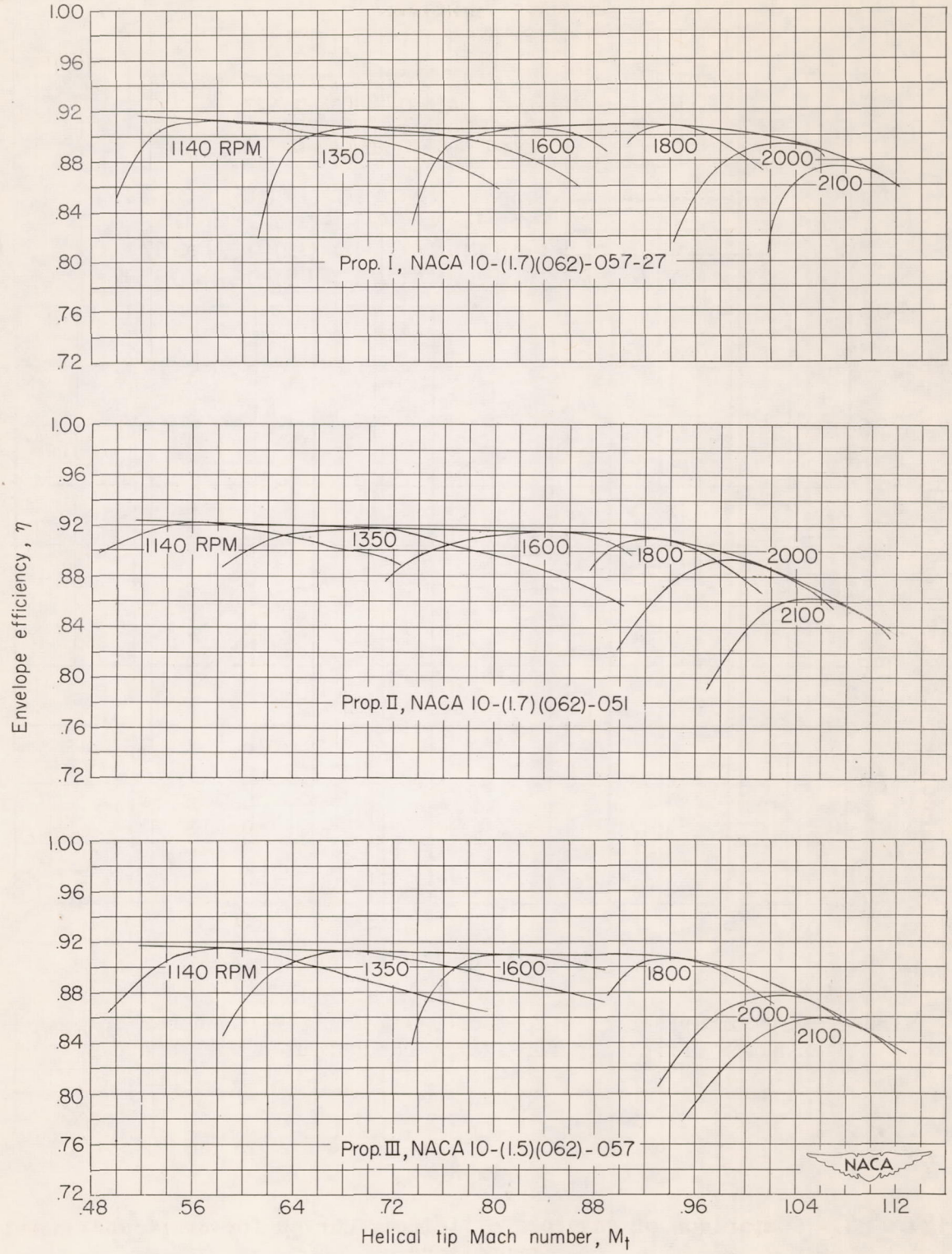

Figure 38.- Effect of helical tip Mach number on peak envelope efficiency.

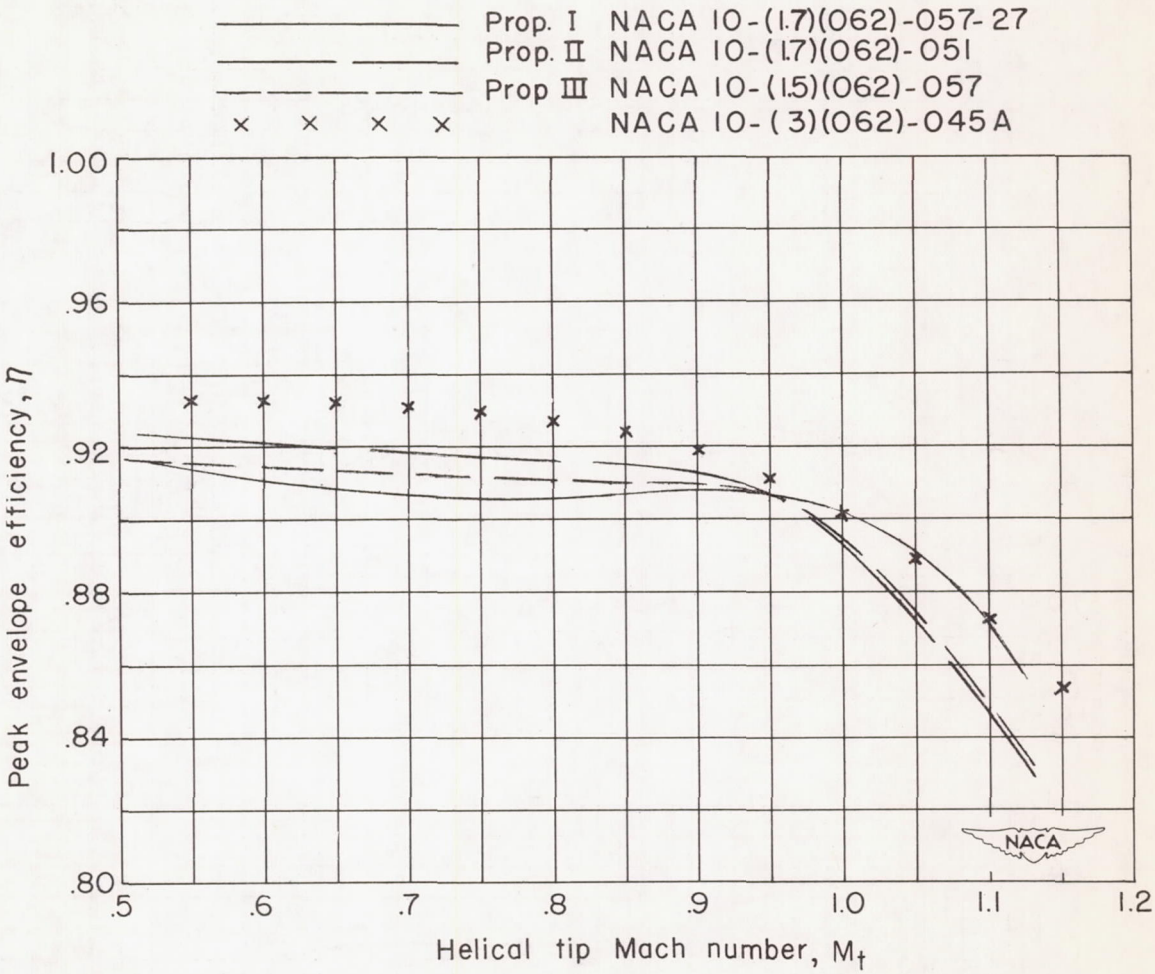

Figure 39.- Comparison of effect of helical tip Mach number on peak envelope efficiency for swept and unswept propellers.

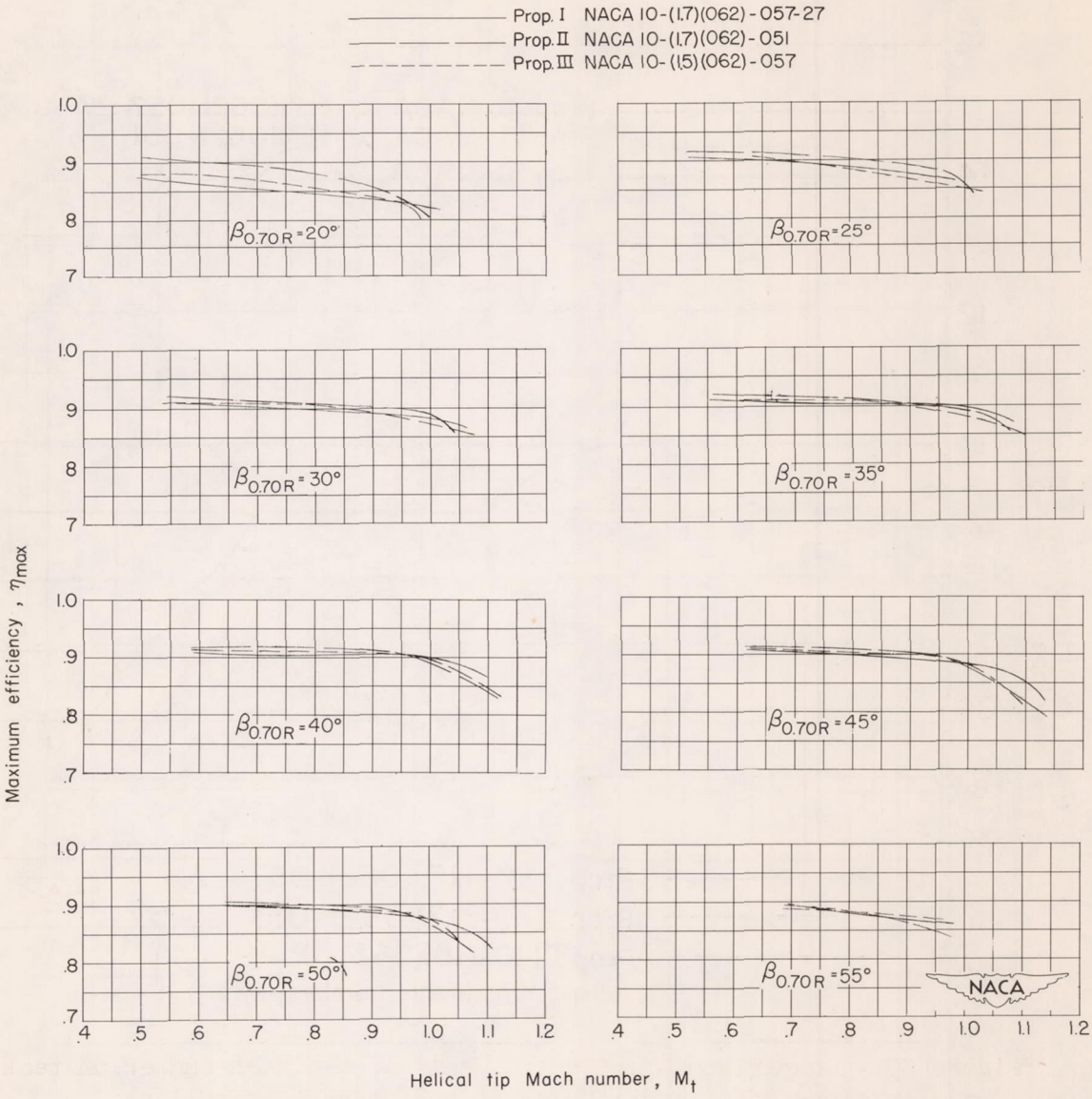

Figure 40.- Effect of helical tip Mach number on maximum efficiency for given blade-angle settings.

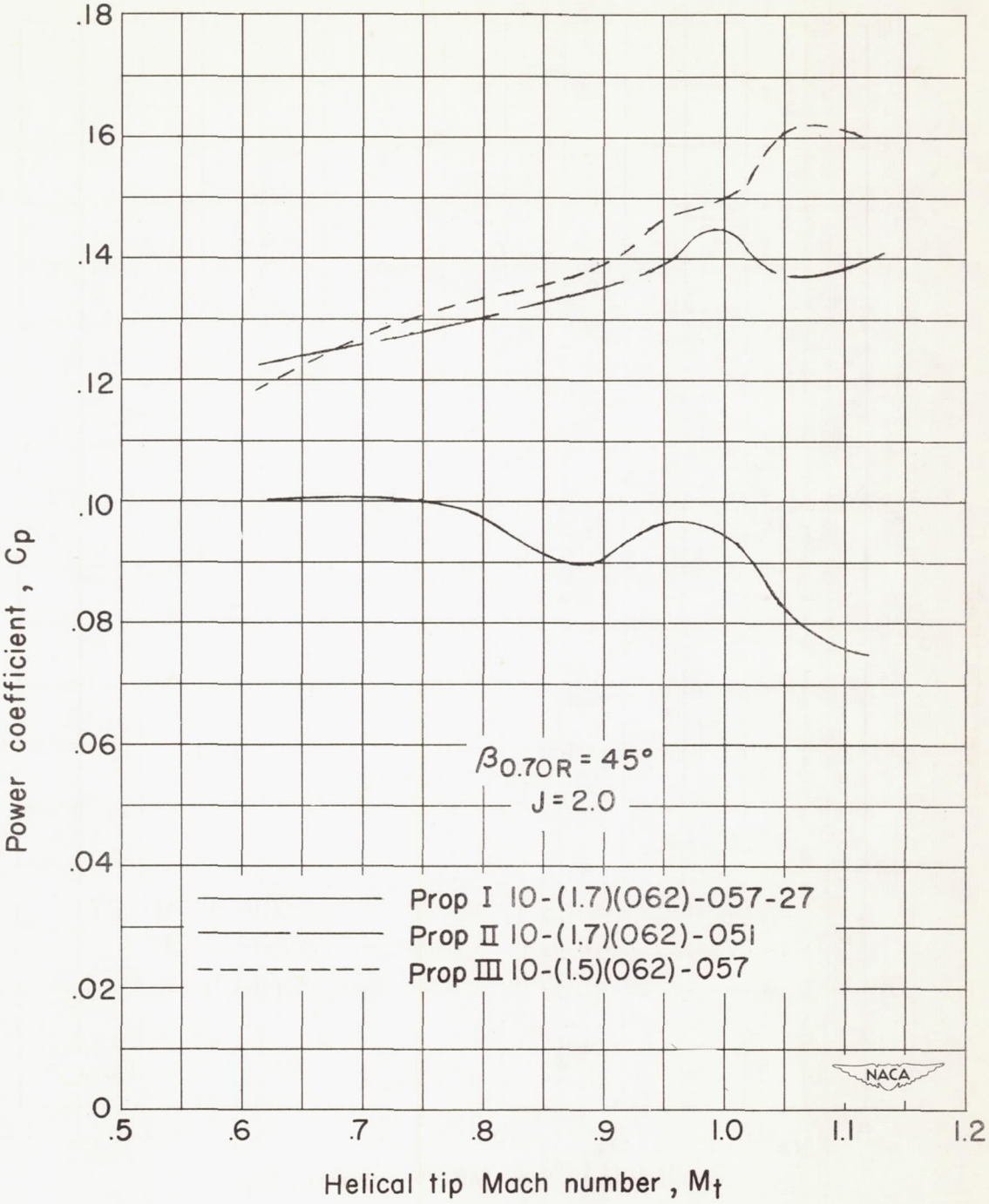

Figure 41.- Variation of power coefficient with helical tip Mach number at the design values of advance ratio and blade-angle setting for the three propellers.

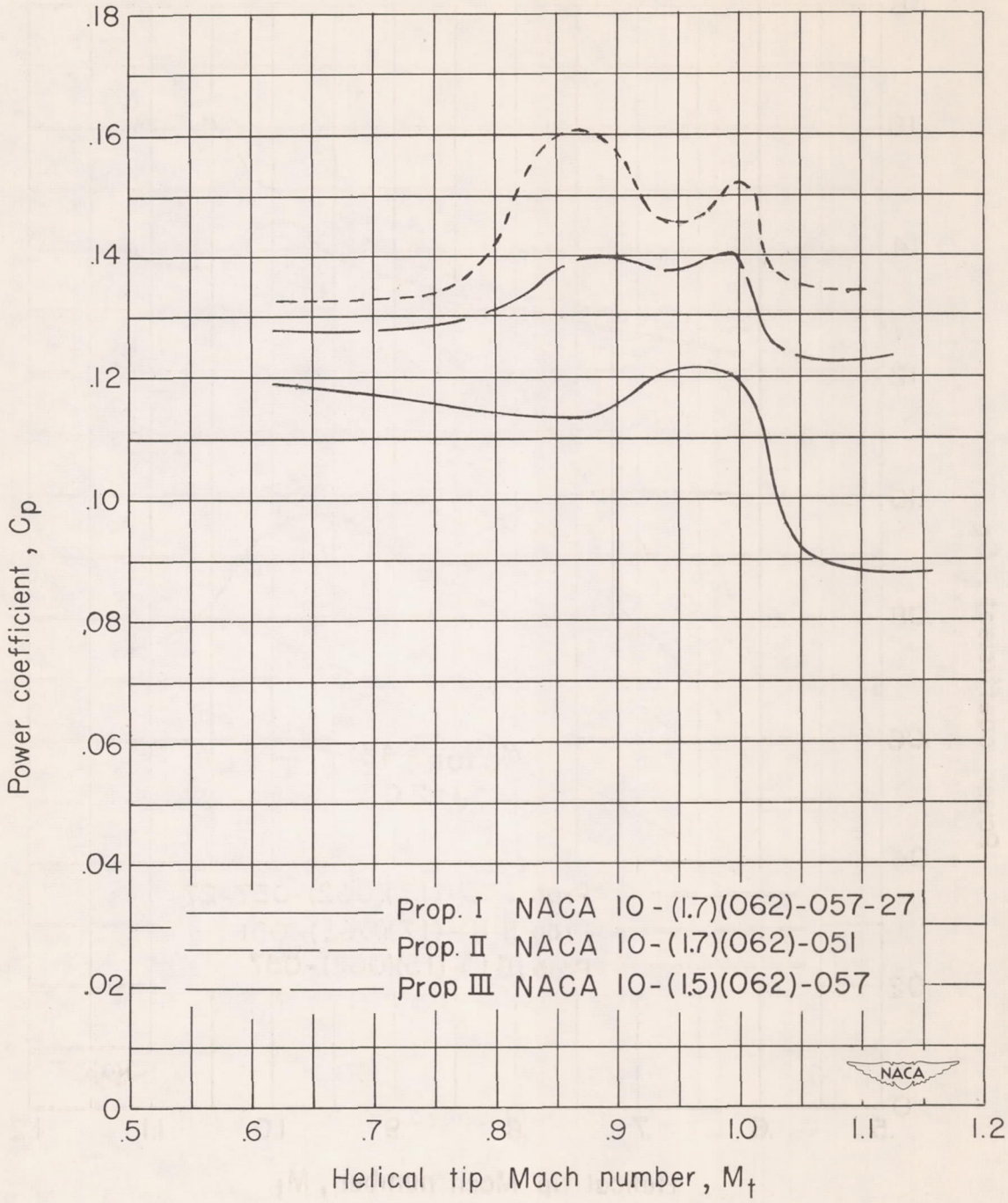

Figure 42.- Comparison of power coefficient for maximum efficiency for swept and unswept propellers. $\beta_{0.70R} = 45^{\circ}$.

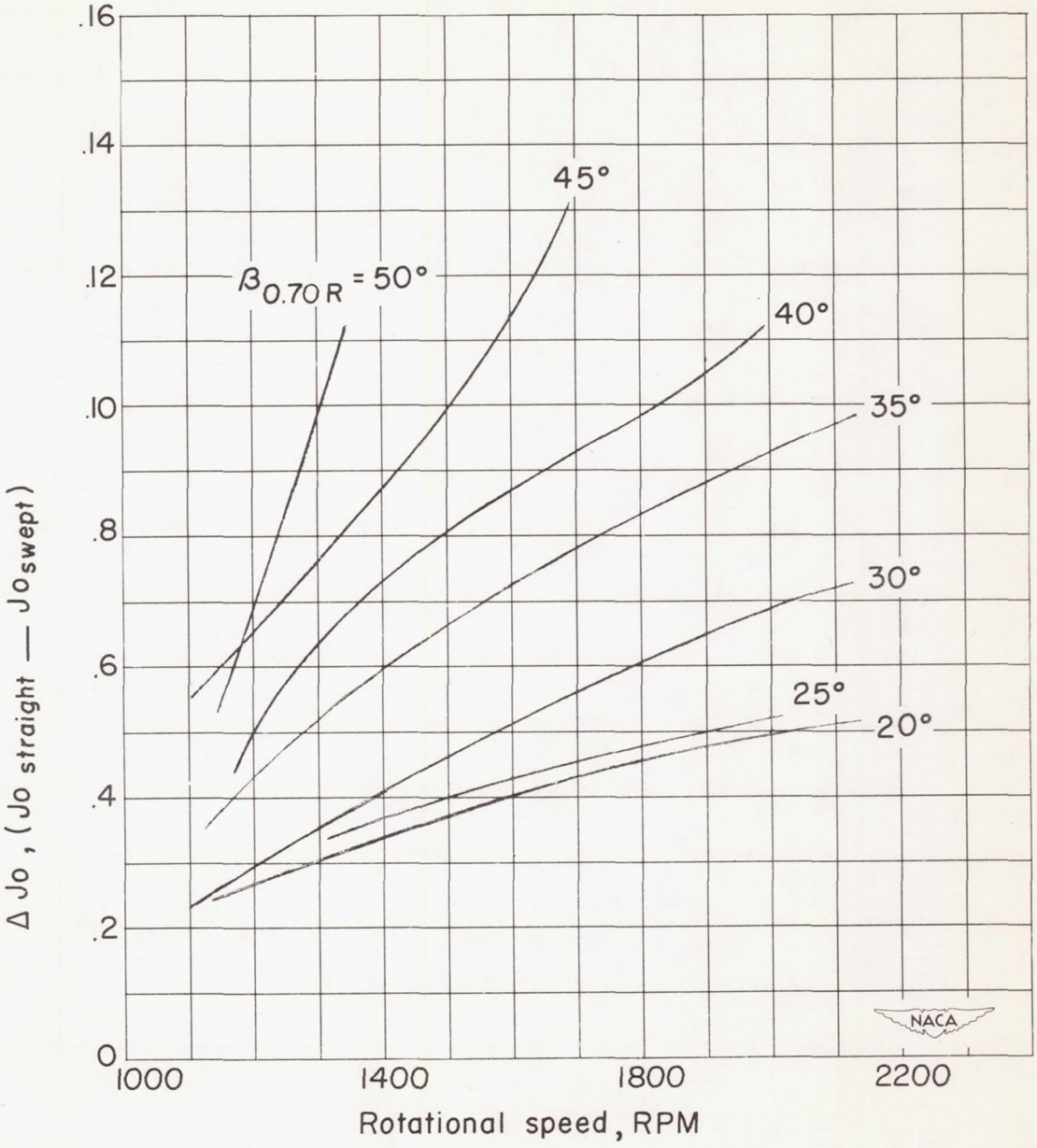

Figure 43.- Effect of rotational speed and blade-angle setting on difference in advance ratio for $C_t = 0$ between swept and straight propellers.

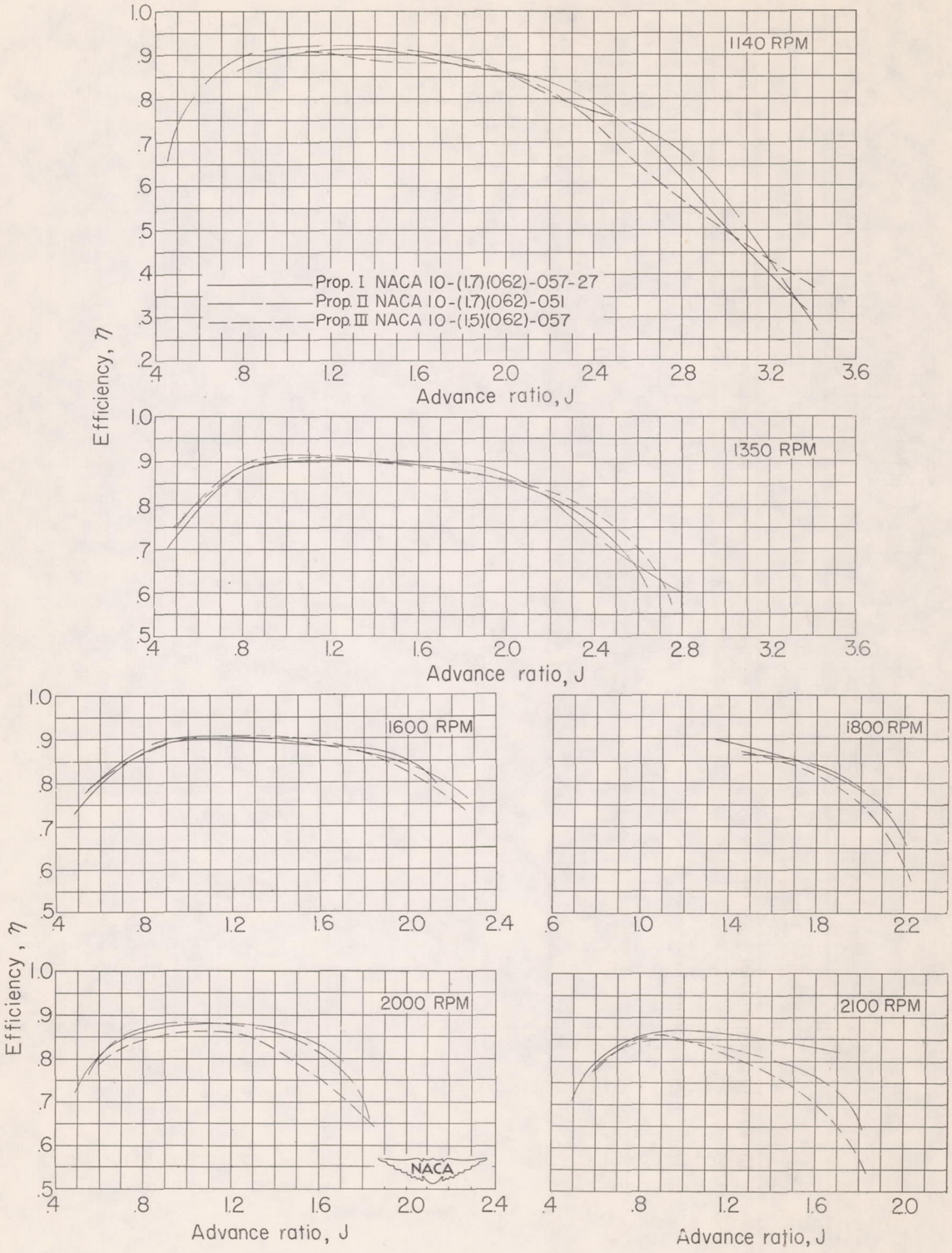

(a) $C_P = 0.05$.

Figure 44.- Comparison of efficiency at given values of power coefficient for swept and unswept propellers.

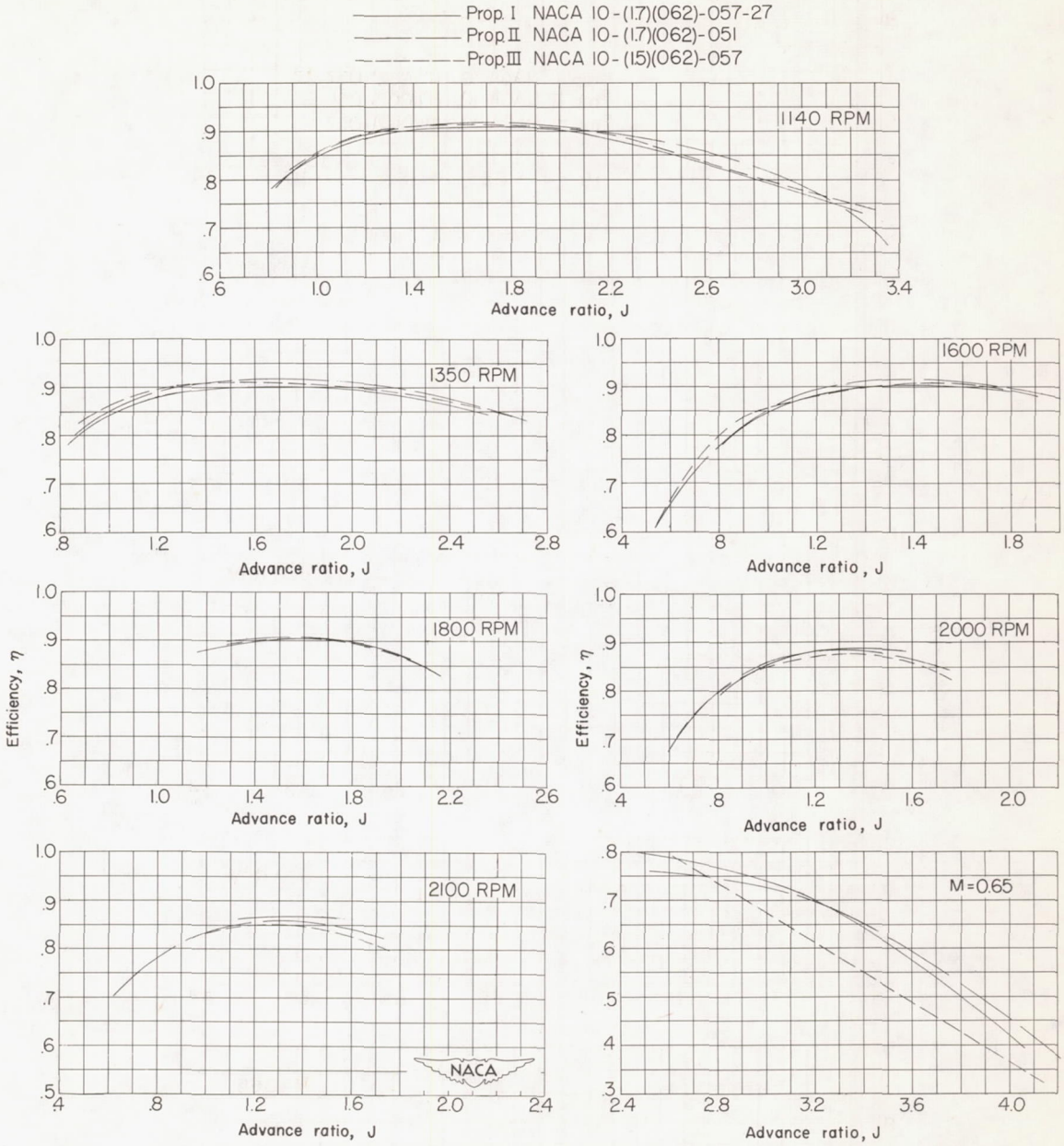

(b) $C_P = 0.10$.

Figure 44.- Continued.

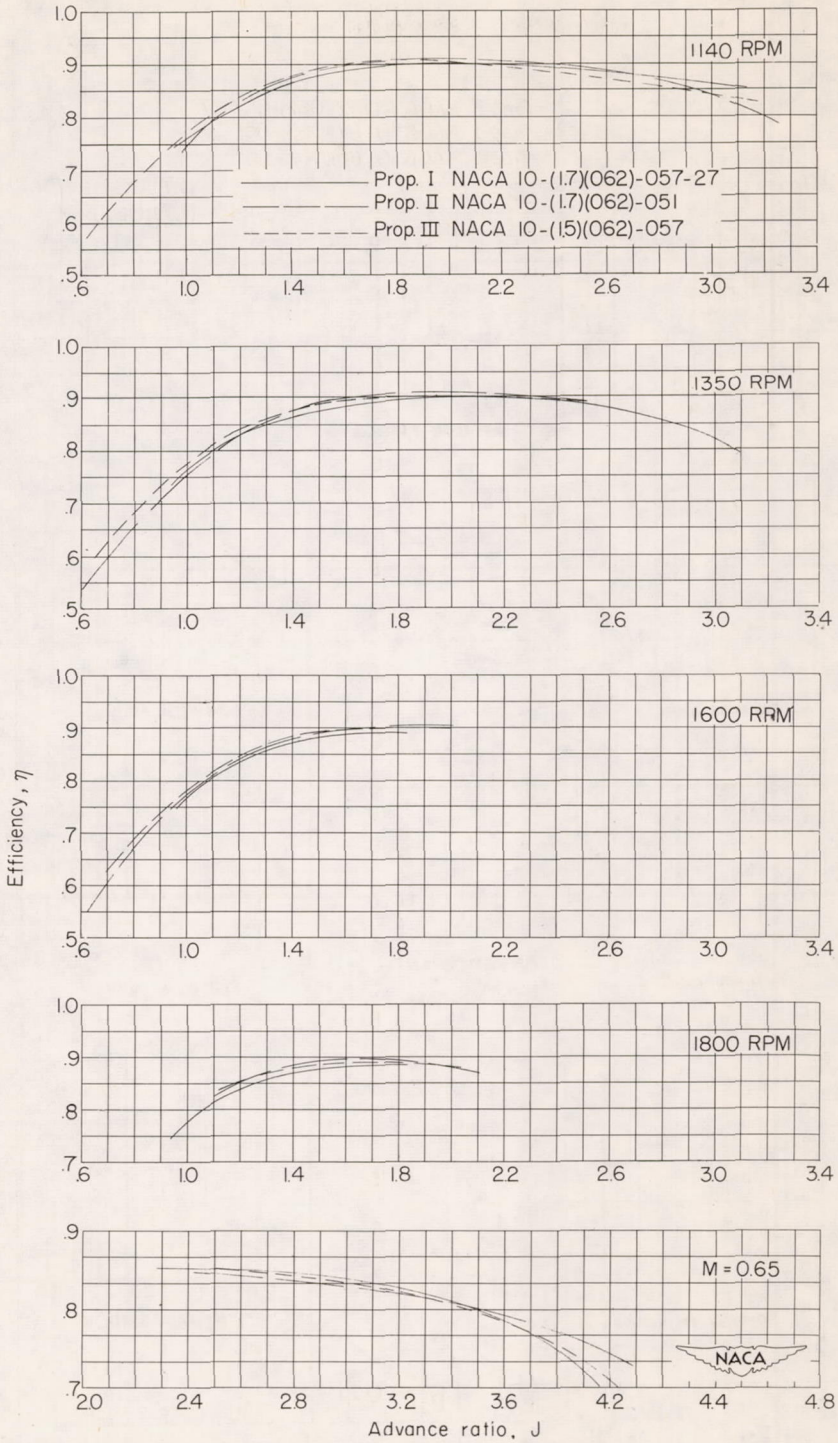

(c) $C_p = 0.15$.

Figure 44.- Continued.

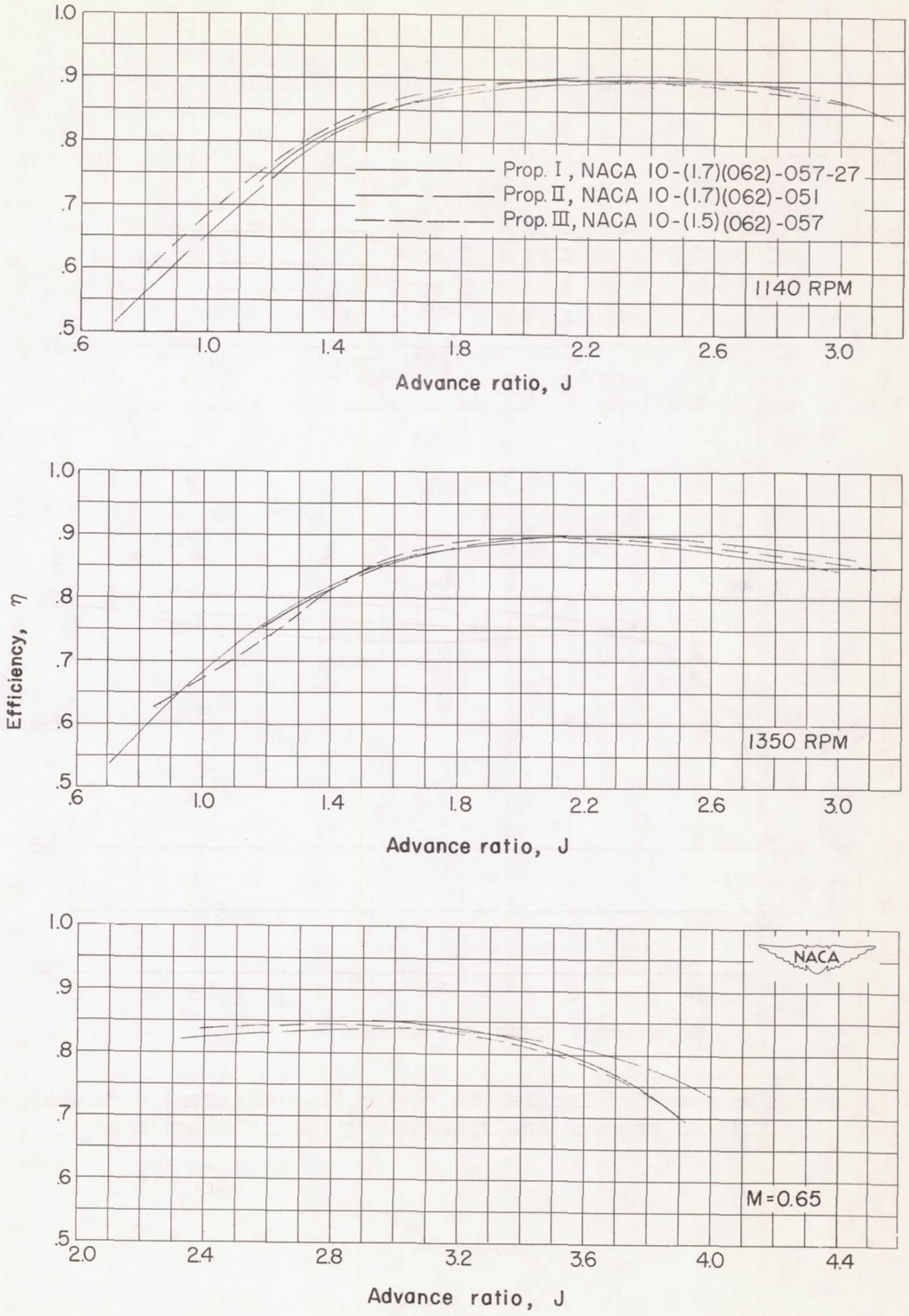

(d) $C_P = 0.20$.

Figure 44.- Continued.

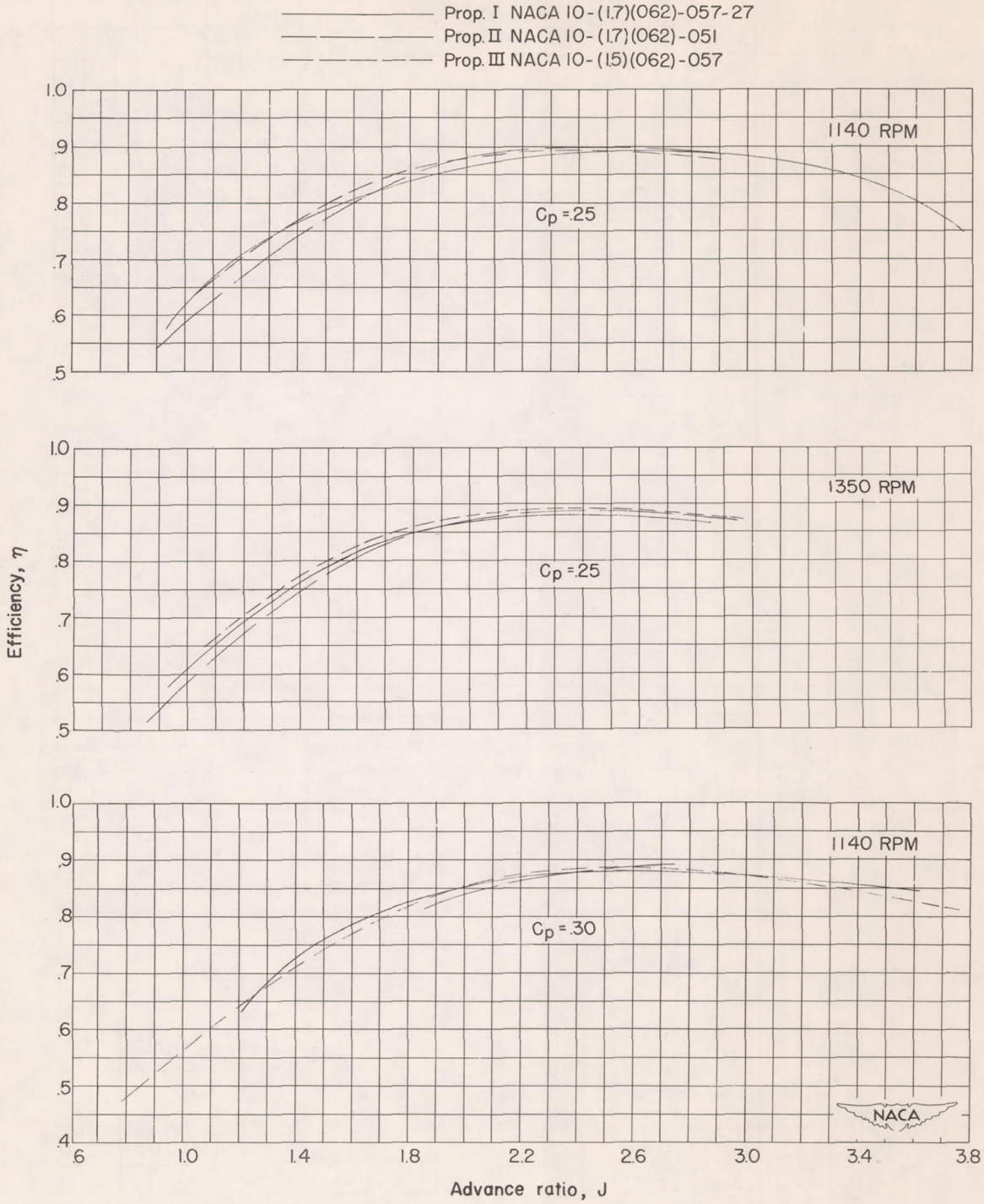

(e) $C_P = 0.25$ and $C_P = 0.30$.

Figure 44.- Concluded.

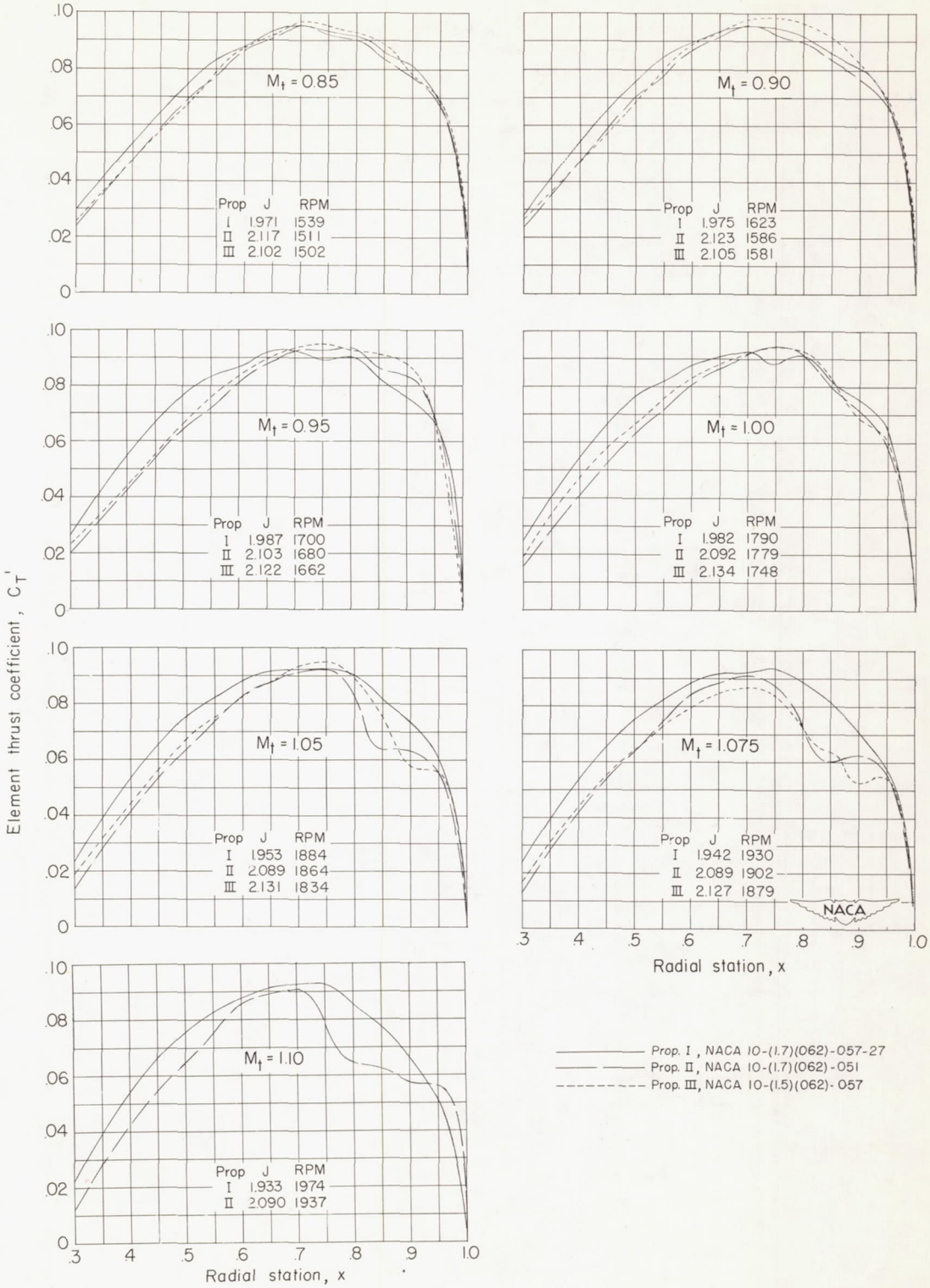

Figure 45.- Effect of helical tip Mach number on blade thrust loading for swept and unswept propellers. $\beta_{0.70R} = 45^{\circ}$; $C_P = 0.10$.